Optogalvanic spectroscopy

Beniamino Barbieri* and Nicolò Beverini

Dipartimento di Fisica, Università di Pisa, 56126 Pisa, Italy

Antonio Sasso

Dipartimento di Scienze Fisiche, Università di Napoli, 80125 Napoli, Italy

The interaction of resonant radiation with atoms or molecules present in a discharge can induce variation in the electrical properties of the discharge. This effect, known as the optogalvanic effect, has been shown to be a powerful and inexpensive technique for the investigation of atomic and molecular species. Many theoretical and experimental articles have been published in the last ten years on this subject. In this review the different types of optogalvanic techniques that have been developed are reviewed and the principal theoretical models are analyzed. The spectroscopic applications are examined. An extensive reference list is included, providing an overview of the literature.

CONTENTS

I. INTRODUCTION

When a self-sustained gaseous discharge is illuminated by radiation resonant with an atomic or molecular transition of the elements within it, a change in its electrical

*Present address: ISS Inc., Champaign, Illinois 61820.

properties occurs. This change is observed as an increase or decrease in the conductivity of the discharge and is known as "the optogalvanic effect" (OGE).

The OGE was first described by Penning (1928), who noted a variation in the impedance of a neon discharge when it was irradiated by an emission from an adjacent neon discharge. Similar observations were later made on Hg and He discharges by Kenty (1950) and by Meissner and Miller (1953). In all cases the pumping effect of the radiation on the metastable levels, which are critically involved in the ion-electron production mechanism inside the discharge, made it possible to observe this phenomenon by using incoherent light sources. Extensive and practical applications of the OGE had to wait for the introduction of tunable dye lasers. The OGE was first discovered in gas-discharge lasers when a change was observed in the discharge current as the laser came over threshold (Garscadden *et al.*, 1964). It was seen in the He-Ne laser (Schiffner and Seifert, 1965; Garscadden and Adams, 1966), in a Xe discharge (Freiberg and Weaver, 1967), and in CO_2 (Carswell and Wood, 1967).

The actual development of the OGE as a useful spectroscopic tool began with the work of Green, Keller, Luther *et al.* (1976). They irradiated a discharge using a tunable dye laser and demonstrated that high-sensitivity spectra of the species present in the discharge could be obtained. The electronic excitation of the atoms in the discharge allowed for the observation of transitions starting from the metastable or excited states, while the use of a hollow-cathode discharge made it possible to perform spectroscopy on a gas-phase sample of refractory elements produced by cathodic sputtering. Figure 1 is a diagram of what became a standard arrangement for continuous-wave (cw) tunable laser applications. The laser beam is amplitude modulated by a chopper, and the optogalvanic (OG) signal is detected by a lock-in amplifier.

The OG technique can be considered as an alternative to absorption or fluorescence techniques. The experimentally observed perturbation of the discharge characteristics induced by laser radiation (even at a high saturation level) is usually sufficiently small so that the OGE can be considered directly proportional to the number of photons absorbed (Lawler, 1980). High-resolution spectroscopy techniques are discussed and compared in Sec. IV, and some of their applications described.

Several papers published since 1976 have suggested a wide range of applications of the OGE—spectroscopy, small-concentration detection, isotopic analysis, laser calibration, and laser stabilization. They have also explored extensions of the technique (molecular and ion spectroscopy; use of cw tunable infrared lasers such as color-center or CO_2 lasers; use of pulsed lasers; and spectroscopy in radio-frequency discharges) and ways of studying the kinetics of OG signal generation. The usefulness of OG spectroscopy has been extended by the demonstration of sub-Doppler techniques for studying species present within the discharge.

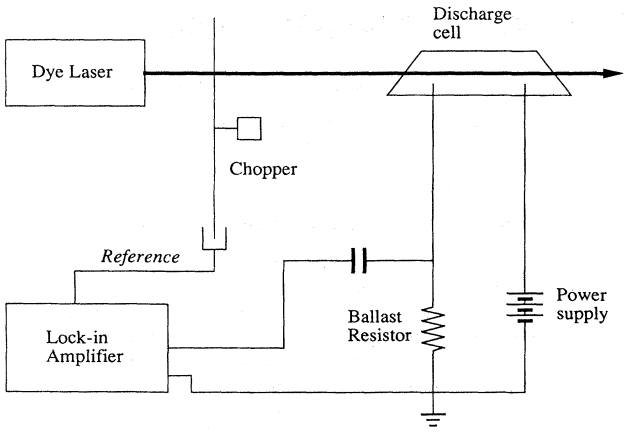

FIG. 1. Typical experimental apparatus for optogalvanic spectroscopy. The signal is detected across the ballast resistor, while the capacitor permits decoupling of the high-voltage power supply.

In this article we review the most important OG techniques to date. Optogalvanic signal generation is analyzed in Sec. II, and the proposed models of the effect in different kinds of discharges are discussed. The typical experimental apparatus is reviewed in Sec. III, while the spectroscopic applications are considered in Sec. IV, with emphasis on high-resolution sub-Doppler techniques. Finally, in Sec. V, we discuss other applications.

In this paper, the interest has been restricted to the optogalvanic effect in self-sustained discharges. Other techniques in which radiation field absorption triggers a discharge are sometimes also referred to as optogalvanic techniques, but they will not be covered by this review. However, in Sec. V we shall briefly consider the optogalvanic technique as applied to flames.

The optogalvanic effect has been the subject of several monographs and review papers, which are listed in the Appendix. An international conference on optogalvanic spectroscopy and its applications was held in 1983, and the proceedings of the conference were published in a special issue of the *Journal de Physique*, Colloque (**C7**, 1983).

In this paper only the most remarkable articles are cited, although in the references we include a complete (to the best of our knowledge) list of the works published in the field.

II. THE OPTOGALVANIC MECHANISM

A. Steady low-pressure discharges

In order to understand fully the mechanisms leading to the OGE, it is useful to recall briefly some of the basics of steady low-pressure gaseous discharge operations (for a

more complete description, see Druyvesteyn and Penning, 1940 and von Engel, 1965).

In order to illustrate the different regimes of a discharge, we show, in Fig. 2, the discharge characteristic $V=f(I)$ for flat parallel electrodes, typical for a gas pressure around 100 Pa (about 1 torr). For low values of V, the gas is a good insulator. Nevertheless, even between cold electrodes and in the absence of photoelectric emission, a very small current flows due to the ionization induced by external agents (such as cosmic rays). This current is subject to statistical fluctuations.

When the dc potential V, applied across the two electrodes in series with a current-limiting resistor R, overcomes the so-called breakdown voltage (of the order of 1000 volts), a self-sustained discharge is produced (Penning, 1928). In this regime a primary electron, generated by external agents, receives from the electric field sufficient energy before a collision to produce secondary ionization. As a consequence, the discharge can be maintained even if the external ionization source is stopped. For a low current, of the order of 10^{-7}–10^{-6} A (i.e., for large values of R), the discharge is characterized by constant voltage and no light emission. This is referred to as a "dark discharge" or "Townsend discharge." As the current increases, the space charge becomes so large that a cathode voltage fall develops. The voltage decreases through a transition region, called a subnormal glow discharge, until it reaches a constant value V. In this condition, usually known as a normal glow discharge, a visible luminescence is produced. The voltage is only slightly above the cathode fall potential, which is of the order of 200–300 V and is relatively constant for current between 1 and 100 mA. A further increase in the current brings the limited cathodic area to saturation. As a result, the voltage rises and the discharge operates in the so-called "abnormal glow region." For greater currents, on the order of 1 A, there is a sudden transition region. The voltage drops to several tens of volts, a level equal to and even lower than the ionizing potential of the gas, with a current of the order of 1–10 A. This is referred to as an arc discharge. This same behavior is maintained in an alternating (ac) excited discharge, provided the frequency is lower than about 10^4 Hz.

In the following section we shall consider only discharges in the glow region, even though the OGE has been observed both in the Townsend region (Kravis and Haydon, 1981) and in the arc region (Van den Hoek and Visser, 1980). Interest in these cases appears to be limited to diagnosing the discharge itself.

On the other hand, a low-pressure glow discharge displays a nice spectroscopic property that is quite useful: unlike the arc discharge, the atomic excitation is not related to the gas temperature but results directly from the electron energy generated by the electric field. Although a certain amount of heat is generated by the ionic cathode bombardment, this thermal energy is not necessary for sustaining the discharge. The discharge can be cooled, and the line broadening is limited.

Alternating dark and luminous zones can be distinguished in a glow discharge. A typical appearance of the glow discharge is shown in Fig. 3, corresponding to a direct-current discharge in a long cylindrical tube filled with rare gas, at a pressure between 10 and 150 Pa (about 0.1–1 torr). Under different conditions the appearance and the properties of a glow discharge can be different.

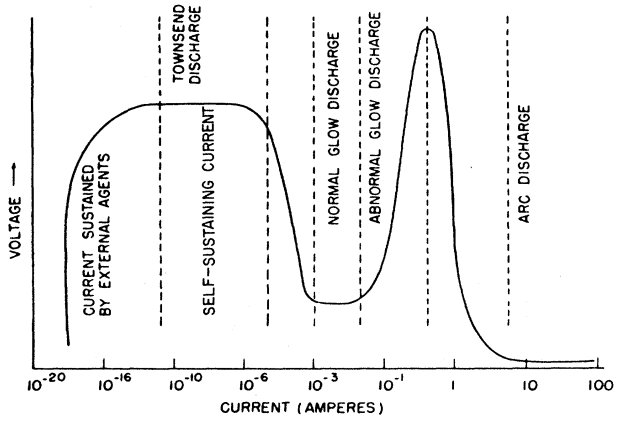

FIG. 2. Schematic of a gas discharge between flat parallel plates.

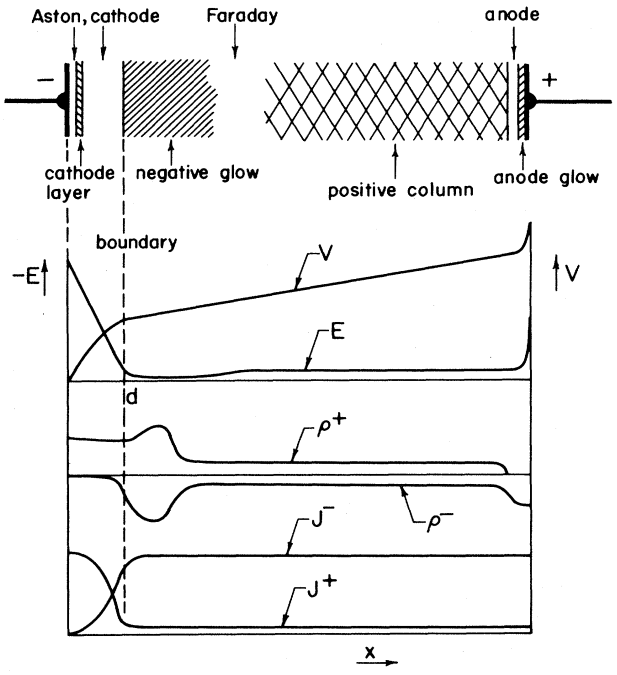

FIG. 3. Spatial distribution of dark and luminous zones, electric field E, potential V, space-charge densities ρ^+ and ρ^-, and current densities J^+ and J^- in a glow discharge.

Later, we shall consider some particular cases that are interesting for their applications in optogalvanic spectroscopy. Figure 3 also shows the behaviors of the electric field, the charge density, and the current density, both for negative (electron) and positive (ion) charge carriers in the different discharge regions.

The generation of these different regions can be explained as follows (von Engel, 1965). The electrons, extracted from the cathode by a collision of positive ions or by the photoelectric effect, leave the cathode with a small initial energy, of the order of 1 eV, and are then accelerated by the strong electric field. The very narrow region near the cathode, where they have not yet achieved enough energy to ionize the gas, is called the "Aston dark space." This is followed by a thin, weakly luminous layer, where the electrons have gained an energy corresponding to the maxima in the excitation function. These regions are followed by the cathode dark space (or Crookes space), characterized by the presence of a few electrons slowed down by inelastic collisions together with many fast electrons whose energy is well beyond the maxima for atomic excitation. The slow electrons are responsible for the faint luminosity of this region, while the fast ones induce ionization with high efficiency, producing a strong electron multiplication. Due to the ionizations, and to the different mobilities of the electrons and the positive ions, a strong positive space charge is generated, which progressively reduces the electric field to a weak value.

A sharp increase in luminosity characterizes the boundary of the negative glow. The number of low-energy electrons becomes very large and their speed decreases with distance from the cathode. The ionization efficiency is now low, while the inelastic collisions produce efficient atomic excitation. The reduced electric field favors recombination between the electrons and the ions. With increasing distance from the cathode, the average electronic energy, and consequently the luminosity, decreases. A new dark region develops, called the Faraday dark space. Just beyond the Faraday space there is a new luminous region, the positive column, characterized by uniform luminosity or by regularly striated zones. The axial component of the electric field in the positive column is found to be nearly constant (this implies that the plasma is at any point neutral) and several orders of magnitude smaller than in the dark space. The motion of electrons is no longer beamlike, as in the negative glow, but essentially random: their drift speed is many orders of magnitude smaller than their random velocity.

In proximity to the anode, a negative charge region is generated by the combination of electron attraction and ion repulsion. Thus the electric field increases again. The electrons arriving from the positive column cross a new dark region and are accelerated against the anode, producing an "anode glow" in front of it.

The nature of the gas, its pressure, the geometry of the cell, the separation of the electrodes, their size, their material, are all parameters that can change the appearance of the glow discharge. Some particularly important parameters are considered here. For instance, when the distance between the cathode and the anode is reduced (keeping the current constant), the axial length of the cathodic region remains unchanged, while the positive column length is progressively reduced. Before the anode enters the Crookes dark space, the voltage on the discharge begins to increase, demonstrating an increasing difficulty in the ionization processes. In this condition the discharge is called "obstructed." A similar effect can be observed if the radius of the discharge tube is reduced. When the mean free ionic path becomes comparable with the tube radius, the voltage rises steeply. The discharge is then in the (Tonks and Langmuir, 1929) free-fall regime.

Other peculiarities of the positive column, the cathode fall region, and particularly the hollow-cathode discharge shall be discussed later with regard to OG processes.

The elementary processes occurring in a glow discharge are numerous and complex. The electrons, accelerated by the electric field, have an energetic distribution that can be described by an elevated electronic temperature, which at low pressure can reach values as high as 5×10^4 K. Collisions with such energetic electrons cause the atoms present in the discharge to be excited or ionized. The relative cross sections are on the order of 10^{-14}–10^{-16} cm^2, being greatly dependent on the particular atomic transition and electronic energy. For example, in Fig. 4 the cross sections for $^3P_0$, $^3P_2$, $^3P_1$, and $^1P_1$ levels of Ar ($1s_5$, $1s_3$, $1s_4$, and $1s_2$ in the Paschen notation) are shown as a function of the electronic energy (Tachibana, 1986). The cross sections corresponding to optically allowed transitions (for example, the $^1S_0$–$^1P_1$ transition in argon) are larger and broader than those involving metastable levels.

The mechanism responsible for direct ionization can be

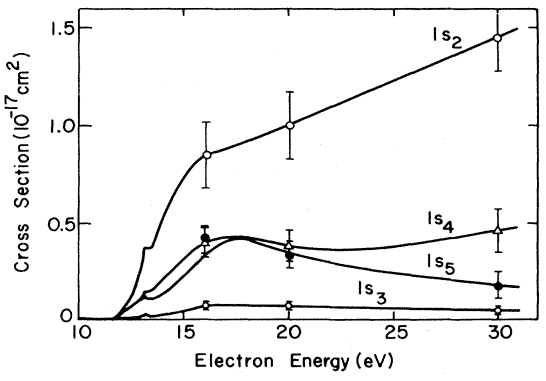

FIG. 4. Excitation cross sections for electronic impact of the lower Ne excited states (from Tachibana, 1986).

summarized as follows.

(1) One-step ionization by electron impact:

$$A + e^- \rightarrow A^+ + 2e^- . \quad (1)$$

(2) Two-step or multistep ionization:

$$A + e^- \rightarrow A^* + e^-, \quad A^* + e^- \rightarrow A^+ + 2e^- . \quad (2)$$

In noble-gas discharges, process (2) is particularly important, where A^* is a metastable level. We shall see later that this fact is of great interest in OGE generation. Direct ionization [process (1)] dominates at low pressure, because the electrons can acquire enough energy between two different collisions.

Besides these processes in which the kinetic energy of the electron is converted into excitation energy, other processes involving collisions between excited atoms compete to build up the excited-state population in the discharge. The most important are the following.

(3) Excitation transfer between an atom A in the ground state and an excited atom B:

$$A + B^* \rightarrow A^* + B + \Delta E , \quad (3)$$

where the difference of excitation energy ΔE is released as translation energy.

(4) Penning ionization:

$$A^* + B \rightarrow A + B^+ + e^- . \quad (4)$$

This process is particularly important for discharges in noble gases where A^* is a metastable level. The typical cross section is about 10^{-16} cm^2.

(5) Associative ionization:

$$A^* + A \rightarrow A_2^+ + e^- . \quad (5)$$

This process is energetically allowed for neon atoms excited to the $5s$ or higher-lying electronic states. The binding energy of Ne_2^+ ions is effectively about 1.3 eV, so that an excitation energy equal to 20.3 eV (equal to the difference between the ionization energy and the binding energy) is required to create an ion-electron pair. The corresponding cross sections in these cases are very large, of the order of 10^{-16} cm^2. For this reason an excitation of Ne atoms to $3s$, $4d$, or more energetic levels is practically equivalent to a direct ionization.

(6) Metastable-metastable collisions:

$$A^* + A^* \rightarrow A^+ + A + e^- . \quad (6)$$

Such collisions are, again in the case of neon, very effective due to the high energy (around 16.6 eV) of the metastable levels.

Other specific processes contribute to the losses of excited atoms, like diffusion and deexcitation against the cell walls. Superelastic collisions, in which excitation energy is transferred in kinetic energy, increase the electronic temperature.

A complete balance of the discharge processes requires the inclusion of other mechanisms such as recombination, loss of charged particles due to ambipolar diffusion to the discharge's walls, and radiative processes.

B. The optogalvanic signal in a steady glow discharge

When laser radiation is tuned around a transition of an atomic or molecular species present in the discharge, the described processes are perturbed and the electrical properties of the discharge are changed.

The mechanisms that translate these effects into current perturbation are essentially the following.

(1) A variation of electron-ion pair production.

(2) A variation of the electron and gas temperatures produced by superelastic collisions with excited atoms.

Both of these processes have been invoked to explain the OGE in different kinds of discharges, and, as we shall see, either process can dominate OG signal generation, depending upon the particular discharge considered. What actually happens is that the environment of a discharge is too complex to be described by a general theoretical model.

The first attempt to explain the optogalvanic effect was based on a qualitative description. Penning (1928) used the effect to confirm the occurrence of collisions between metastable neon atoms and ground-state argon [process (4)].

A quantitative understanding of the OGE is possible only if a reasonable model of the discharge can be made and the cross sections of the involved processes are known. Usually a rate equation formalism has been used to describe the different processes. However, it is impossible to give a complete set of rate equations for all of the levels and processes involved in the discharge. This is due to the very large number of equations required and the unavailability of most cross-section values. Thus knowledge of the properties of a particular discharge is usually largely empirical, and establishing a general model for a quantitative description of the OGE is a very difficult task.

The problem can be solved for a specific transition by making reasonable approximations, such as considering the levels immediately connected to the two resonant levels by the larger cross sections, and eventually introducing empirical parameters, such as discharge impedance.

During recent years considerable effort has been made in this direction. Some models have been obtained for particular kinds of discharges (positive column, hollow cathode, radio frequency) that provide good explanations of the experimental observations under typical conditions. The more important models are discussed below.

1. Positive column in a noble-gas discharge

The positive column of an inert gas discharge is a region of the glow discharge characterized by uniform brightness, whose color depends on the particular gas or vapor. The properties of the positive column of a glow

discharge, as a function of the pressure p and the current i, can be scaled with the dimension using the scale-independent parameters pr and i/r, where r is the discharge radius, p the pressure, and i the current.

For a low-pressure column ($pr < 10^{-2}$ torr cm), the positive column is homogeneous; it can be described by a theory first developed by Schottky (1924) and then generalized by Franklin (1976). This theory is based on the assumptions that single-step electronic ionizing collisions dominate ion production and that ion loss is due only to ambipolar diffusion (i.e., the Debye length for the electron is much smaller than the tube radius, and recombination occurs on the wall). As a consequence, the densities of negative and positive charge are locally equal (neutral plasma), with a maximum value on the axis and practically zero on the wall. At higher pressure, or in the presence of impurities, the discharge appears striated. The different regimes of a positive column have been described by Tonks and Langmuir (1929), Smits and Prins (1979), and Cherrington (1979). When operating in a higher-pressure regime, stepwise ionization becomes comparable to direct ionization or dominant. However, typical conditions in OG investigations involve low-pressure columns, because they correspond to the more stable regime of the discharge; thus the theoretical models of the OGE that we shall discuss here refer to such discharges.

A model that provides not only qualitative, but also quantitative, comparison with experimental data was developed by Lawler (1980) for the OGE in a positive helium column. Lawler's model is based on a rate equation approach. The rate equations concern the levels, whose populations are greatly perturbed by the laser radiation, and the ion density. The model was tested by studying a single He transition, the 2^3P-3^3D transition at 587.6 nm, which involves levels with well-understood kinetics and well-known reaction rates, and which occurs at a convenient wavelength for dye lasers.

The process of OG signal generation is split into two steps. First, the number of ion-electron pairs produced in excess per absorbed photon (ionization efficiency ϵ_i) is calculated by solving the equations for the level populations perturbed by the laser radiation. This ionization efficiency depends on the change in the excitation and ionization rates for the two resonant levels and can be expressed, in general, as

$$\epsilon_i = \frac{\gamma_{ui}}{\gamma_u} - [(\gamma_u - A)/\gamma_u]\frac{\gamma_{li}}{\gamma_l} , \tag{7}$$

where γ_u and γ_l are the total decay rates for the upper and lower levels, respectively (summed over all possible decay channels); γ_{ui} and γ_{li} are the total decay rates (except the direct decay from the upper to the lower level) producing an ion-electron pair; and A is the spontaneous radiative transition rate between the two levels. For the considered transition, the dominant ionization process is associative ionization of the 3^3D state, while deexcitation is primarily radiative, so that Eq. (7) can be simplified to

$$\epsilon_i = a/A , \tag{8}$$

where a is the associative ionization rate for the 3^3D level. It should be observed that ionization efficiency is not generally related to the energy of the absorbed photons. An infrared photon may produce a large ionization effect, as demonstrated experimentally by Jackson *et al.* (1980) on the 2.65 μm multiplet transitions in He. In this case the interconnected levels have almost the same ionization cross sections, but their lifetimes differ by more than one order of magnitude. A direct application of Eq. (8) gives, in the case of the $4d$-$6f$ transition, a value of ϵ_i as high as 0.56. Al-Chalabi *et al.* (1983) have confirmed these assertions.

The second part of Lawler's model considers the response of the discharge plasma to perturbation due to ion-electron pair production induced by the radiation, assuming a small perturbation. The variation of the current ΔI, flowing through the ballast resistor R_b, enters into the equation

$$R_b \Delta I = -l \Delta E , \tag{9}$$

where l is the positive-column length and ΔE is the variation in the axial electric field induced by the light. The phenomenological equations are solved in terms of a collection efficiency ϵ_c, defined as the number of excess electrons that flow through the ballast resistor per ion-electron pair produced.

As a final result, the current signal ΔI is expressed in terms of the calculated values of ϵ_i and ϵ_c as

$$\Delta I = eQ\epsilon_i\epsilon_c , \tag{10}$$

where Q is the number of absorbed photons and e the electron charge.

The complete analytical equation for the OG signal for the considered transition is derived as

$$\Delta I = -\frac{a}{A} Q \left[\frac{er\mu E}{s_0 l} (2kT_e/m_p)^{1/2} \right] \frac{R_d}{R_d + R_b} , \tag{11}$$

where μ is the electron mobility, whose dependence on the E/p ratio is well known (Brown, 1961); m_p is the ion mass; R_d is the dynamic resistance given by dV/dI and T_e is the electron temperature, a function of pr (Pfau *et al.*, 1969). The coefficient s_0 is a constant, defined by Tonks and Langmuir (1929), related to the average and axial electron densities.

This model is satisfactory for the 2^2P-3^3D transition in He, which is particularly simple because the variation in the population of the two involved levels can be directly related to the perturbation in the discharge properties. For transitions involving the metastable levels of noble gases, the situation is more complex. Indeed, the metastable levels play an important role in sustaining the discharge. The absorption of a photon, not followed by an immediate ionization, results in depletion of the metastable-states population because the radiative decay to ground state can be more than one order of magnitude faster than the metastable-level lifetime, particularly at

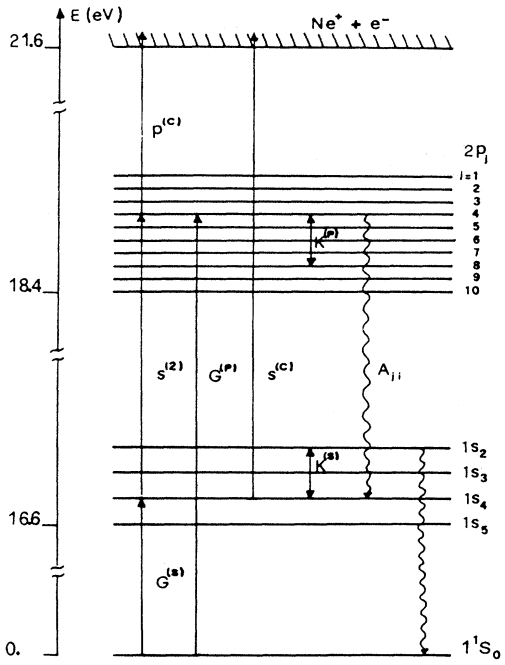

FIG. 5. Simplified energy-level diagram for Ne, including the ground state, the four $1s$ levels, the ten $2p$ levels, and the continuum. The main collisional and radiative processes are represented (from Sasso, Ciocca, and Arimondo, 1988).

low current. A scheme of the more relevant levels in OG signal generation is shown in Fig. 5 for neon. The principal excitation and deexcitation channels are shown. The lowest excited electronic configuration $2p^5 3s$ yields four states, designated in the L-S coupling scheme as $^3P_2$, $^3P_1$, $^3P_0$, and $^1P_1$ or, in Paschen notation, as $1s_5$, $1s_4$, $1s_3$, and $1s_2$, respectively. The $^3P_2$ and $^3P_0$ are metastable, with a radiative lifetime of the order of 1 s, while the $^3P_1$ and $^1P_1$ levels decay to the ground state with a lifetime of 16 ns and 1.2 ns, respectively, by emitting VUV photons. At pressures greater than 1 torr, radiation trapping determines the effective lifetime of the $^3P_1$ level, so that in the discharge it becomes comparable with the effective lifetime of the two metastable levels.

In Fig. 6 a typical OG spectrum obtained in a low-pressure neon positive-column discharge at low current is displayed. A cw dye laser is tuned in the range 580–640 nm, which covers many Ne atomic transitions originating from the $1s_i$ levels. In this spectrum both positive and negative variations of the current appear. This behavior can easily be understood (Erez *et al.*, 1979). At low current, when the laser is resonant with a transition starting from a metastable level, the resulting depletion of the metastable population reduces the rate of two-step ionization by electron impact [Eq. (2)]. Consequently, photon absorption can cause a net reduction in the ion-electron pair production, making the ionization efficiency negative, even if the ionization cross section for the upper level is one order of magnitude greater than that for the metastable lower state. Higher current levels, where the lifetime of the metastable state is quenched by electron collisions, cause the signal to be positive, as is usually the case.

A model that can be successfully applied to the OGE in a Ne positive column was developed by Doughty and Lawler (1983a). In this model the neon metastable and "quasimetastable" levels $1s_5$, $1s_4$, and $1s_3$ are lumped together as a single metastable level whose population M evolves according to the following rate equation:

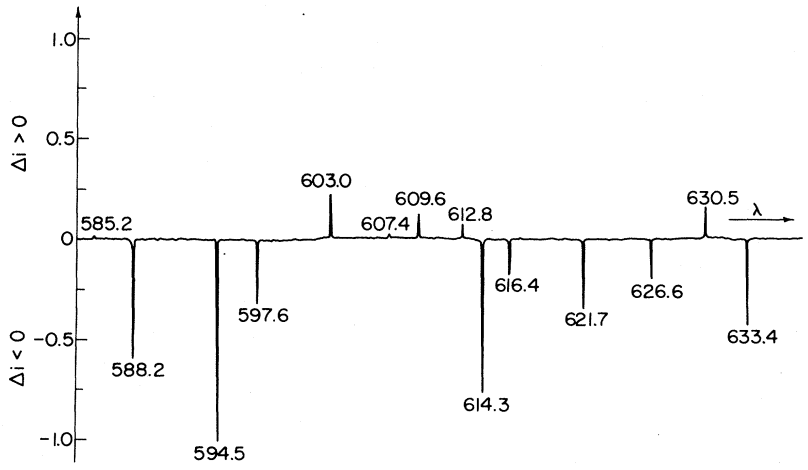

FIG. 6. Broadband optogalvanic spectrum of a neon positive-column discharge. The current was 1 mA and the pressure 0.8 torr.

$$\frac{d}{dt}M = Pn_eN - wM - TM^2 - Sn_eM - S'n_eM/4 - \beta Q = H(n_e, M, E) , \quad (12)$$

where P represents the production rate of metastable atoms due to electron impact with ground-state atoms N and due to radiative refilling from excited levels; w is the loss rate of metastable atoms due to diffusion against the wall; T is the rate for metastable-metastable collisions leading to ionizations; S and S' are the rates for electron-impact collisions producing ionization and excitation into the $2p$ levels, respectively; and β is the branching ratio for radiative decay of the laser-excited $2p$ levels to the nonmetastable level. Obviously, many of these coefficients are functions of the discharge parameters.

A second rate equation describes the production and destruction of electrons with density n_e:

$$\frac{d}{dt}n_e = \alpha v_d N + Sn_eM + TM^2/2 - D(2.4/r)^2 n_e = G(n_e, M, E) , \quad (13)$$

where single-step ionization is represented by the product of the first Townsend coefficient α and the electron drift velocity v_d, both strong functions of E/p; D is the ambipolar diffusion coefficient; and r is the column radius.

Finally, a third equation relates the discharge current to the electron density:

$$I = en_e c v_d r^2 = F(n_e, E) . \quad (14)$$

Assuming that radiation absorption is a small perturbation, this set of equations can be solved by a linear, steady-state approximation, and the following formula for the OG signal can be derived:

$$\Delta I = \beta QI(Sn_e + TM)\{(1 + R_b/R_d)[(Sn_eM + TM^2/2)w + (S - S'/4)n_eTM^2/2]\}^{-1} , \quad (15)$$

where the dynamic resistance $R_d = dV/dI$ has been introduced.

A comparison between experiment and a theoretical model is shown in Fig. 7 as a function of discharge current intensity. The agreement between theory and experiment is, however, good only under restrictive experimental conditions, because under different conditions many neglected processes may become important.

This model was generalized by Sasso, Ciocca, and Arimondo (1988). The evolution of the $1s_i$ and $2p_j$ levels has been separately considered and collisional mixing between these levels and the neighboring levels has been included. In this model, the properties of the discharge in the absence of laser absorption are also predicted from the atomic properties, instead of being derived from empirically measured discharge impedance. The system of steady-state equations becomes too complex to be solved analytically. Numerical solutions in the presence and in the absence of laser radiation were obtained for a large set of transitions in the neon spectrum. A knowledge of the $2p_j$ populations also allows a comparison between the OG and the simultaneously observed fluorescence spectrum.

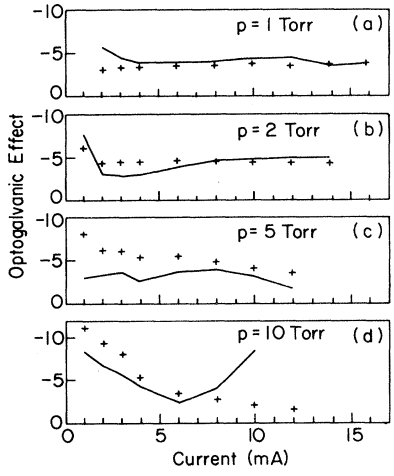

FIG. 7. Optogalvanic signal in a neon positive column as a function of the current at several pressures. Solid lines represent the value calculated from Eq. (15). The crosses are from experimental data (from Doughty and Lawler, 1983a).

The models we have considered up to now are based on the assumption of local-field approximation. Both the change in the electron density and in the electron temperature are included in a self-consistent way. The change in the local electron energy, and its effect on all excitation rates, ionization rates, and transport coefficients, is parametrized in terms of the perturbation to the reduced field E/N. Models based on the local-field approximation may not be appropriate to strong discharges, where recombination and superelastic collisions, and, in general, the transfer between internal and translational energy, play an important role. These conditions are quite usual in the OG signal generation in a molecular discharge (Rettner *et al.*, 1981; Haner *et al.*, 1983; Webster and Menzies, 1983a) and in a hollow cathode discharge (Keller and Zalewski, 1980).

This temperature effect has also been observed in the positive column of a He-Ne discharge by simultaneously detecting the OG signal and the acoustic disturbance signal via a microphone in the same experimental arrangement used for optoacoustic (OA) spectroscopy (Arimondo *et al.*, 1984). The OA signals can be explained in terms of the energy deposited into the gas and then, indirectly, in terms of the energy deposited on the tube walls. The total power dissipated in a positive column illuminated by a laser radiation

$$P_{\text{tot}} = IlE + Qh \tag{16}$$

disperses into different output channels: visible fluorescence transmitted by the cell and ultraviolet fluorescence absorbed by the walls; energy released by the deexcitation of metastable atoms and recombination of ions diffusing to the walls; and heat conduction of ground-state atoms. All of these contributions, except the last one, are easily related to the discharge parameters (Doughty and Lawler, 1983a).

The presence of resonant radiation modifies the energy balance (Sasso, Di Vito, and Arimondo, 1988), and the acoustic signal monitors changes in the gas temperature.

The experimental observation of the OA signal in a He-Ne positive column demonstrates that either heating or cooling of the discharge can follow the radiation absorption, depending on the discharge parameters.

To conclude this section, we note that the OG signal measured in a positive column is usually a spatial average over the length of the discharge. May (1985a) has investigated a positive column with steady striation using transverse illumination. He found periodic polarity changes in the signal.

2. Metallic vapor in a positive column

The first attempt at outlining a general theoretical framework was made by Pepper (1978) for a discharge operating in a metallic vapor in the presence of buffer gas. He considered a simplified atomic system (ground state, excited state, ion) in a noble-gas glow discharge. The superelastic collision rates of electrons against these two-level atoms or the metastable buffer gas atoms determined the electron temperature of the discharge. The absorption of radiation changed the densities of these species and then affected the electron temperature and, as a consequence, the discharge impedance. Numerical calculations based on this model were, however, only partially satisfactory.

Some modifications to the model have been made by Maeda *et al.* (1981), who studied a sodium discharge in noble gas. They also took into account the changes induced in the electron density and calculated the following equation for the relative amplitude of the OG signal:

$$\Delta V = 1.96 \frac{(2m_e kT_e/\pi)^{1/2}}{e^2 r^2 \lambda_e n_e} J \left[\frac{\Delta T_e}{2T_e} - \frac{\Delta n_e}{n_e} \right], \tag{17}$$

were λ_e is the electron mean free path and J is the axial current density.

3. Optogalvanic effect in the cathodic region

As we have seen in Sec. II.A, the cathodic region is characterized by nonuniform electric properties. Effectively, the electric field is very large at the cathode surface, dropping almost to zero in a few millimeters. The basic mechanism for production of an OG signal in the cathodic region is very different from that occurring in the positive column. The presence of strong accelerating electric fields amplifies, by ionization avalanche, the number of electron-ion pairs produced by the radiation. Moreover, the changes in the metastable density and in VUV photon generation can strongly modify the rate of electron emission from the cathode surface. As a result, the OG signal observed in this region is usually much larger than the signal in the positive column.

A model for OG signal generation in the cathodic region (De Marinis *et al.*, 1988) can be obtained by generalization of the theory of Little and von Engel (1954). For a neon glow discharge with two plane-parallel elec-

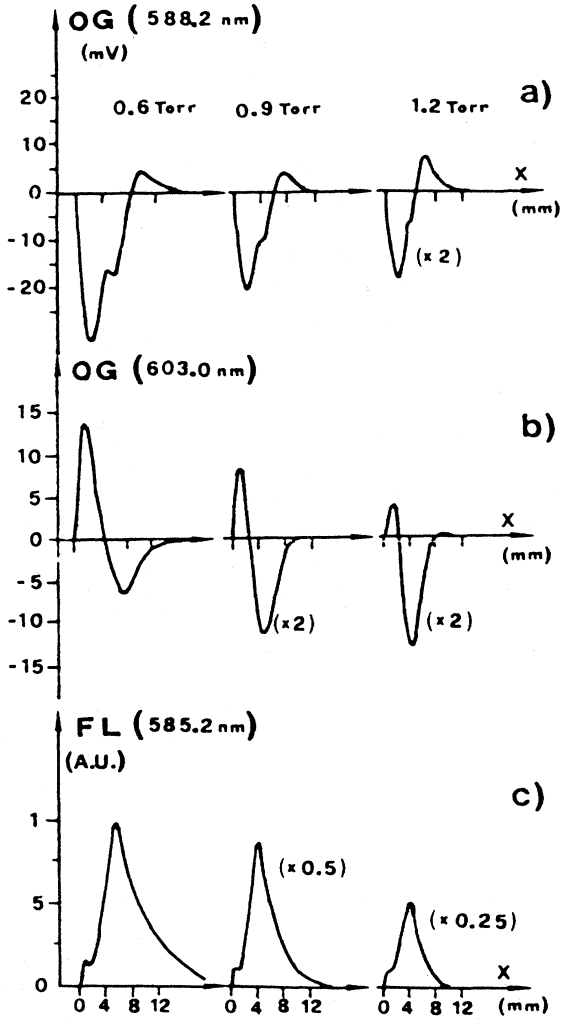

FIG. 8. Experimental OG and fluorescence signals as a function of the distance from the cathodic surface: (a) OG for a laser excitation at 588.2 nm ($1s_5 \rightarrow 2p_2$); (b) OG for a laser excitation at 603.0 nm ($1s_4 \rightarrow 2p_2$); (c) fluorescence at 585.2 nm ($2p_1 \rightarrow 1s_2$) in the absence of laser radiation. The discharge current was 4 mA. The pressures were 0.6, 0.9, and 1.2 torr, respectively (from De Marinis *et al.*, 1988).

trodes, a relation can be obtained between the discharge current I and the cathodic voltage V_c in terms of the coefficients γ_i, γ_m, γ_p for the secondary electron emission from the cathode due to the ions, the metastable atoms, and the photons, respectively:

$$I(V_c)=V_c^{3/2}K\left[\frac{1-D+\gamma_i}{1-D-G}+\frac{M}{1-D-G}\right]S\ , \tag{18}$$

where S is the cathode surface area and

$$\begin{aligned} K&=2\epsilon_0/d\{8/em\,[2l/d-(l/d)^2]\}^{1/2}\ ,\\ D&=f_d n_d \gamma_p\ ,\\ G&=f_g n_g \gamma_p\ ,\\ M&=f_m \Gamma \gamma_m \end{aligned} \tag{19}$$

are coefficients that are functions of the dark space length d, the mean free path for charge transfer l, and the number of VUV photons n_d and n_g created by each electron entering the Crookes space and the negative glow, respectively. Γ is the density of metastable atoms; f_d, f_g, and f_m are geometric factors, giving the cathodic collection efficiencies for photons and for metastable atoms.

In the limit of small perturbation, a variation of the discharge current when laser radiation excites a transition can be obtained by differentiating Eq. (18):

$$\Delta I=\partial I/\partial n_d \Delta n_d+\partial I/\partial n_g \Delta n_g+\partial I/\partial\Gamma\Delta\Gamma\ . \tag{20}$$

The strong nonuniformity of discharge properties near the cathode gives a large variation in the OG signal amplitude as a function of the distance of the excitation region from the cathode. Figure 8 reports typical OG spatial behaviors in a neon discharge for two different radiation wavelengths, corresponding to transitions starting from (a) metastable and (b) radiative levels.

Optogalvanic and conventional (fluorescence and absorption) spectroscopic techniques have been used in parallel by Den Hartog *et al.* (1988) to investigate a helium discharge in order to map the electric field and the gas temperature. Their results were compared to an analytic treatment of the ion transport and a Monte Carlo simulation of the current balance at the cathode surface.

4. Hollow-cathode discharge

The hollow-cathode discharge is a particular kind of glow discharge with an enlargement of the negative glow region as one of its main characteristics. Let us imagine that the cathode is formed by two flat electrodes, parallel to each other. If the distance between the two electrodes is quite small with respect to their typical dimensions, the two negative glows coalesce into a single negative glow displaying a high radiation intensity. Often, instead of two parallel flat electrodes, a cylindrical cathode is used. This design allows the discharge to handle large currents, up to many amperes, in the glow regime in a relatively cold carrier gas. Another advantageous property of a hollow-cathode discharge is the strong electric field in the cathodic dark region, which strongly accelerates ions against the cathodic surface, producing very effective sputtering at high current values (of the order of 100 mA). In this way the discharge can be used as a source of free atoms of refractory elements (Fig. 9).

Electron heating effects are important in the case of a hollow-cathode discharge when the minority carriers (i.e., the atoms sputtered from the cathode) are excited by laser radiation. This statement is supported by a series of experiments (Keller *et al.*, 1979; Keller and Zalewski, 1982) in which the amplitude of the OG signal was measured for hollow-cathode lamps of different materials (U, Eu, Na, Zr) irradiated by resonance lines, as a function of the absorbed laser energy. Keller and co-workers found that the amplitude of the signal was independent of the ionization potential of the absorbing atom and of the energy difference between the laser-excited level and the continuum.

This effect can be explained easily if it is assumed that the atomic system simply transfers the excitation energy into the electrons. The equilibrium established in a hollow cathode between the electrons and the atoms, resulting from numerous elastic and superelastic collisions, makes the electron temperature approximately equal to the electronic excitation temperature in the atom. Laser irradiation slightly perturbs this process. However, the electron collisions are so frequent that a significant change in the level population is prevented. The energy supplied by absorbed photons is transferred to electrons. Since the equilibrium in the discharge is strongly affected

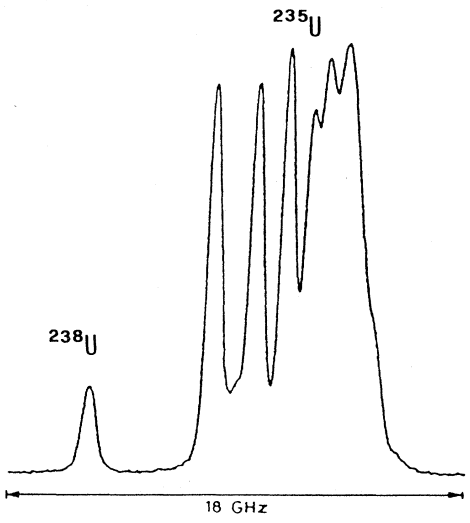

FIG. 9. Doppler-limited optogalvanic recording of the hyperfine structure of the 591.5 nm transition in ^{235}U. A hollow-cathode lamp with a small isotopically enriched uranium foil was used (from Barbieri *et al.*, 1984).

by the electron energy distribution, this extra energy causes a decrease in the impedance of the discharge.

This explanation was confirmed by the experience of Drèze *et al.*, 1982. They detected simultaneously the OGE and laser-induced intensity variations in the emission lines of a uranium hollow-cathode discharge filled with Xe as a buffer gas. When the laser was tuned at the 591.5 nm transition of U, the emission lines of all the species present in the discharge (U I, U II, and Xe) showed an increase in intensity. The intensity variation of the Xe lines was particularly interesting, because a direct energy transfer from the laser-excited U atoms to Xe atoms in the ground state or in metastable states is impossible. Drèze *et al.* also measured the electronic excitation temperature of the atoms with and without laser radiation and found that there was an increase on the order of a few degrees Kelvin on a steady value of about 3500 K.

Keller *et al.* (1983), using a standard model of a hollow-cathode discharge, performed a calculation that shows that the OGE generation mechanism involving direct collisional energy transfer from absorbing atoms to electrons was approximately 100 times more effective than direct ionization of a laser-excited level. The change in conductivity σ induced by the laser radiation was determined by differentiating the conductivity with respect to electron temperature and electron density. The relative variation of the conductivity was

$$\frac{\Delta\sigma}{\sigma}=\frac{\Delta Z}{Z}=1.5\frac{\nu_{ei}}{\nu_{ei}+\nu_{ea}}\frac{\Delta T_e}{T_e}-\frac{\nu_{ea}}{\nu_{ei}+\nu_{ea}}\frac{\Delta N_e}{N_e}\ , \tag{21}$$

where ν_{ei} and ν_{ea} are the electron-ion and electron-neon collision frequencies.

A theoretical and experimental investigation of the role of photoionization in a hollow-cathode discharge was the subject of a recent paper by Broglia *et al.* (1987).

C. Optogalvanic effect in high-frequency discharges

1. Radio-frequency discharges

A low-pressure glow discharge can also be supported by a radio-frequency (rf) field. The rf oscillator can be coupled to the plasma by placing the sample inside the oscillator circuit, in a coil (inductive coupling) or in a capacitor (capacitive coupling). This kind of discharge has some useful properties. The absence of internal electrodes in the inductively coupled system eliminates sputtering and contamination, even in the presence of reactive or corrosive species. An rf discharge can also be driven with high stability in a range of pressure often much larger than that allowed for dc discharges. Working at lower pressures can minimize the pressure broadening when high resolution must be achieved, while higher pressure can produce excimer molecules present only when three-body collisions become important.

The impedance changes in the discharge induced by atomic or molecular transitions can be monitored with a good signal-to-noise ratio on the oscillator current if a regenerative oscillator, such as a Colpitt circuit, is used. This device works in a regime of negative dynamic resistance. When the vapor cell is coupled capacitively or inductively with it, the impedance Z of the sample becomes a part of the series impedance of the circuit. In this way, the amplitude of the OG signal (detected as $\Delta I/I$ in the oscillator circuit) is enhanced, because the negative resistance $-R$ of the oscillator lowers the total unperturbed impedance. The resulting OG signal is thus proportional to $\Delta Z/(Z-R)$. This detection scheme, suggested by Goldsmith *et al.* (1979), was demonstrated for the first time by Stanciulescu *et al.* (1980a).

Other methods of extracting information on the impedance variations inside the discharge include monitoring of the signal induced in a pickup coil wound around the sample (Suzuki, 1981) or direct measurement of the dc discharge impedance using two electrodes placed inside the cell (Labastie, Biraben, and Giacobino, 1982). In this latter method, the detected impedance also gives a measurement of the discharge intensity. This is useful when extrapolation to zero discharge intensity must be performed in order to correct for shifts and broadening due to spurious phenomena in the discharge.

Any theory of electrodeless discharge must consider a complicated self-consistent system of equations describing the distribution of electron density, electron temperature, and electromagnetic fields in the skin layer. In the presence of laser radiation, a detailed balance equation for the perturbed level must be considered.

A simplified model was developed by Bulyshev and co-workers (Bulyshev and Preobrazhenskii, 1984; Bulyshev *et al.*, 1988). The relative change of the power Q injected into the discharge was shown to be simply related to the relative change in the electron temperature T_e by the equation

$$\Delta Q/Q=\tfrac{1}{2}h\nu/T_e(\Delta T_e/kT_e)\ . \tag{22}$$

The theoretical results were compared with the experimental results of Suzuki (1981) in an argon rf discharge and with those of Roesch (1983) in cesium.

2. Microwave discharges

The OGE has also been observed in discharges excited by microwaves (mw). This case is different from that of rf excitation. In a typical glow discharge, the collisional frequency is greater than the field oscillation frequency, while the opposite is true for mw excitation. Since the collisional processes are very important in OG signal generation, the OG signal obtained in a mw excitation contains additional information. Suzuki *et al.* (1983) analyzed methods for mw excitation and their applications. The study of free radicals, which are easily created in a mw discharge, and their kinetics, was suggested as one application. The OG signal was detected by using a

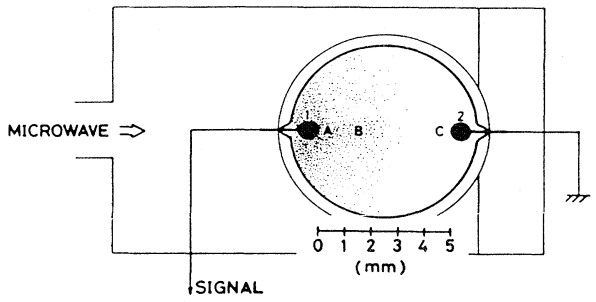

FIG. 10. Schematic drawing of the bright region in the discharge cell with microwave excitation. At high pressure the bright region is restricted around the probe. As the pressure decreases, the bright region increases (from Suzuki, *et al.*, 1983).

diode to monitor the reflected microwave power extracted by a directional coupler, or by observing the potential induced in a pair of probes inside the chamber. Suzuki *et al.* demonstrated that, even using a quite noisy mw source such as a magnetron, a good signal-to-noise ratio could be achieved if the OG signal were extracted by means of a pair of parallel rods. With this arrangement, the sensitivity (measured as the voltage on the electrodes divided by the laser power absorbed) was found to be one to two orders of magnitude greater than the sensitivity obtained from the usual OG signal in a dc discharge. This observed high sensitivity cannot be explained with the electron-gas heating mechanism. In order to explain the OGE with a double probe, it is necessary to consider the position of the discharge cell inside the cavity (Fig. 10). The mw field is more intense at probe 1 than it is at probe 2. As a result, there is a difference in electron temperature and in electron density close to the two probes. A space-charge potential is then generated, which is a function of the pressure in the discharge and of the specific mechanisms of the discharge in different gases. The model presented to explain this signal generation fits the experimental results quite well for three different discharges (Ar, Ne, and O_2).

D. Transient effects

When a dc discharge is excited by a pulsed dye laser, an important change is observed in the OG signal. The high laser power density easily saturates the transitions, allowing observation of multiphoton processes. Ultraviolet wavelengths can be produced more easily, and the corresponding spectra can be investigated. Finally, the short duration of the pulses allows time-resolved studies of the OGE, which give additional information about the kinetics (at the price of a more complex theoretical interpretation).

The first phenomenological analysis (Erez *et al.*, 1979) obtained qualitative agreement with the experiments by fitting the experimental curves with a sum of exponential functions whose constants were given by the effective lifetimes of the levels involved in the excited transition.

A complete model describing the pulsed OGE must take into account the great perturbation induced in the level populations and interpret the complex phenomenology observed, such as multiple sign reversal in time evolution, amplified spontaneous emissions, and nonlinear effects due to two-step photoionization (van de Weijer and Cremers, 1985a). Yasuda *et al.* (1985) developed a model for a particular transition in the He I spectrum (the 2^3S-3^3P transition at 388.9 nm), in which they considered the sharp spike observed in the early time stage of the OG current signal. From available data on the radiative and collisional cross sections, they found that relaxation of the OG signal in the He positive column was primarily governed by ion current to the walls, followed by wall recombination. It was shown that the Rp product is a good parameter for characterizing the discharge, along the Tonks and Langmuir model, in the considered pressure range (0.18–0.8 torr cm).

The calculated values obtained in this model using the data of Bickerton and von Engel (1956) were quite satisfactory compared to the measured values. The analysis considered only the first fast response, and no attempt was made to explain the continuing evolution of the signal. It should be noted, however, that the amplitude of this first sharp signal is more than an order of magnitude greater than the signal that follows it. In the case of molecular discharges, the time-resolved OGE can give much information on the chemical processes in the discharge. This is discussed in the next section.

E. Molecular discharges

As we have pointed out in Sec. II.B, in a molecular discharge the OGE arises primarily through a heating mechanism. It was the observation of an OGE during absorption of low-energy infrared photons in pure vibrational transitions, without any modifications of the electronic states, that first led to this hypothesis (Webster and Menzies, 1983a). The absorbed radiation energy is translated into a gas temperature increase through vibrational relaxation. Many important processes in the discharge, such as the electron-impact ionization, the electron attachment, or the electron-ion recombination, are gas-temperature dependent. Consequently, the impedance of the discharge is changed. Evidence of this effect also results from the generation of a weak OG signal when iodine molecules are irradiated outside the region in a pure iodine discharge (Rettner *et al.*, 1981; Webster and Menzies, 1983a). A time-resolved investigation showed that the perturbation induced by the laser was primarily a pressure wave traveling at the velocity of sound.

This is the same mechanism that gives rise to the optoacoustic effect. As a matter of fact, an important optoacoustic effect was observed in conjunction with the

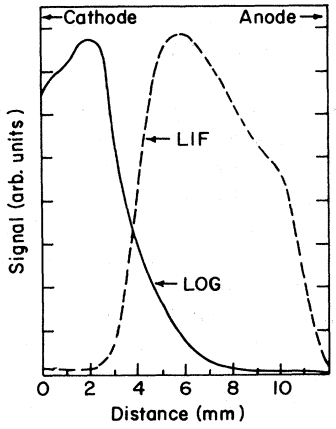

FIG. 11. Spatial dependence of the optogalvanic signal (LOG) and laser-induced fluorescence (LIF) of N_2^+ ion vs the distance from the cathodic surface in a 1.0 torr nitrogen discharge (from Walkup *et al.*, 1983a).

OGE by Hameau *et al.* (1985) in vibrational excitation of CO_2. NH_3, and SF_6. The amplitude of the optoacoustic effect and its temporal evolution give additional information on the mechanism of the OGE.

A detailed quantitative analysis of the OGE in a molecular discharge would require a complete knowledge of the chemistry of the discharge. The experimental results demonstrate that different mechanisms interact in the generation of an OG signal and that their relative weight depends on the specific molecules as well as on the irradiated region of the discharge. A very peculiar case is the detection of molecular ions, described by Walkup *et al.* (1983a, 1983b). In this case, the authors suggest a mechanism in which ion mobility is modified by laser excitation due to the difference between collisional properties of the ions in the ground state and in the excited state. Note that the OG signal was observed only while using laser irradiation within the cathode dark space, which is the only region where positive ions are significant current carriers (Fig. 11).

III. EXPERIMENTAL APPARATUS

In this section we briefly analyze the typical experimental apparatus that has been used to study the OGE. The detection of an OG signal depends both upon the excitation—whether the laser is continuous wave or pulsed—and the lamp—whether it is dc or ac sustained.

A. Light sources

1. Continuous-wave lasers

The basic setup for OG spectroscopy using a cw laser is shown in Fig. 1. The laser beam is amplitude modulated by the chopper before irradiating the discharge. The OG signal is detected through the ballast resistor R_B and analyzed by the lock-in amplifier, whose reference comes from the chopper. A capacitor blocks the high voltage.

The laser beam can be frequency modulated as well (Goldsmith *et al.*, 1979). In this case the output of the lock-in is the derivative of the absorption signal. The technique of frequency modulation of a dye laser is quite sophisticated, so this method has rarely been applied in the visible region. By contrast, this is a very simple technique when a diode laser is used, because frequency can easily be modulated by current modulation (Webster and Menzies, 1983a, 1983b).

The choice of a proper laser source in an experiment is linked to the spectroscopic study required. Experimentalists first used commercial multimode cw lasers to observe the OG effect in both volatile and refractory elements. As soon as the potential of the method for high-resolution spectroscopy was recognized, more sophisticated lasers were employed.

The use of a single-mode laser with active frequency stabilization was introduced by Johnston (1978a, 1978b), and since then similar sources have contributed much to high-resolution spectroscopy through OG detection.

The tunable cw *F*-center laser was introduced by Jackson *et al.* (1980) in infrared OG spectroscopy of transitions induced between highly excited atomic states in helium.

The tunable IR diode laser is expected to be more important in the near future for OG studies of molecular spectra and (with the new short-wavelength diode) for OG studies of atomic spectra.

Optogalvanic detection in the infrared range has been extended by the use of CO_2 and NO_2 lasers (Hameau *et al.*, 1984).

2. Pulsed lasers

Where pulsed lasers are used as the excitation source to observe the OGE, a boxcar integrator typically replaces the lock-in amplifier (Fig. 12). Pulsed dye lasers were successfully used in the visible region mainly to study high-lying levels by two-step excitation (Camus *et al.*, 1979, 1982, 1983a, 1983b; Delsart *et al.*, 1981; Shuker *et al.*, 1981; Aymar *et al.*, 1982; Caesar and Heully, 1983b). Extension of the technique to multistep OG laser spectroscopy was demonstrated by Broglia *et al.* (1983a).

The short pulse duration of some pulsed lasers enables one to study the temporal evolution of the OG signal, an approach first taken by Miron *et al.* (1979) and then by Rosenfeld *et al.* (1979); Shuker *et al.* (1982); Caesar and Heully (1983a); Shuker *et al.* (1983b, 1984); Fujimoto *et al.* (1983); and Broglia *et al.* (1983b).

The use of pulsed lasers can also open the region of the near-ultraviolet to spectroscopic investigation. It has, moreover, enhanced the applicability of the OGE in the study of several processes, such as quasiresonant Penning ionization, electron detachment, and laser-induced

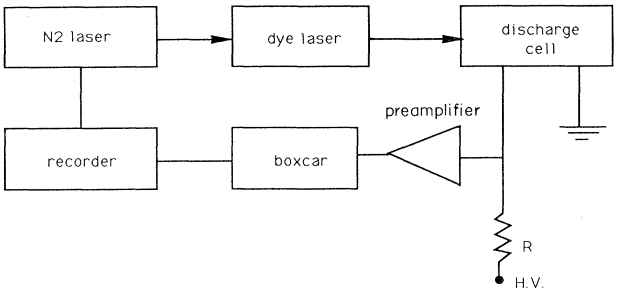

FIG. 12. Schematic diagram of the experimental layout for pulsed optogalvanic spectroscopy.

dipole-dipole pair absorption. These applications are the subject of Sec. V.

So far we have considered changes in the experimental apparatus in connection with sources, either cw or pulsed. In the next section we shall discuss the different discharges used in OG experiments.

B. Cell discharges

A discharge is often a noisy medium, but if some essential operating conditions are fulfilled, the noise can be reduced to the level of shot noise, or statistical fluctuations in the number of charges reaching the electrodes.

The useful working region of the voltage-current plot is a function of the geometry of the discharge, of the pressure of the carrier gas, and of the particular element under study. The pressure range in which the glow is stable is proportional to the inverse of the discharge transversal dimension (or cathode diameter in a hollow-cathode discharge).

Many kinds of glow discharge have been used for OGE detection: He-Ne laser tubes, commercial hollow-cathode discharges, heat-pipe discharges, and even Ne indicator lamps (Nestor, 1982) and mercury vapor germicidal lamps (Bridges, 1978). Specially designed apparatus have been developed for high-resolution spectroscopy.

1. Positive column

The detection of the OGE in noble gases in positive columns does not present any particular difficulty once cleanliness of the discharge tube environment has been assured. In the case of molecular discharges, a continuous flow of gas is usually maintained.

The positive column is more easily modeled than any other region of the glow discharge because of the spatial uniformity of this region. As we have seen in Sec. II.B.1, positive-column models have produced satisfactory explanations of the OGE.

In 1983 Kushner proposed that isotope enrichment of copper ions in positive columns of Cu-Ne discharge should be possible. Previous proposals for isotope enrichment by cataphoresis in hollow-cathode discharges had not been successful. Kushner's proposal is still awaiting realization.

When the vapor pressure of an element being studied is low, a heat-pipe structure permits the observation of the OGE in a positive column. The design is the same as that commonly used in absorption spectroscopy. An example is shown in Fig. 13 (Camus, 1974). Two nickel or stainless-steel hollow electrodes are assembled at the extremities of a ceramic tube by means of aluminum holders, which also provide a cooling system. In the inner part of the ceramic tube a 20-cm-long stainless tube is mounted. The inner walls of this tube are covered by three layers of 100-mesh stainless steel, forming the wick of the heat pipe. The cell is heated over the central part by an electrical oven; a thermocouple provides temperature measurements. The metal vapor is controlled by noble buffer gas at some torr pressure. This apparatus was used for barium Rydberg-state analysis (Camus, Dieulin, and Morillon, 1979; Camus, Dieulin, and El Himdy, 1982, 1983a, 1983b). Similar devices were used by Bridges (1978) and Roesch (1983) for cesium.

2. Commercial hollow-cathode discharges

Commercial hollow-cathode lamps were extensively used for the first OG applications. They are relatively inexpensive (where not yet present in the spectroscopic laboratories) for almost all of the elements of the Periodic Table, and their electrical noise is very low—at the level of shot noise. However, their design can be incompatible with some specific applications. Essentially, the problem is the design of the cathode, which is a cylinder closed at one end. This design does not usually allow propagation in the cathodic region of two counterpropagating beams, a characteristic feature in sub-Doppler saturation techniques (see Sec. IV). Moreover, at the shortest wavelengths, photoelectric emission produced by the laser striking the cathodic surface can give an unwanted background signal.

For these reasons, the need to make hollow cathode tubes with a clear optical path through the cathode was recognized early. On the other hand, since the magnitude, the signal strength, and even the sign of the OG signal can change when different regions in the discharge are irradiated (Zalewski *et al.*, 1979), it would be desirable to work with discharges in which one could probe the different regions independently. In particular, in order to collect spectroscopic data, it would be useful to have available discharge tubes that permitted a probe of the negative glow region because of the interesting features to be found there.

It is not easy to design a discharge geometry that satisfies all of these requirements, offers a sufficient concentration of sputtered refractory elements, and permits one to work in a wide range of currents and buffer gas pressures. We shall describe some hollow-cathode discharges developed for OG spectroscopy applications.

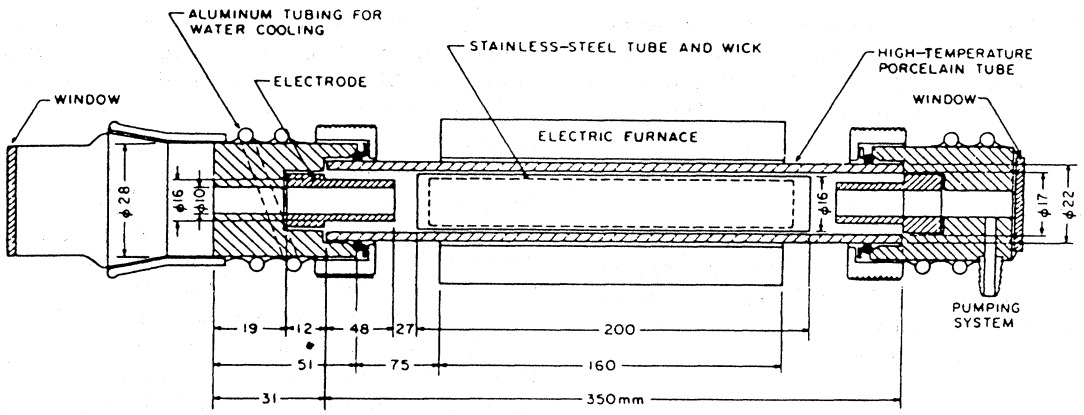

FIG. 13. Cross section of a heat-pipe discharge (from Camus, 1974).

3. Hollow-cathode discharges for high-resolution spectroscopy

A hollow-cathode lamp designed specifically for OG spectroscopy usually provides both a clear optical path through the cathode and a cooling system for the cathode. The need for cooling results from the relatively high current required to obtain active sputtering. The heat generated by ion collisions against the cathode is significant and must be dissipated to avoid instability, collective motion of the gas carrier, and degassing of the cathodic materials, as well as to reduce the Doppler width of the spectral lines.

Feldmann (1979) was the first to introduce a discharge with a clear path through the electrodes. Such a discharge, however, was not devised to obtain Doppler-free spectra, but to perform operations under continuously flowing buffer gas, the aim being OG detection of molecular spectra in the visible part of the spectrum.

Miyazaki *et al.* (1983a, 1983b, 1983c) modified Feldmann's discharge by positioning the hollow cathode between two hollow anodes to ensure that the whole length of the bore was covered with the negative glow. In this design the electrodes were cooled with flowing water.

A similar lamp was used by Behrens and Guthorlein (1983) and Behrens *et al.* (1983) for the investigation of refractory elements.

Lawler *et al.* (1981) developed a hollow-cathode lamp [Fig. 14(a)] to be used for high-resolution spectroscopy. The cathode had a large internal diameter that allowed for operation at low pressure. This assured a minimum perturbation due to the electric field near the center of the hole. The cathode was 50 mm long, with an internal diameter as large as 27 mm. The anode, in the form of a tungsten bar pin, 1.5 mm in diameter, was placed in front of the cathode in order to suppress the positive column. With such a lamp, the discharge operated at a current of about 150 mA without cathode cooling, allowing the recording of a molybdenum homogeneous linewidth of less than 30 MHz. Operation at higher currents is possible, but it quickly produces a deposit of sputtered material on the inside of the glass tube, increasing the probability of arcing.

Another design has been reported by Keller *et al.* (1983), which allowed the use of a small cathode with currents up to 1 A for extended periods of time. In all of these designs, the importance of a very good cleaning of the apparatus was stressed. This can be achieved by degassing in a good vacuum (10^{-5}–10^{-6} torr) and by running the discharge at high currents with high-purity gases for some time.

A very simple design of a hollow-cathode lamp for high-resolution spectroscopy was reported by Barbieri *et al.* (1984). Its main characteristics are simplicity of construction and easy demountability [Fig. 14(b)]. The different components of the lamp were mounted on glass cones. The anode was a tungsten or nickel pin or an aluminum rod. The cathode was inserted into a holder made of copper and fastened to a massive copper rod cooled by flowing water. The cathode was made either of the element to be studied or of a stainless-steel cylinder into which a role of foil of the sample to be studied was inserted. Typical dimensions were 6 to 12 mm in diameter and 16 mm long. The larger cathodes permitted low-pressure operation, while the smallest diameters were used when high current densities were required for an efficient sputtering operation. All of the metallic parts in the discharge tube, excluding the extremity of the cathode holder and the anode tip, were shielded by glass tubes to force the discharge between the anode tip and the inner cathodic region.

An interesting hollow-cathode geometry that prevents selective excitation of either negative glow or cathode dark space and restricts extension of the positive column to a few millimeters was used by Webster and Menzies (1983) in their studies of the infrared OG spectra of molecules. The glass cell was 16 cm long with a 1 cm internal diameter and had cross-connected O-ring joints with quartz windows mounted 5 cm apart for transverse laser

probing of the discharge. A tungsten rod anode and molybdenum hollow cathode were each mounted on sliding O-ring connections, which allowed the region of the discharge probed by the laser to be adjusted. The length of the discharge could be reached in the same way.

4. Radio-frequency and microwave discharges

Discharges sustained by variable fields (radio frequency or microwave) overcome some of the inherent limitations of dc discharges, so that they can be a useful complement to the conventional OG method. The variable fields produce a homogeneous plasma with an electron temperature relatively high compared to that of a dc discharge. Moreover, their ability to run a discharge without the need of internal electrodes is an interesting feature that will certainly increase their importance in future applications. They make possible, for example, the study of corrosive gases that would damage the usual electrode materials. They allow the study of organic compounds, which in dc discharges can cause arcing even at moderate currents, because their tendency to cause carbon deposition on the electrodes. They are also not affected by shot noise, which is the ultimate contribution to the signal-to-noise ratio deterioration in dc discharges. On the other hand, the study of refractory elements is strictly linked to the use of discharges with internal electrodes, from which atoms of interest can be sputtered in the plasma.

Optogalvanic detection of both atomic and molecular gas species in rf discharges has been undertaken by way of three main approaches, all described by Stanciulescu *et al.* (1980b) and later summarized by Camus (1983). These are sketched in Fig. 15. In all of the schemes, the

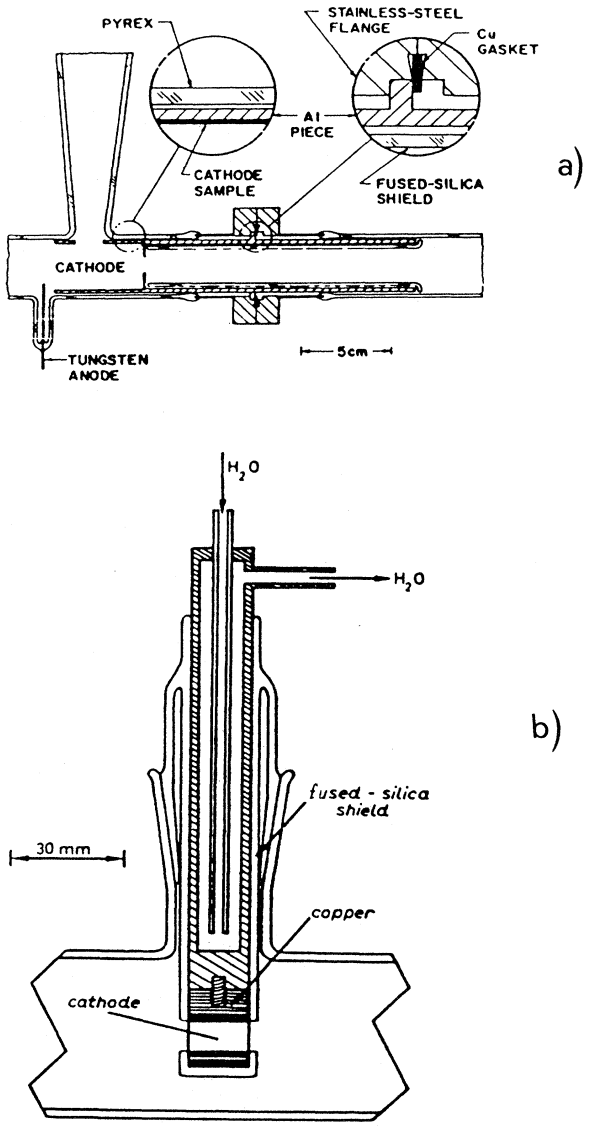

FIG. 14. Hollow-cathode designs for sub-Doppler OG spectroscopy: (a) hollow-cathode discharge tube (from Lawler *et al.*, 1981); (b) cross section of the central part of a simple, water-cooled hollow-cathode lamp (from Barbieri *et al.*, 1984).

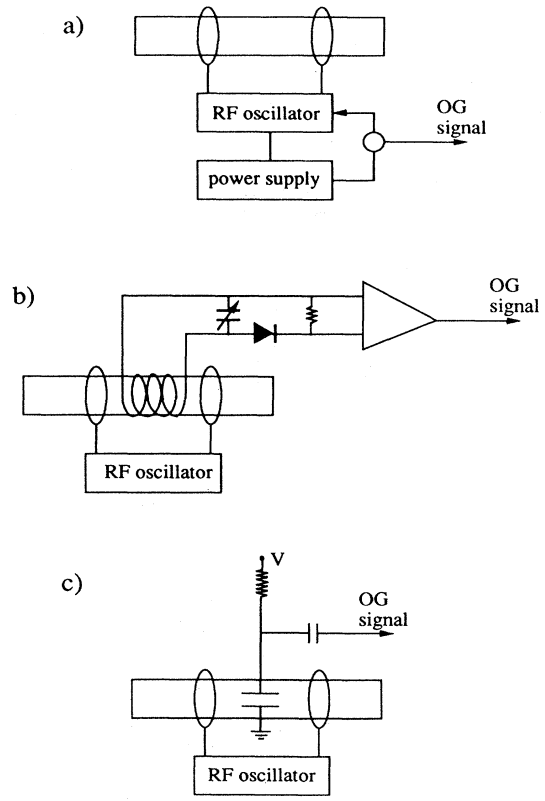

FIG. 15. Different schemes for OG detection based on laser-induced change in the impedence of a rf discharge: (a) The regenerative signal of the rf oscillator is monitored; (b) the OG signal is extracted by a pickup coil would around the discharge cell; (c) two active electrodes are placed inside the cell to monitor current fluctuations.

discharge is sustained by external electrodes coupled to a regenerative oscillator delivering about 100 mW of power, typically in the frequency range 10–50 MHz. They differ from one another in the way that they detect the perturbation in the plasma.

In the first scheme, shown in Fig. 15(a), a laser-induced change in the plasma impedance is monitored through corresponding changes in the regime of the oscillator. Any oscillator adjusts its level of oscillation so that losses are balanced by regenerative amplification. If the losses are slightly increased, the oscillator amplitude is correspondingly decreased, and this produces an observable change in the oscillator's anode current. So, in this rearrangement, the same oscillating circuit represents the detection and the excitation system of the high-frequency discharge.

A detection circuit capacitively coupled to the plasma discharge, instead of inductively coupled, has been suggested by Stanciulescu *et al.* (1980c).

Suzuki (1981) introduced a different scheme for detecting impedance changes in the discharge [Fig. 15(b)]. The OG signal is monitored by a pickup coil wound outside of the cell, so that the discharge plays the part of a transmitting antenna and the coil that of a receiving antenna. An rf field at 13.56 MHz is applied to the discharge tube, which is 40 cm long with diameters between 10 and 30 mm, through two copper-ring electrodes wound to the tube and separated by 5–10 cm. The output power of the rf transmitter is in the range of 4–45 W. The gas is continuously pumped through the discharge at a pressure between 0.01 and 0.4 torr. The pickup coil (10 nH) and a capacitor form a tank circuit, which is adjusted to be resonant with the 13.56 MHz rf field. The signals picked up by the coil are rectified and passed through an amplifier tuned to the modulation frequency of the laser beam. The output is measured with a lock-in amplifier.

The third scheme [Fig. 15(c)], in some ways intermediate between the first two, was applied by Labastie *et al.* (Labastie, Biraben, and Giacobino, 1982; Labastie, Giacobino, and Biraben, 1982). They used an rf discharge to populate excited levels of atoms, but placed two electrodes inside the cell to detect the impedance variation. A voltage V of about 10 volts was applied between the electrodes, and the plasma impedance variation was measured by way of the current variations through an external resistance. This experimental arrangement allowed Labastie *et al.* to operate at very low discharge currents, in order to minimize the shift and the broadening due to the discharge.

Recently Francesconi *et al.* (1990) developed a new approach to impedance spectroscopy. In this technique the physical parameter probed is the dielectric constant of the medium under investigation. The atomic or molecular sample (not necessarily a discharge) is introduced as a component in a radio-frequency resonant circuit by capacitive coupling. A change in the dielectric constant of the sample introduces variations of both the resonant frequency and the merit factor Q of the resonant circuit. The measurement of these changes has been performed by a frequency heterodyne scheme with respect to a stable unperturbed oscillator. This new technique has been applied as a demonstration to dc and rf discharges and to a sample of sodium vapor. In the case of discharges, Francesconi *et al.* observed an improvement in sensitivity by more than one order of magnitude compared with conventional optogalvanic detection.

A similar approach has also been developed by Yan *et al.* (1990). They operated with a neon discharge bulb as a relaxation oscillation. The relaxation oscillation is generated by a simple RC circuit in which the neon lamp is connected in parallel with a capacitor C charged through a resistor R. The relaxation oscillations occur at a frequency determined by the time constant RC. Resonant irradiation causes a change in the electron density perturbing the discharge breakdown and, as a consequence, the relaxation oscillation frequency. A change of a few percent in the oscillation frequency was observed with resonant irradiation of tenths of microwatts for some neon transitions.

A peculiar method for detecting atomic transitions in rf plasmas, very similar to the conventional optogalvanic method but not directly connected with the change in the discharge impedance, was introduced by Brandenberger (1987). He placed inside a Kr rf discharge two electrodes connected to an external passive circuit (Fig. 16). Each electrode, when hit by the metastable Kr atoms, ejected electrons into the discharge. Because the electrodes were placed symmetrically inside the discharge, in the absence of resonant laser radiation no net current flowed in the

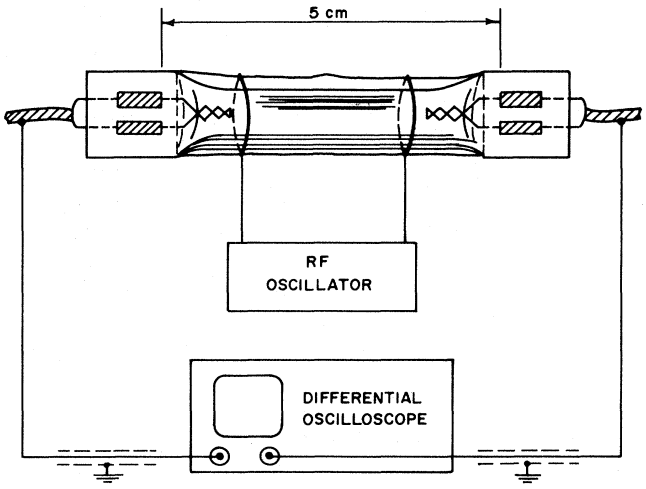

FIG. 16. Optovoltaic detection scheme. The ohmic electrodes at the opposite sides of the cell probe the optovoltaic signal by using a differential oscilloscope (from Brandenberger, 1987).

external circuit. However, when laser radiation resonant with a transition involving a metastable level crossed the discharge in an area around electrode A, the concentration of metastable atoms was then no longer symmetric and a net current flowed from electrode A to electrode B through the external circuit. Brandenberger stressed the difference between this technique and conventional OG detection by calling it "optovoltaic" detection. Suzuki *et al.* (1983) used a similar device in preliminary studies of He_2 transitions detected by the double-probe method. Their discharge was sustained by a microwave field instead of an rf field. The cell was placed in an Evenson-type microwave cavity coupled to a commercial magnetron, with a current-regulating circuit, through a coaxial cable. The microwave power was variable only within a limited range around 20 W. The probes were tungsten wires 0.5 mm in diameter, placed inside the cell. Best performances were obtained with the wires arranged parallel to the cell axis, 5 mm from each other. When the discharge was sustained, a potential difference of several volts appeared across the two probes due to the inhomogeneous electric fields inside the cavity.

These first applications of rf discharges to OG spectroscopy have produced very promising results. It is to be hoped that successful applications of these schemes to the study of unstable molecules, molecular ions, and radicals, easily produced in the plasma of such discharges, will follow.

IV. SPECTROSCOPIC METHODS

A. Linear spectroscopy

The application of the OGE to spectroscopy dates from the availability of tunable lasers. The usefulness of the effect for laser stabilization or wavelength calibration was immediately evident. At the same time, it offered the possibility of other applications—observing spectra from nonvolatile gases in hollow-cathode lamps, for example, or using a single-mode laser to adapt sub-Doppler techniques already developed for saturation spectroscopy.

The main objections to the use of OG spectroscopy were concerned with the problems of performing high-resolution spectroscopy in a discharge. One anticipates a nonlinear response from the plasma with respect to parameters such as the number densities of the species, the electron density, the temperature, and the intensity of the incoming light.

Bachor *et al.* (1982) compared the integrated absorption on a spectral line and the line profile, recorded by OG detection and by conventional absorption spectroscopy on the same dc hollow-cathode discharge. The OG technique is not equivalent to absorption spectroscopy. As Bachor *et al.* pointed out, while OG detection can be usefully applied to wavelength determination of the transition, one should not expect to deduce from the signal intensity an absolute quantitative measurement of oscillator strength. This result is not surprising, considering the complex mechanism of OG signal generation. The oscillator strength is only one of many parameters that affect the relation between the absorbed photons and the variation in discharge current. For comparison, we present in Fig. 17 the spectrum of neon in the range 560–620 nm, observed on the same discharge by different methods (fluorescence spectroscopy, optogalvanic spectroscopy, and optoacoustic spectroscopy). The relative intensities of the lines recorded with the three spectroscopic techniques show dramatic differences.

The OG recorded line profiles are clearly dependent upon the current running the discharge and, especially at high values of current (>100 mA), may be sensitively different from profiles obtained by absorption spectroscopy. These differences can be particularly dramatic in observing transitions starting from metastable levels in noble gases (Kane, 1984), as explained in Sec. II B (Fig. 18).

Engleman *et al.* (1985) studied the effect of saturation on the spectrum profile of hyperfine structure when the individual components were partially overlapped. They compared the Fourier-transform emission spectrum with an OG spectrum of the hyperfine structure of the 22 125

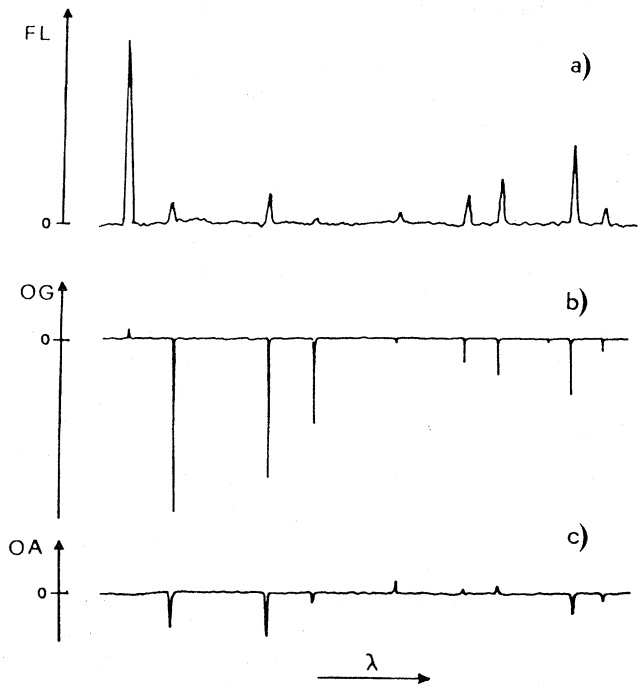

FIG. 17. Neon transitions between 580 and 620 nm, observed on the same discharge with three different techniques: (a) fluorescence spectroscopy; (b) optogalvanic spectroscopy; (c) optoacoustic spectroscopy. Neon pressure was 2.7 torr and the current intensity 3 mA (from Sasso, Ciocca, and Arimondo, 1988).

cm^{-1} $^2D^0_{3/2}-{}^2D_{3/2}$ transition of ^{175}Lu and ^{176}Lu in a commercial Lu hollow-cathode lamp. They obtained a good fit to the hyperfine OG spectrum by introducing a single saturation parameter, and their OG values for hyperfine constants and isotope shifts were of the same order of accuracy as those for the Fourier-transform spectrum case.

To conclude this discussion, we can assert that with a minimum of care OG spectroscopy can give useful information for state assignments of high-lying levels and for measurements of isotope shifts, fine and hyperfine structures, etc., while great care must be taken in the utilization of the data for line shape and linewidth.

Within these limits, many features make OG spectroscopy attractive when compared to other conventional spectroscopic techniques in the ultraviolet, visible, and near-infrared regions of the spectrum. First, it is an economical technique, since it does not require the use of such devices as monochromators or photomultiplier tubes. The direct observation of variations in the discharge parameters can also greatly simplify the detection apparatus: no special designs are needed to collect the fluorescence emission (the detection of the transmitted light is not usually convenient because the medium is optically thin, too) and commercial lamps can be used. A glow discharge is an inexpensive way to obtain quite large densities of excited states in volatile elements, especially in metastable states. Gaseous states of refractory elements are easily produced in hollow-cathode discharges. A remarkable population of atoms in excited levels is present in the discharge due to electron-neutral-atom collisions. In this way transitions between excited levels with different values of total angular momentum J can be recorded. Optogalvanic spectroscopy permits one to record atomic and molecular lines that, otherwise, would be possible only on an atomic or molecular beam. In molecular spectroscopy, OG techniques are the most natural way to investigate atomic and molecular species and radicals available from parent molecular compounds that are present in a discharge.

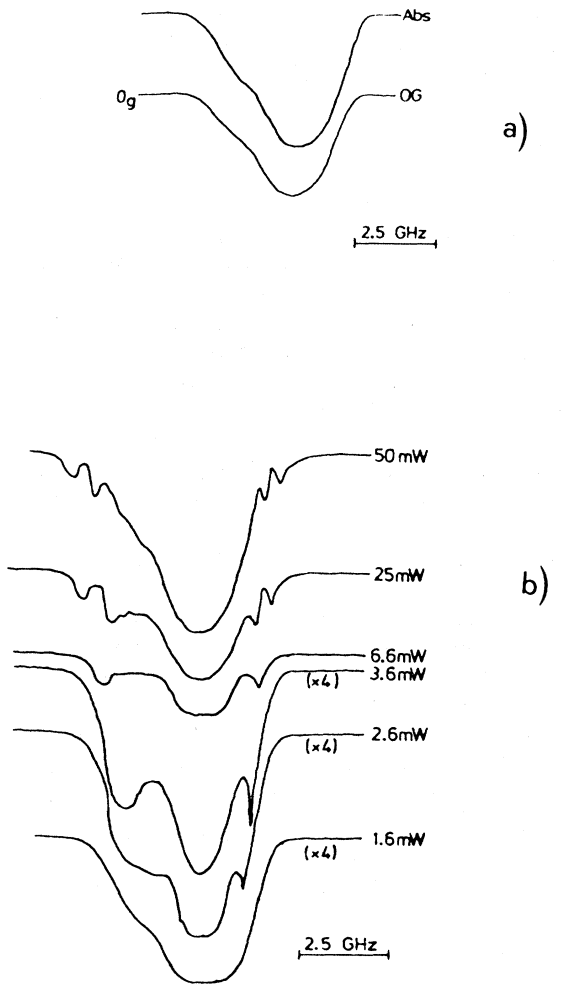

FIG. 18. Line shape of the $1s_5-2p_2$ neon transition at 588.2 nm in a positive-column discharge: (a) saturated absorption and optogalvanic line profile, simultaneously recorded; (b) optogalvanic line profiles as a function of the dye laser power (from Kane, 1983).

Optogalvanic spectroscopy is intrinsically more sensitive than absorption spectroscopy, the former being based upon a signal on a zero background, the latter recording a small variation superimposed on a large signal. When OG spectroscopy is compared to fluorescence techniques, one sees that it offers the advantage of not being affected either by the background signal due to the discharge luminosity or by the scattering of the excitation signal. This is particularly important when the fluorescence must be detected at the same wavelength as the absorbed radiation.

Highly efficient detection and collection of charges produced by radiation are the bases of the high sensitivity of OG spectroscopy. From this point of view, OG spectroscopy may be compared with resonance ionization spectroscopy (RIS), in which, starting from neutral atomic or molecular species, ionizations are induced by resonant multiphoton absorption and the created electron-ion pairs are collected by electrodes.

We shall examine below some applications of OG spectroscopy at moderate resolution (Doppler-limited linewidths) and then consider the high-resolution applications.

Going beyond the many papers that demonstrate the technique and study the discharge mechanism (see Sec. II), we find that to date, the main application of linear OG techniques for original spectroscopic measurement has been the study of highly excited states in atoms or in molecules. Both rf and dc discharges have been utilized; the laser sources were primarily cw or pulsed dye lasers, although color-center lasers, diode lasers, and CO_2 lasers have also been used.

Apart from probes of the Rydberg levels of Xe (which

can be reached directly from the metastable states by cw dye lasers), most other studies utilize the two-step technique in which two different transitions are excited in sequence by two laser beams. It has been demonstrated that this provides greater amplification of the signal than does the single-photon technique for transitions starting from the intermediate level (Shuker *et al.*, 1981). In complex atoms, such as uranium, a three-step excitation can be useful (Broglia *et al.*, 1983a).

The amplification of the signal in two-step and three-step techniques can be used to identify the intermediate level in a complex spectrum. This opportunity is completely developed in the intermodulated double-resonance technique, suggested by Vidal (1980). Here the two laser beams are separately amplitude modulated at two different frequencies f_1 and f_2, and the signal at the sum or difference modulation frequency is detected by the lock-in amplifier. The result is that only atoms interacting with both laser beams give a signal without the background of single-photon absorption. This method is particularly useful for identifying lines embedded in dense and complex molecular spectra (Fig. 19). The theory of the double-resonance technique is detailed in Miyazaki *et al.* (1983b).

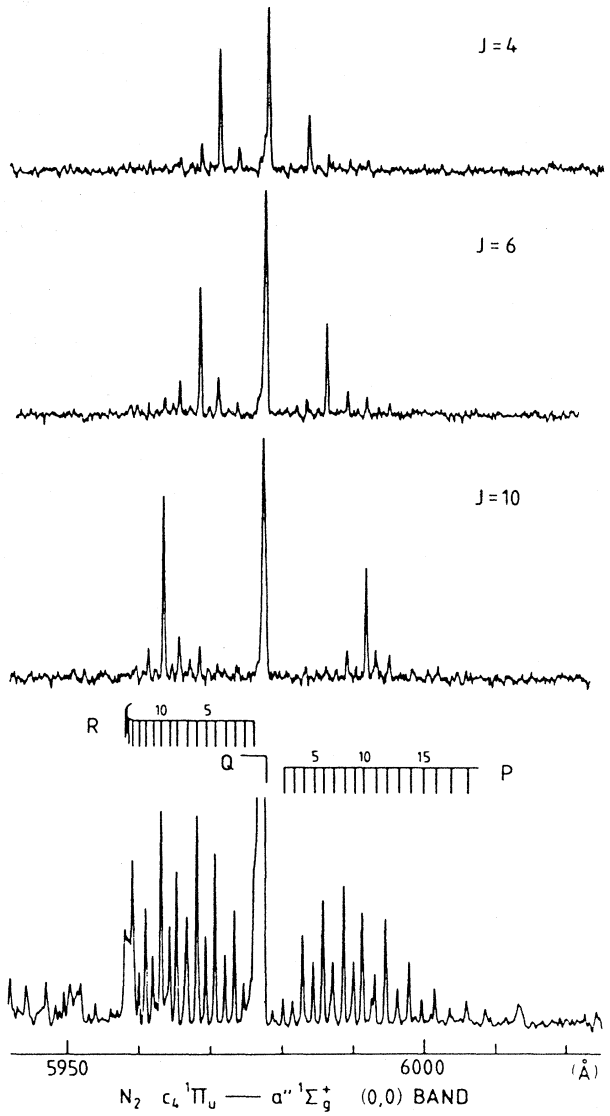

FIG. 19. Optogalvanic single-resonance spectrum (lowest spectrum) and examples of the OG double-resonance spectra (upper three spectra) for the (0,0) band of the $c_4\,{}^1\Pi_u - a''\,{}^1\Sigma_g^+$ system of N_2 (from Miyazaki *et al.*, 1983a).

An experimental apparatus that permits similar observation of the two-step signal without single-photon background in the case of pulsed laser excitation has been presented by Wakata *et al.* (1981). They made an electronic comparison of the OG signals in the presence and in the absence of one of the two lasers, thereby extracting a signal proportional to the relative enhancement, which they called an alternated enhanced double-resonance optogalvanic signal (AEDROGS).

B. High-resolution spectroscopy techniques

As our understanding of atomic and molecular structure improves, the resolution imposed by the linewidth of the recorded resonances becomes more important.

Let us consider an atom in a low-pressure environment ($p \sim 1$ torr). For transition occurring in the visible part of the spectrum, the Doppler broadening contributes 100 times more to the linewidth than broadening due to the finite lifetime of the levels; collisions with atoms, ions, electrons; and perturbations of the electromagnetic field. Purging the linewidth of the Doppler contribution to the broadening has become one of the main problems that spectroscopy is called upon to solve. With the advent of lasers, several techniques have been developed to eliminate Doppler broadening. They can be grouped in three classes: saturation spectroscopy techniques; two-photon spectroscopy; and trapped-particle spectroscopy. To date, only the first two classes of techniques have been combined with OG detection.

The different methods developed for sub-Doppler spectroscopy can also be applied using the OG technique. The OG signal is actually proportional to the absorption of radiation by the atoms of the discharge, so that the same saturation methods used for other detection techniques, such as optoacoustic or fluorescence spectroscopy, can be used.

1. Intermodulation optogalvanic spectroscopy

In 1978, Johnston made the first sub-Doppler observation with OG detection. A He-Ne discharge was irradiated by a dye laser, and the transmitted beam was reflected by a mirror back into the discharge. The profile

of the line, recorded by tuning the dye laser frequency, displayed the characteristic Lamb dip at the center of the resonance due to the saturation effect for atoms with a zero-velocity component along the light direction. In order to avoid this background, it is necessary to develop a technique that is sensitive only to the saturated signal due to the atoms absorbing photons from both beams; that is, the signal to be observed must arise directly from the nonlinear mechanism.

This effect can be obtained using the intermodulation technique. This sub-Doppler technique, first introduced by Sorem and Schawlow (1972) for fluorescence spectroscopy, was applied by Lawler *et al.* (1979a) to OG spectroscopy. The laser beam is split into two beams of about the same intensity (Fig. 20), which are mechanically chopped at two different frequencies f_1 and f_2 and sent through the discharge in opposite directions. In this way they interact with atoms whose velocity component along the direction of propagation is zero. Because of the nonlinearity of the absorption under saturated conditions, signals at the frequency (f_1-f_2) and (f_1+f_2) can be detected when the same atoms interact with both beams. The intensity of the intermodulated signal can be calculated easily (Lawler *et al.*, 1979a) using a two-level model in the Doppler-broadened weak-saturation limit. The change in the density of atoms in the upper and lower levels at the line center, modulated at the sum frequency (f_1+f_2), can be calculated as

$$\Delta n_u=\Delta n_l=(n_u-n_l)(\Delta\nu_H/\Delta\nu_D)I_1I_2/8I_S\ , \qquad (23)$$

where n_u and n_l are the densities of atoms in the upper and lower levels, respectively; $\Delta\nu_H$ and $\Delta\nu_D$ are the homogeneous and inhomogeneous widths; I_1 and I_2 are the counterpropagating beam intensities; and I_S is the saturation intensity.

Intermodulated optogalvanic spectroscopy (IMOGS) was first applied by Lawler *et al.* (1979a) to the study of hyperfine splitting in ^{3}He. Since then it has been applied to the detection of lines in both volatile and refractory elements. The elimination of Doppler broadening allowed isotope shifts to be recorded in Ne I (Jackson *et al.*, 1981; Lyons *et al.*, 1981; Belfrage *et al.*, 1983b; Inguscio, 1983), in Mo I (Siegel *et al.*, 1981; Belfrage *et al.*, 1983b), in Sr I and Sr II (Lorenzen and Niemax, 1982); in O I (Ernst, Minutolo, *et al.*, 1989), and in Ar (Murnick *et al.*, 1986; Moscatelli *et al.*, 1988). Behrens and Guthorlein (1983) determined hyperfine coupling constants and isotope shifts for some Yb I, Eu I, and Eu II transitions and recorded Doppler-free hyperfine structures of Mn I, Ca I, and La I; Barbieri *et al.* (1984) reported hyperfine structure of the transition at 591.5 nm in ^{235}U I. Transitions between highly excited states of the oxygen atom (Fig. 21), populated through the dissociation of O_2 molecules in the discharge, were observed by Inguscio *et al.* (1988). Zeeman Doppler-free OG spectroscopy by IMOGS has been carried out by Beverini, Galli, *et al.* (1982) in a study of transitions of Ne I and Ca I. IMOGS spectra were extended from the visible to the infrared by Jackson *et al.* (1981) studying highly excited states in He.

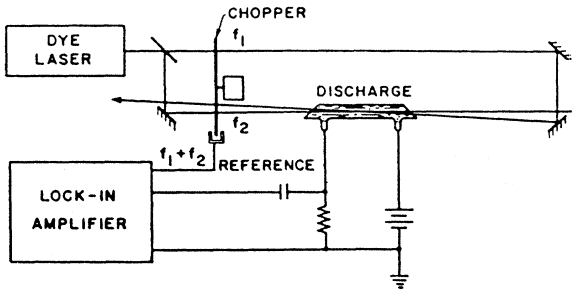

FIG. 20. Experimental apparatus for intermodulated optogalvanic spectroscopy. the two counterpropagating beams are chopped at two different frequencies f_1 and f_2, while the signal is synchronously detected at a frequency f_1+f_2 (from Lawler *et al.*, 1979a).

A characteristic of this method is the appearance of a crossover signal when two lines with a common level fall inside one Doppler width. In this case some atoms have a velocity component in the beam direction such that they are in resonance with photons from both of the beams because of an opposite Doppler shift.

The IMOGS spectra usually display a narrow homogeneous profile superimposed on a large Gaussian pedestal of a width corresponding to the Doppler linewidth, as first outlined by Gerstenberger *et al.* (1979). This effect is due to elastic velocity-changing collisions. A saturation signal can arise if an atom with a velocity component in the light direction v, and resonant with one radiation beam at a frequency $\Omega+kv$, is changed by an elastic collision to $-v$, and is then resonant with the other beam (Letokhov and Chebotayev, 1977). The relative weight of the collision mixing on the homogeneous signal is clearly a function of the effective lifetime of the levels, so that the effect is particularly evident in transitions starting from ground state or metastable levels (Fig. 22). Moreover, the crossover signal is affected by the velocity-changing collisions. This phenomenon has been studied both experimentally (Bréchignac *et al.*, 1977, 1978; Tenenbaum *et al.*, 1983; Gough and Hannaford, 1985; Sasso, Tino, *et al.*, 1988) and theoretically (Smith and Hänsch, 1971; Kolchenko *et al.*, 1973; Berman, 1976, 1978).

Velocity-changing collisions can be described by a model that distinguishes between two possible regimes of elastic collisions according to the value of the mean change of the velocity component $\langle\Delta v_c\rangle_z$ in one collision. If $k\langle\Delta v_c\rangle_z\geq\Delta\nu_D$, a single collision completely thermalizes the atomic velocity distribution (a "strong collision"). By contrast, if $k\langle\Delta v_c\rangle_z<\Delta\nu_D$, which can occur when a heavy active atom is perturbed by a light buffer gas, the off-resonance signal is due to multiple collision effects.

In the case of "strong" collisions, the line shape of the

saturated signal has been calculated by Smith and Hänsch (1971) as

$$S = A\left[\frac{\Delta\nu_H^2}{\Delta\nu_H^2/4+(\nu-\nu_0)^2}+C\exp\left[-\frac{2(\nu-\nu_0)}{0.6\Delta\nu_D}\right]^2\right], \tag{24}$$

where A is a normalization constant. The parameter C represents the relative weight of the collisional background with respect to the narrower homogeneous peak and is a function of the collisional and radiative cross sections. When the effective lifetime of the lower level is much longer than that of the upper, it can be expressed as

$$C = 2(\pi \ln 2)^{1/2}\Gamma_a \Delta\nu_H/\gamma_a\Delta\nu_\Delta), \tag{25}$$

where Γ_a is the cross-relaxation rate of the lower level $|a\rangle$ and γ_a takes into account all the decay channels of the transition.

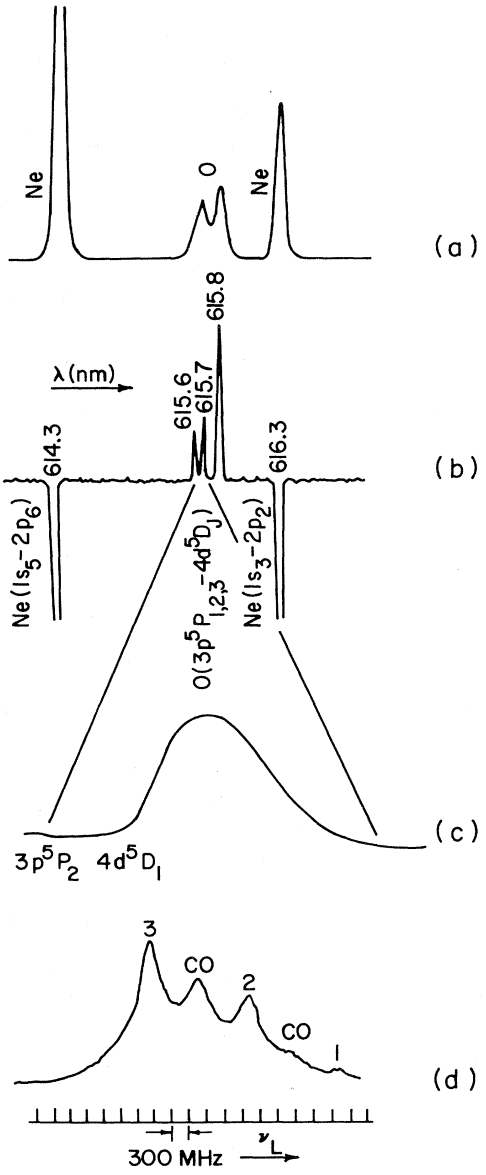

FIG. 21. Spectrum of an O_2-Ne discharge around 616 nm: (a) fluorescence spectrum recorded through a grating monochromator with 0.1 nm resolution; (b) OG signal obtained by frequency scanning a multimode dye laser; (c) Doppler-limited line profile; (d) IMOGS Doppler-free registration of the O $^5P_2-^5D_{3,2,1}$ transitions.

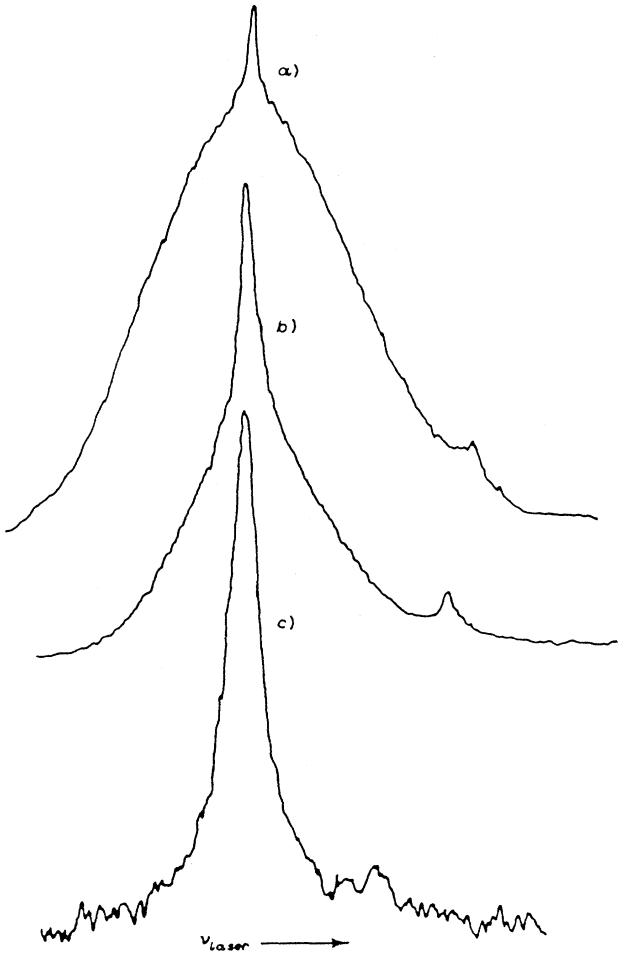

FIG. 22. Intermodulated optogalvanic signal in a hollow-cathode discharge containing natural-abundance neon. Three different transitions are recorded: (a) $1s_2-2p_3$ at 616.3 nm; (b) $1s_4-2p_3$ at 617.4 nm; (c) $2p_4-4s'_1{}''$ at 590.2 nm. The change in the line shape is caused by the different effective lifetimes of the lower (longer) level of each transition; (a) $\sim 10^{-4}$ s, (b) $\sim 10^{-5}$ s, (c) $\sim 10^{-6}$ s (from Sasso, Tino, *et al.*, 1988).

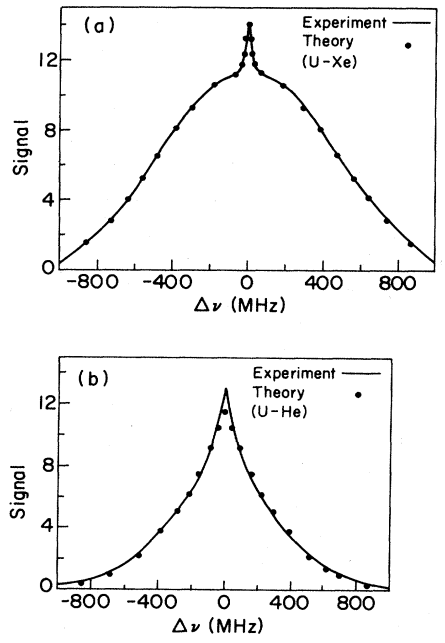

FIG. 23. Saturated absorption signal profile for the (a) U-Xe and (b) U-He systems, demonstrating the different regimes of the velocity-changing collision. Buffer gas pressure was 2.5 torr in both cases (after Tenenbaum *et al.*, 1983).

The model has been refined by Bréchignac *et al.* (1977), who include additional terms in Eq. (24) that take into account the different collisional partners in the discharge of the active atom.

The "weak" collision regime occurs only in extreme cases in which there is a very large ratio between the mass of the active atom and the perturber, like that of uranium in helium. Tenenbaum *et al.* (1983) developed a model, based on Fokker-Planck diffusion equations, to fit the experimental results. The observed line shape was qualitatively different from the "strong" collision case, resulting in an exponential function superimposed on a Gaussian profile (Fig. 23).

The study of the physics of velocity-changing collisions can be of interest both in the search for optimum experimental conditions for sub-Doppler resolution and in useful information about collisional processes.

2. Polarization intermodulation excitation spectroscopy

Hänsch and co-workers have demonstrated that the intermodulated technique can be improved by modulating the polarization, instead of the amplitude, of the two counterpropagating beams. This method is referred to as polarization intermodulation excitation (POLINEX). When the laser is tuned within the homogeneous width, the total rate of excitation will still be modulated at the sum or difference frequency, because the combined absorption of the two beams will, in general, depend on their relative polarization. When the two beams have the same polarization, they will be preferentially absorbed by atoms of the same orientation with a resultant increase in saturation; when the polarizations are different, the two beams will tend to interact with atoms of different orientation, and there will be less total saturation.

One important way in which POLINEX spectroscopy differs from intermodulated spectroscopy is that a signal beam cannot produce a modulated signal because the total rate of absorption in an isotropic medium does not depend on the sign or direction of the light polarization. As a consequence, any modulation of the excitation rate gives a nonlinear signal, and good selectivity for the Doppler-free signal can be maintained even when one polarization modulation is removed. The fact that the cross section for disorientation of atoms is usually of the same order as, or greater than, the velocity-changing collisions also eliminates the broad pedestal present in intermodulated spectroscopy.

Another advantage of POLINEX over intermodulated spectroscopy is that the crossover signal is frequently of opposite sign, so that it can easily be distinguished in complicated spectra. It must be noted that if an amplitude modulation is present together with the polarization modulation, a spurious signal is produced.

The theory of POLINEX spectroscopy has been presented by Hänsch and Toschek (1970) in a density-matrix formalism and by Teets *et al.* (1977) in a simpler rate equation approach. The amplitude of the POLINEX signal for a transition between two levels of angular momentum J and J' can easily be calculated from the Clebsch-Gordon coefficients. In cases of low saturation, this leads to an analytical equation given by

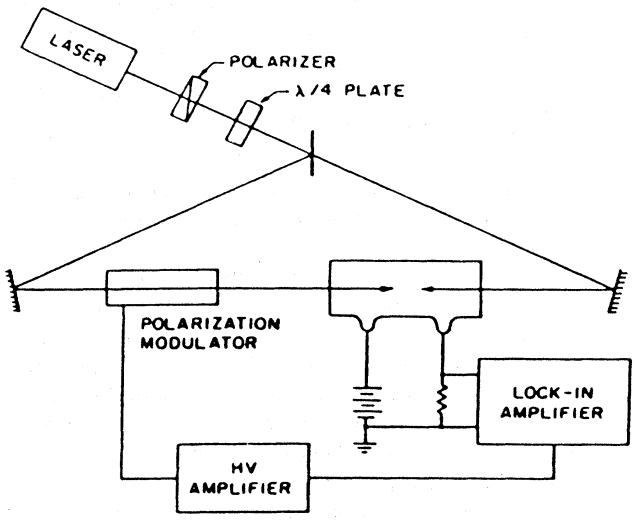

FIG. 24. Experimental setup for Doppler-free POLINEX spectroscopy (from Hänsch *et al.*, 1981).

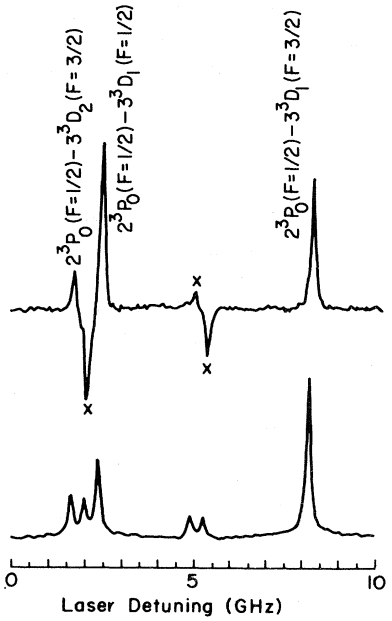

FIG. 25. POLINEX optogalvanic spectroscopy compared with IMOGS. Upper part: a section of the hyperfine spectrum of the 2^3P-3^3D line of ^{3}He. Lower part: the same spectrum recorded by the intermodulated technique (from Hänsch *et al.*, 1981).

Hänsch *et al.* (1981) that can be used for both linear and circular polarized beams.

POLINEX with OG detection was first demonstrated on a He transition (Dabkiewicz *et al.*, 1981; Hänsch *et al.*, 1981) and subsequently used to detect transitions of Ne (Lyons *et al.*, 1981; Julien and Pinard, 1982; Belfrage *et al.*, 1983a, 1983b; Pinard and Julien, 1983).

An experimental setup for Doppler-free POLINEX spectroscopy is shown in Fig. 24. In Fig. 25 a typical POLINEX spectrum is shown.

3. Other saturation techniques: beam-overlap modulation and Doppler-free double-resonance spectroscopy

Another method of obtaining sub-Doppler spectra was recently suggested by Duffey *et al.*, 1985. Instead of modulating the intensity or the polarization of the two opposite laser beams at different frequencies and detecting the intermodulated signal, they modulated the degree of overlap between the beams. One of the two beams was reflected by a high-frequency vibrating mirror, which provided the overlap modulation. In this scheme the Doppler background was suppressed without the need for an intermodulation technique. The advantage of the method consists in a simplification of the apparatus and the ability to use the full laser power.

Doppler-free optical double-resonance spectroscopy can be performed essentially in two ways. The first method, already mentioned in Sec. IV.A.3, was proposed by Vidal (1980) as a state-selective technique. Two counterpropagating laser beams are intensity modulated at different frequencies f_1 and f_2 and directed collinearly through the discharge. Laser beam 1 is fixed on the transition ω_{12}, and the signal is detected at the frequency (f_1+f_2) scanning the wavelength of lasers beam 2 over the Doppler profile of the transition ω_{13}. A homogeneously broadened signal appears on a large background due to velocity-changing collisions. Inguscio (1983) reported the first such measurement on Ne transitions.

The second method comes directly from the optical-optical double resonance. In this case, laser beam 2 is fixed on the transition ω_{23} and modulated at frequency f_2. The transmitted intensity of the unmodulated laser beam 1, tuned over the Doppler profile of transition ω_{12}, is detected at frequency f_2.

The first OG experiment using this method was carried out by Behrens *et al.* (1983) on Ga I and In I transitions. Once again they recorded Doppler-free signals on a large Doppler pedestal. Both of these techniques are expected to be used successfully in clarifying collisional roles in energy transfer inside the plasma.

4. Two-photon optogalvanic spectroscopy

Doppler-free two-photon spectroscopy is based on an entirely different principle from saturation spectroscopy for the elimination of Doppler broadening. It is well known that two-photon spectroscopy gives a sub-Doppler resolution if the atoms can absorb two photons from two laser beams propagating in opposite directions. In effect, the Doppler shift on the first photon, due to atomic motion, is exactly compensated by the second one. Two-photon transitions have low probabilities, being proportional to the square of the intensity, so that usually it is necessary to have quite a strong radiation power, unless a quasiresonant intermediate state is present to increase the transition probability.

The first experiments with two-photon OG spectroscopy (Goldsmith *et al.*, 1979) were performed by placing the discharge cell in the dye laser cavity. Goldsmith and his co-workers observed some transitions starting from the $3s$ levels of neon with a power of the order of 20 kW/cm^2 in the waist.

Another method is to use a pulsed laser, as did Goldsmith and Smith (1980) for the transition 2^3S-5^3D of ^{4}He. They were able to observe the 284 MHz $(J=2)$-$(J=1)$ fine-structure splitting of the 5^3D state.

5. Level-crossing spectroscopy and the nonlinear Hanle effect

It is known from classical spectroscopy that one can obtain sub-Doppler information on levels connected by an optical transition by observing the evolution of the

coherent states generated by suitable polarized radiation as a function of an applied static magnetic (or electric) field. This evolution shows up as a variation of the fluorescence polarization, when the applied field is swept across zero (Hanle effect) or a crossing value of the Zeeman levels (level crossing).

Such an effect cannot be observed by OG detection, which is sensitive to the absorption. However, when the power density of the radiation is high enough so that it must be taken into account for saturation, then the absorption coefficient may also experience variations as a function of the applied field. In order to understand the physics of this phenomenon, let us consider the simplest case, a $(J=0)$-$(J=1)$ transition. An atomic sample is placed in a static magnetic field and interacts with a monochromatic resonance radiation linearly polarized orthogonally to the field (σ polarization). When the magnetic field is not present, an atom can be excited by the σ photon to a coherent superposition of the $M=+1$ and $M=-1$ sublevels; however, when the Zeeman splitting is greater than the homogeneous width of the transition, a single atom can see only the σ^+ or the σ^- component of the incident radiation. As a consequence, the whole power is effective on a single atom in the case of zero field, while only half power is effective in the case of resolved levels: in the first case the saturation is twice that experienced by an atom in the second case. The absorption k on a Doppler-broadened line is given, in the presence of saturation, by the equation

$$k=k_0/(1+S)^{1/2}\,, \tag{26}$$

where k_0 is the unsaturated absorption coefficient and S the saturation parameter. The ratio R between the absorption coefficient in the two cases is then

$$R(S)=[(1+S)/(1+2S)]^{1/2}\,. \tag{27}$$

For $S\gg 1$, the absorption is enhanced by a factor of $\sqrt{2}$.

The case of different $J\rightarrow J'$ transitions is more complex, but it can be treated similarly. The value of the enhancement $R(J,J')$ of the absorption coefficient between the extreme cases of completely degenerate and completely resolved Zeeman sublevels has been calculated as a function of the saturation value by Beverini *et al.* (1985) in a simple rate equation formalism, which well describes the typical situation of an OG experiment (Fig. 26).

A theory intended to evaluate the profile of the effect at intermediate field strength requires the explicit calculation of the atomic matrix density evolution. Feld *et al.* (1974) derived a formal equation for the absorption coefficient for the $0\rightarrow 1$ transition for low saturation values by a perturbation calculation. Their solution is, however, quite involved and is difficult to compare directly with experimental data.

The observation of the nonlinear Hanle effect (NLHE) in an optoacoustic cell (Inguscio *et al.*, 1980; Strumia *et al.*, 1981; Inguscio *et al.*, 1982) suggested that the OG technique might be used for detecting the NLHE and

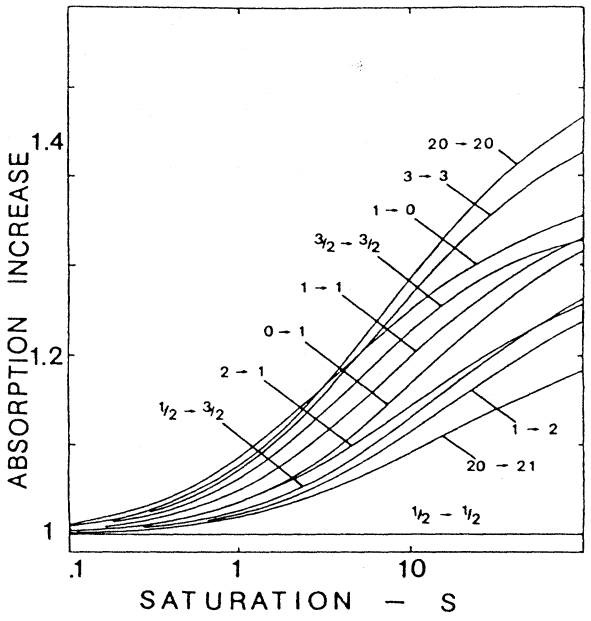

FIG. 26. Enhancement of the optogalvanic signal as a function of the saturation value for different $J\rightarrow J'$ transitions (from Beverini *et al.*, 1985).

stimulated level crossing (Beverini and Inguscio, 1980). Experimental results were presented by Hannaford and Series (1981a, 1981b), by Barbieri *et al.* (1983), and by Beverini *et al.* (1985) on different transitions of Zr I, Ca I, Ar I, and Ne I (Fig. 27) in hollow-cathode discharges. The width of the observed NLHE can give useful information about collisional broadening (phase-changing col-

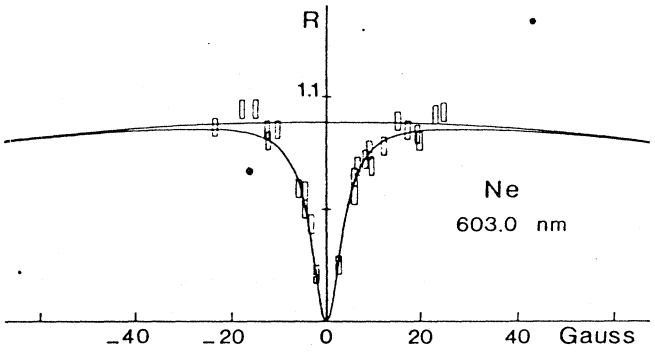

FIG. 27. Optogalvanic detection of the nonlinear Hanle effect for the $J:1\rightarrow 1$ transition at 603 nm in Ne. The width of the effect is comparable in upper and lower levels of the optical transition, and the experimental points can be fitted to the difference of a single Lorentzian and a Gaussian line shape. Gas pressure was 1.07 torr, discharge current was 65 mA, and laser power was 80 mW (from Beverini *et al.*, 1985).

lisions) at very low pressure (of the order of 1 torr), for which it is very difficult to obtain significant measurements by other methods (Beverini *et al.*, 1985).

It must be observed that the NLHE is directly related to removal of the degeneracy between Zeeman sublevels of the level connected by the optical transition and not to removal of the degeneracy between Zeeman components of the transition itself. This means that in general the profile of the NLHE appears as a superposition of two curves corresponding to removal of degeneracy from the upper and the lower states. If the lower level is the ground state or a metastable state, the width of the curve corresponding to this level can be very narrow, and may be narrower than the natural width of the transition (Fig. 28).

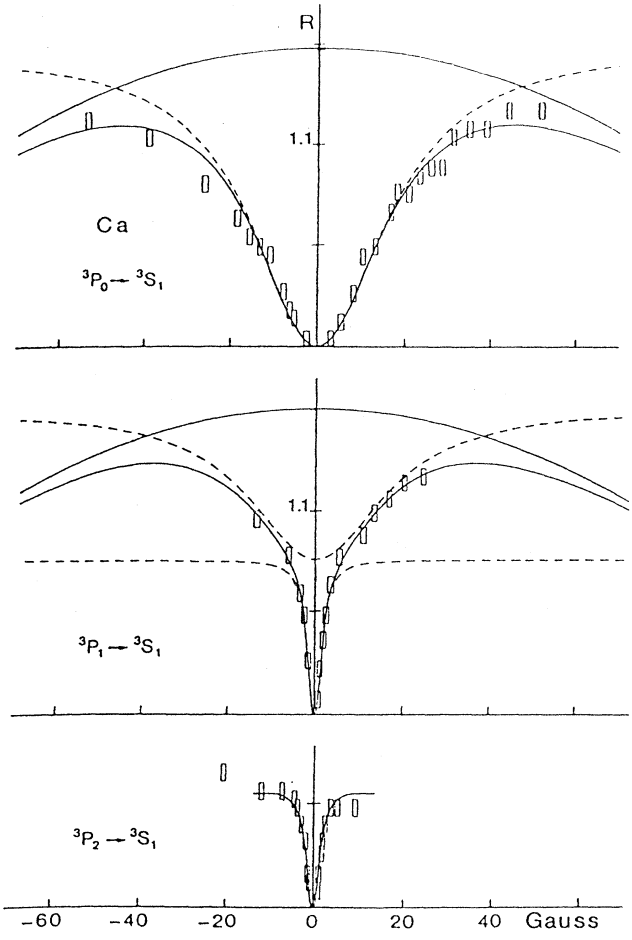

FIG. 28. Optogalvanic nonlinear Hanle effect recorded using a hollow-cathode lamp for the 610.2, 612.2, and 616.2 nm Ca transitions starting from the metastable $^3P_{0,1,2}$ triplet. For the $^3P_0 - {}^3S_1$ transition, the experimental points can be well fitted (eliminating the Doppler contribution) by a Lorentzian curve of width $\gamma = 100$ MHz, comparable with the linewidth measured by means of the intermodulated technique (130 MHz). For the $^3P_1 - {}^3S_1$, the profile can be fitted by the superposition of two Lorentzian curves of the same amplitude, the larger with a width $\gamma = 100$ MHz and the narrower with a width corresponding to about 6 MHz, due to the removal of degeneration in the lower metastable levels. The same narrow structure, of the order of 7 MHz, can be observed for the $^3P_2 - {}^3S_1$ transition. This width is smaller than the natural linewidth of the transition (10 MHz). From Barbieri *et al.* (1983).

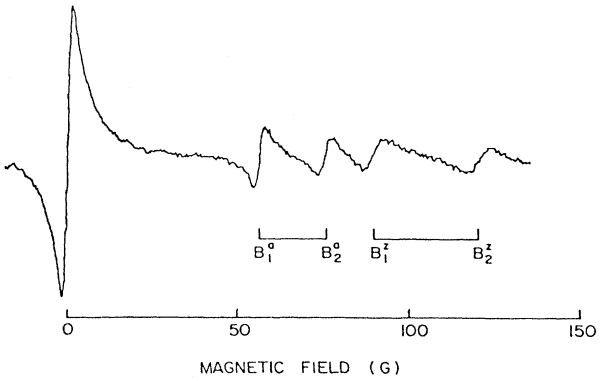

FIG. 29. Stimulated level-crossing resonances for the 619.2 nm ($a^2D_{3/2} - z^2D_{3/2}$) transition in Y I detected by the optogalvanic technique in a hollow-cathode discharge (from Hannaford *et al.*, 1983a).

Extension of the technique to nonzero-field level crossing (Hannaford and Series, 1981a, 1982a; Hannaford *et al.*, 1983a, 1983b) makes possible the measurement of the hyperfine structure of refractory elements present in hollow-cathode discharges (Fig. 29). Moreover, the stimulated level crossing, which is different from the classical one, is sensitive to the level crossing occurring both in the upper and in the lower level of the transition, thereby extending the possible applications.

The NHLE, combined with the use of a multimode laser, provides a further tool for measuring the atomic g_J factor. The method is based on a "mode crossing" effect occurring when the Zeeman splitting in the upper or in the lower level is equal to the laser mode separation. This technique has been applied to the measurement of the Landé factor of several levels of Zr (Hannaford and Series, 1982b).

C. Advantages and limits of optogalvanic spectroscopy

In Sec. IV.A some useful properties of the OG technique were outlined: OG spectroscopy is less expensive and involves the use of fewer electronics than the usual optical detection techniques. With regard to the signal-to-noise ratio, the current noise in a discharge can be reduced practically to the shot noise—that is, the statisti-

cal fluctuation of the number of charged particles—when the discharge is driven in the correct regime. In this condition the rms noise current $(I_N)_{\rm RMS}$ is given by

$$(I_N)_{\rm RMS}=(2eI\Delta\nu)^{1/2}\ , \tag{28}$$

where I is the current in the discharge and $\Delta\nu$ is the detection bandwidth. With typical current in a hollow cathode of 30 mA, this formula gives $I_N\sim 1$ nA in a bandwidth of 1 Hz.

Keller *et al.* (1980) discussed the signal-to-noise ratio from experimental data for typical transitions in a uranium hollow-cathode lamp. They estimated from the observed OG signal that the detection limit for uranium atom concentration, with 1 watt laser radiation power, was of the order of 10^6 atoms/cm^3, while the metastable $^3P_2$ state of Ne yielded a detection limit of about 3×10^2 atoms/cm^3. These considerations show the usefulness of the OG technique in many applications, such as laser wavelength calibration, detection of small impurities, etc., which are the subject of the following section.

One possible disadvantage that should be noted is that the useful regime of a discharge is limited to a narrow range of discharge parameters and that these conditions are particularly delicate when the current is increased (as is necessary for efficient sputtering in hollow-cathode lamps). It might be difficult, for instance, to perform measurements at significantly different pressure values in order to determine the pressure dependence.

In the case of sub-Doppler techniques, Belfrage *et al.* (1983b) have compared intermodulated fluorescence spectroscopy, polarization fluorescence spectroscopy, and the corresponding OG technique. The polarization technique demonstrated a larger signal-to-noise ratio, while the intermodulated technique was affected by a large pedestal due to elastic velocity-changing collisions (see Sec. IV.B.1).

In general, it can be demonstrated that the OG techniques perform almost the same as traditional optical techniques, with the real advantage of inherent simplicity. However, they cannot offer the maximum signal-to-noise ratio in detecting spectra. Hollberg *et al.* (1983) showed that, with highly sophisticated FM spectroscopy, the signal-to-noise ratio in the recording of a sub-Doppler spectrum of an erbium hollow-cathode discharge could be enhanced by a factor of greater than 1000 over the best OG results. The price paid for the best performance is the use of much more electronics.

V. APPLICATIONS

A. Spectrum analysis

1. Rydberg states

The optogalvanic technique has been extensively applied to the study of Rydberg states. These can be reached by exciting radiative transitions starting from metastable levels, which are well populated in the discharge. This is particularly true for the noble gases or for alkaline-earth atoms. An analysis of the $np\,^1S$ ($n=14$–36) in He was performed by Katayama *et al.* (1979) using an ultraviolet pulsed dye laser. Delsart *et al.* (1981) observed some Rydberg levels of Kr with an accuracy of 0.03 cm^{-1} using a two-step technique and a pulsed dye laser. The Rydberg spectrum and some autoionizing states of Xe, which can be reached from the metastable states with the absorption of a single photon in the visible region, were measured with greater accuracy (10^{-3} cm^{-1}) using a cw dye laser in an rf discharge by Grandin and Husson (1981); Labastie *et al.* (Labastie, Biraben, and Giacobino, 1982; Labastie, Giacobino, and Biraben, 1982); and Lemoigne *et al.* (1983, 1984). Camus *et al.* (1979, 1982, 1983a, 1983b) applied the technique to Ba in a heat-pipe discharge with a two-step excitation, obtaining a long list of new observed and assigned levels. Begemann and Saykally (1982) obtained the infrared spectrum of Ar and Ne between 3600 and 4100 cm^{-1} using a color-center laser. The application of the intermodulated sub-Doppler technique allowed Lorenzen and Niemax (1982) to determine isotopic shifts of some transitions starting from the metastable levels.

Doppler-free two-photon spectroscopy has been utilized by Beigang and Timmerman (1983) to investigate isotope shifts and hyperfine structures of *msns* and *msnd* Rydberg series of alkaline-earth elements for n values up to 150.

The optogalvanic technique is very efficient for the investigation of autoionizing levels. Caeser and Heully (1983b) have studied the $3p'$-ns',nd' series of Ne in a hollow-cathode discharge. Wada *et al.* (1986, 1987) have explored the Kr autoionizing transition in the region between 16 700 and 17 250 cm^{-1}.

2. Complex atoms

In the programs for laser-induced isotope separation, optogalvanic spectroscopy has been extensively used in conjunction with beam spectroscopy as a quick way to investigate transitions between highly excited levels of uranium. Beam spectroscopy is more accurate, but the technology is more complex because of the high temperature required for the oven and the high reactivity of uranium. Palmer *et al.* (1981) published a wavemeter measurement of spectral lines, while Broglia *et al.* (1983a) used a three-step technique to identify high-excitation-level transitions. Many papers on OG mechanisms in hollow-cathode discharges refer to U lamps (see Sec. II). Optogalvanic investigation of doubly excited uranium (U III) has been reported by Piyakis and Gagné (1989).

A systematic study of the spectra of Pr I and Pr II in the range from 576 to 625 nm, using a commercial hollow cathode, has been reported by Reddy and Rao (1988). The sub-Doppler intermodulated OG technique

TABLE I. Atomic spectroscopy studies using optogalvanic detection: dc, direct current (positive column); hc, hollow cathode; hp, heat pipe; mw, microwave; rf, radio frequency.

Authors	Element	Kind of discharge	Laser source	Experimental results
Begemann and Saykally, 1982	Ar, Ne	dc	col, center	IR spectrum (3600–4100) cm^{-1}
Su *et al.*, 1987	Ar	hc	cw dye	Wavelength calibration
Suzuki *et al.*, 1983	Ar	mw	cw dye	First OG spectroscopy in microwave discharge
Murnick *et al.*, 1986	Ar	rf	cw dye	Isotope shift in optical transitions for ^{36,38,40}Ar (IMOGS)
Moscatelli *et al.*, 1988	Ar	rf	cw dye	Isotope shift (IMOGS)
Camus *et al.*, 1982	Ba	hp	cw dye	Two-step excitation of Rydberg states
Rinneberg and Neukammer, 1983	Ba	hp	cw dye	Rydberg-states spectroscopy of the states $6snp\,^{1,3}P$ and $6snf\,^{1,3}F$ by two-step excitation
Beigang, Schmidt, and West, 1983	Be, Mg	hp	pulsed dye	Rydberg series of *msns* and *msnd* configurations ($n=10$–70)
Inguscio, 1983	Ca, Ne, U	hc	cw dye	Doppler-free spectroscopy, isotope shifts
Barbieri *et al.*, 1983	Ca	hc	cw dye	hf structures (IMOGS)
Bobulescu *et al.*, 1980	Cs	rf	nonlinear	Hanle effect
Aymar *et al.*, 1986	Cd	rf	pulsed dye	Autoionizing profiles of resonances $5s5p\,^3P_J-5p^2\,^3P$
Gerstenberger *et al.*, 1979	Cu	hc	cw dye	Hyperfine structure, isotope shifts (IMOGS)
Beverini, Bionducci, *et al.*, 1982 Beverini, Galli, *et al.*, 1982	Cu	hc	cw dye	Hyperfine structure, isotope shifts (IMOGS)
Lawler *et al.*, 1981	Cu,Mo	hc	cw dye	Doppler-free spectroscopy
Babin *et al.*, 1987	Fe	hc	pulsed dye	Wavelength calibration
Hänsch *et al.*, 1981	He,Ne	dc	cw dye	Hyperfine structure of ^{3}He 3^3P-3^3D transitions
Katayama *et al.*, 1979	He	dc	pulsed dye	Rydberg-levels investigation $np\,^1S$ ($n=14$–36)
Goldsmith and Smith, 1979	He	dc	pulsed	Demonstration of two-photon OG spectroscopy in ^{4}He 2^3S-5^3S transitions and 2^3S-5^3D
Jackson *et al.*, 1981	He,Ne	hc	col. center	IR Rydberg series
Ganguly and Garscadden, 1985	He	dc	cw dye	Allowed and forbidden Rydberg series $2s\,^1S-ns\,^1S, np\,^1P, nd\,^1D$ ($n\leq 46$)
Lawler *et al.*, 1979a	He	dc	cw dye	First demonstration of IMOGS of ^{3}He 2^3P-3^3D transition at 587.5 nm
Hänsch *et al.*, 1981	He	dc	cw dye	First demonstration of POLINEX with OG detection of ^{3}He 2^3P-3^3D transition
van de Weijer and Cremers, 1985a, 1985b	Hg	dc	pulsed dye	Two-step photoionization
Wada *et al.*, 1986, 1987	Kr	hc	cw dye	Autoionizing visible transitions: $5p'$-$7d'$, $5p'$-$9s'$
Delsart *et al.*, 1981	Kr	dc	pulsed dye	Rydberg states $nd[3/2]_2$, $nd[7/2]_3$, ($n=15$–25)
Behrens *et al.*, 1983	I,Ga	hc	cw dye	Hyperfine constants of $8p\,^2P$ and $6p\,^2P$ levels; isotope shifts
Engleman *et al.*, 1985	Lu	hc	cw dye	Hyperfine structure of the $^2D^0_{3/2}-{}^2D_{3/2}$ transition and isotope shifts in ^{175,176}Lu
Behrens and Guthorlein, 1983	Mn, Co, La	hc	cw dye	Doppler-limited and Doppler-free spectroscopy (IMOGS)
Beigang and Timmermann, 1983	Yb, Eu I, Eu II Mg, Ca, Sr, Ba	hp	cw dye	Hyperfine structure and isotope shifts of Rydberg series by Doppler-free two-photon spectroscopy

TABLE I. (*Continued*).

Authors	Element	Kind of discharge	Laser source	Experimental results
Siegel *et al.*, 1981	Mo	hc	cw dye	Isotope shifts
Wakata *et al.*, 1981	Na	hc	pulsed dye	Two-step and two-photon excitation
Singh and Rao, 1989	Nb	hc	cw dye	Doppler-limited hyperfine structure
Beverini *et al.*, 1985	Ne	hc	cw dye	Optogalvanic nonlinear Hanle effect
Goldsmith *et al.*, 1979	Ne	dc	cw dye	Demonstration of Doppler-free two-photon OG spectroscopy
Nestor, 1982	Ne, Ar	dc	pulsed dye	Two-photon OG spectroscopy
Belfrage *et al.*, 1983a, 1983b	Ne, Mo	hc	cw dye	Comparison of Doppler-free techniques (IMOGS, POLINEX, polarization)
Lyons *et al.*, 1981	Ne	rf	cw dye	Doppler-free spectra of $1s^2-2p_1$ transition at 585.2 nm
Julien and Pinard, 1982	Ne	rf	cw dye	Optical pumping
Miyazaki *et al.*, 1983a, 1983b, 1983c, 1983d	Ne	hc	cw dye	Double resonance
Bickel and Innes, *et al.*, 1985	Ne	hc	pulsed dye	Two-photon and two-color OG investigations
Caesar and Heully, 1983a, 1983b	Ne	hc	pulsed dye	Rydberg series ($3p'$-ns,nd) and autoionizing series ($3p'$-ns',nd')
Keaton *et al.*, 1987	O	dc	pulsed dye	Highly excited atoms detection
Inguscio *et al.*, 1988	O	rf	cw dye	Fine structure of $4d^5D_{4-0}$ levels (IMOGS)
Ernst *et al.*, 1989	O	rf	cw dye	Isotope shift in ^{16,18}O optical transitions
Reddy and Rao, 1988	Pr I, Pr II	hc	cw dye	Doppler-limited hyperfine structure of optical transitions
Lorenzen and Niemax, 1982	Sr I, Sr II	hp		Isotope shifts measurements
Naveedullah and Naqvi, 1985	Th	hp	pulsed dye	Pressure broadening and isotope shifts of $6^2P_{1/2}-8^2P_{1/2,3/2}$ transitions
Langlois and Gagné, 1987	U	hc	cw dye	OG detection of Zeeman patterns (IMOGS)
Broglia *et al.*, 1983a	U	hp	pulsed dye	Highly excited spectrum for isotope separation study
Palmer *et al.*, 1981	U	hc	cw dye	Wavemeter measurements of spectral lines
Piyakis and Gagné, 1989	U III	hc	cw dye	Identification of doubly ionized uranium transitions in noble-gas discharge
Pianarosa *et al.*, 1984	U	hc	cw dye	Doppler-limited isotope shifts (^{234,235,236}U) measurements
Dovichi *et al.*, 1982	U	hc	pulsed dye	Wavelength calibration
Kroll and Persson, 1985	^{51}V	hc	cw dye	Hyperfine structures of the $3d^44s^6D-3d^44p^6F$ transition
Grandin and Husson, 1981	Xe	rf	cw dye	Rydberg states $np[1/2]_1$ ($n=15-19$); $nf[3/2]_1$ ($n=11-43$)
Labastie, Biraben, and Giacobino, 1982	Xe	rf	cw dye	Rydberg series: $6p[5/2]_3$-$nd[7/2]_4$,$ns[3/2]_2$ $6p[5/2]_2$,$6p[3/2_1$-$ns[3/2]_1$ ($n=12-27$) $5p^5ns[3/2]_2$;$5p^5ns[3/2]_1$ ($n=12-27$)
Labastie, Giacobino, and Biraben, 1982	Xe	rf	cw dye	Collisional shift and broadening of the Rydberg levels
Lemoigne *et al.*, 1983, 1984	Xe, Kr	rf	cw dye	Rydberg states in magnetic field
Hannaford *et al.*, 1983a, 1983b	Zr, Y	dc	cw dye	Demonstration of level crossing
Chevalier *et al.*, 1988	Zr	hc	cw dye	Hyperfine constants for the levels $^3F_2^0$, $^5F_1$, $^3F_3^0$, $^3D_1^0$, $^3F_4^0$, $^3D_2^0$, $^3D_3^0$ (POLINEX, IMOGS)
Chevalier *et al.*, 1987	Zr	hc	cw dye	Isotope shifts measurements of optical transitions for ^{90,91}Zr (POLINEX, IMOGS)
Bourne *et al.*, 1986	Zr	hc	cw dye	Hyperfine structure and isotope shifts for $a^3F_2-z^3F_2^0$ transitions (IMOGS)

has been applied to the measurement of hyperfine separations and isotopic shifts in excited levels of atoms such as molybdenum (Siegel *et al.*, 1981), lutetium (Engleman *et al.*, 1985), and zirconium (Bourne *et al.*, 1986; Chevalier *et al.*, 1987).

A summary of work done in atomic spectroscopy with optogalvanic detection is given in Table I.

3. Molecules

The OG detection of molecular transitions was first demonstrated by Schenck *et al.* (1978), who observed the absorption spectra of metal oxides. Feldman (1979) recorded transitions in NH_2, NO_2, N_2, and H_2 in the spectral range 570–620 nm and managed to observe

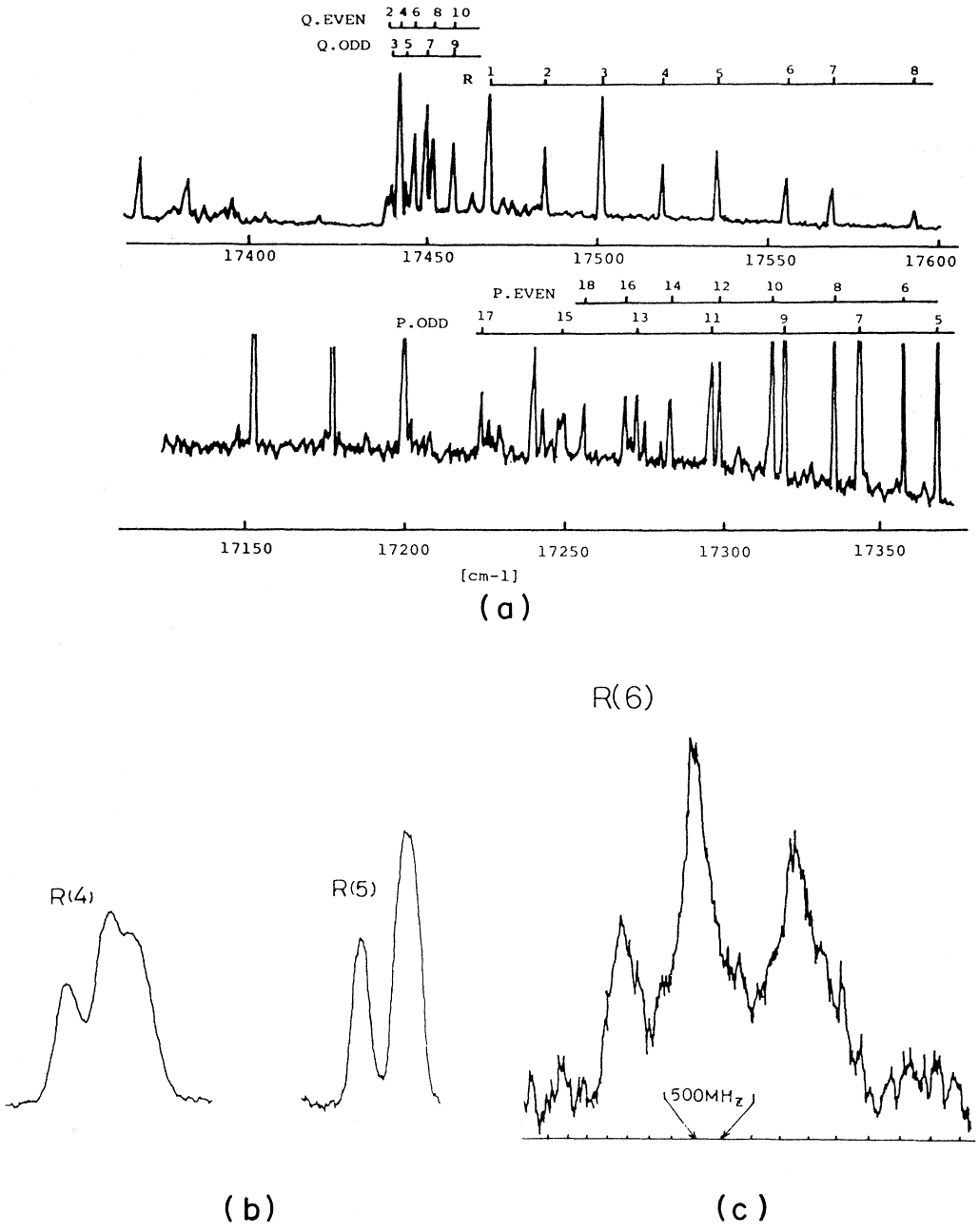

FIG. 30. Optogalvanic spectrum of the He_2 dimer: (a) low-resolution spectrum of the $b\,^3\Pi_g - f\,^3\Delta_u$ transition; (b) high-resolution Doppler-limited spectrum of the $R(4)$ and $R(5)$ components; (c) Doppler-free intermodulated spectrum of the $R(6)$ component (from Kawakita *et al.*, 1985).

weak transitions, such as the Ledbetter band, representing transitions between the Rydberg states $C_4\,{}^1\Pi_u - {}^1\Sigma_g^+$, in N_2. Molecular iodine transitions were detected by Demuynck and Destombes (1981) in the range 578–630 nm, as well as by Rettner *et al.* (1981) in the range 520–630 nm. These last investigators obtained OG signals irradiating even the cell far from the discharge region, a result renewing the interest in the nature of the OG signal. Iodine was also chosen by Haner *et al.* (1983) in their time-resolved study of the OG effect.

Suzuki (1981) detected OG spectra of N_2, NH_3, and NO_2 in the wavelength region between 580 nm, and 630 nm in an rf discharge. In subsequent work (Suzuki and Kakimoto, 1982) a more detailed study of N_2 Rydberg states, in the spectral range covered by rhodamine 6G, is presented. Lines from the Ledbetter band are resolved using intermodulated Doppler-free OG spectroscopy. Carlson *et al.* (1985) have observed the TiO diatomic molecules produced in a glow discharge by sputtering titanium metal and TiO_2 from the inner surface of a hollow cathode composed of a compressed mixture of these two substances; they recorded the optogalvanic spectrum of the (0,0) band of the $B\,{}^3\Pi - X\,{}^3\Delta$ transition.

Miyazaki *et al.* (1983a, 1983c), using the optical-optical double-resonance method proposed by Vidal (1980), have verified the assignments made by Suzuki (1981). The same technique was also used in a study of H_2 transitions (Miyazaki *et al.*, 1983d).

Webster and Menzies (1983a, 1983b) extended OG molecular studies to infrared wavelengths. They recorded portions of the NH_3 ν_2 band at 9.5 μm and the NO_2 ν_3 band at 6.2 μm using cw tunable diode lasers to probe the dc electrical discharge in pure NH_3 and in NO_2/He gas mixture. An isotopic CO_2 laser was used by Muenchausen *et al.* (1984) in the detection of OG signals in rf discharges with D_2O, H_2CO, NH_3, SO_2, H_2S, and H_2O_2. Van Roozenadael *et al.* (1986), using an isotopic CO laser, have examined the optogalvanic spectrum of a low-pressure rf discharge in NO, NO_2, HNO_3, HCO_2, H_2CO, and $C_2H_2O_2$.

Suzuki *et al.* (1983) detected, in a discharge produced by a microwave field, transitions in the dimer He_2. The same system was studied with sub-Doppler techniques by Kawakita *et al.* (1985; see also Fig. 30).

Reactive radical species that can be produced in a discharge can also be usefully studied using the OG technique. Vasudev and Zare (1982) presented a study of HCO performed with a cw single-mode dye laser in an rf discharge in acetaldehyde vapor. They were able to measure the linewidths in a band of excited-state transitions, demonstrating mixing between some levels in the upper state of the transition and nearby strongly predissociated levels.

B. Wavelength calibration

The OG effect can provide an accurate and economical way to calibrate the wavelength of a tunable dye laser (King *et al.*, 1977) by means of a suitable discharge lamp in any spectral region. The use of a hollow cathode made by an element with a high density transition spectrum, such as uranium, is particularly straightforward. The region between 348.8 nm and 908.5 nm is covered by an atlas published by Palmer *et al.* (1980), which reports the Fourier-transform spectrum emitted from a uranium hollow-cathode discharge in Ne. The wavelengths of the stronger transitions (about a thousand) were tabulated with an estimate accurate of 0.005 cm^{-1}. A comparison with the OG spectrum (Keller *et al.*, 1980) showed an agreement in the relative intensity of about 30%, apart from occasional anomalous lines.

Dovichi *et al.* (1982) analyzed the application of the same atlas for wavelength calibration of pulsed lasers. They found the atlas useful for this purpose and the relative intensity of the lines similar to that observed with cw laser sources. A commercial hollow-cathode lamp was used for the visible region, while at wavelengths shorter than 350 nm it was necessary to use a drilled hollow cathode to avoid the background signal due to photoelectric emission from the cathode surface, as discussed in Sec. III.

Other elements—like Na (King *et al.*, 1977), Th (Keller *et al.*, 1980; Sansonetti and Weber, 1984), Ne (Begemann and Saykally, 1982), and Ar (Su *et al.*, 1987)—have been used occasionally for wavelength calibration.

For wavelength calibration of a tunable UV pulsed laser, Babin *et al.* (1987) have published an optogalvanic spectrum of iron. The accuracy of the measured wavelength is limited to 0.05 cm^{-1} by the spectral width of the pulsed laser.

Special care must be taken when high-intensity pulsed lasers are used or when the discharge is driven at high current, because asymmetries and shifts of the line profiles caused by saturation effects and self-absorption phenomena can arise. Beenen and Piepmeier (1981) observed a shift of the peak maximum up to 0.15 cm^{-1}. They analyzed the phenomenon and conceived a model that fit the experimental results quite well (Piepmeier and Beenen, 1982) and indicated the experimental conditions that minimized the effect. By contrast, no observable asymmetry or shift was observed by Dovichi *et al.* (1982).

Webster (1982) suggested a special technique for wavelength calibration, which could be used in laser monitoring of reactive atmospheric species: the reactive species of interest (molecules or radicals) are produced in a discharge, and the OG spectrum is compared with the atmospheric fluorescence spectrum produced by the same laser beam.

C. Laser frequency stabilization

Widespread use is being made of OG signals to stabilize laser frequencies, as in the case of the cw CO_2 laser. The standard technique is based on the impedance change in the excitation discharge as a function of the

output power of the laser. A laser working in a single-mode and single-line regime is frequency modulated by tuning the length of the laser cavity using a piezoelectric transducer (PZT). The OG signal is observed as an ac voltage signal across the ballast resistor of the power supply line by a phase detector. The error signal is amplified and sent to drive the PZT in order to correct the cavity length. A stabilization on the peak power of the order of 5×10^{-8} was obtained using this method (Skolnick, 1970; Thomason and Elbers, 1975; Smith and Moffatt, 1979; Moffatt and Smith, 1984).

When the modulation frequency was increased, the OGE was observed to decrease; it vanished in low-pressure lasers at 2–3 KHz. Moffatt and Smith (1984) explained this phenomenon by analyzing the collisional relaxation processes in the discharge plasma; they found that the OG effect reappeared at higher frequencies (with an opposite phase). A better performance was achieved by modulating at a frequency of 10–20 kHz (long-term stability better than 5×10^{-9}), because of the lower-density spectral noise of the discharge in this frequency region. This relatively high frequency modulation makes possible rapid corrections to reduce the laser noise in the audio-frequency band.

Kavaya *et al.* (1982) have reported optogalvanic stabilization of a high-pressure (200 torr) wave-guide CO_2 laser, with a feedback stabilization loop that allowed continuous tuning of the laser frequency over a wide portion of the broadening gain profile. The optogalvanic signal could be greatly improved by picking up the signal from a low-pressure amplifier discharge (Bourdet and Houmault, 1986).

The stabilization of CO_2 lasers by OG monitoring of the Doppler profile is now widely practiced in laboratories, when ultimate stability properties are not important, because of its simplicity and low cost when compared with other more sophisticated methods such as saturation fluorescence. The method is particularly well suited for output equipment, because it requires no additional instrumentation or detector to obtain the error signal.

The optogalvanic signal can also be obtained without any direct connection with the high-voltage electric circuit of the laser discharge: Abramski *et al.* (1985) used a simple needle probe placed in the water cooling jacket to detect capacitively the signal.

A more accurate stabilization can be reached by locking a low-pressure laser on a homogeneous line by means of a sub-Doppler technique. This was done in 1973 by Bourdet *et al.* in a CO_2 laser with a total linewidth of 50 MHz and a homogeneous width, according to the pressure, between 4 and 8 MHz. They were able to stabilize the laser on the Lamb dip of the gain profile by modulating the reflection grating with a PZT: in this way they obtained a stability of the order of 2×10^{-10} over a period of some ten seconds. However, in order to observe the Lamb dip in a CO_2 laser, one must have a pressure lower than 1 torr, and at this pressure the laser can operate only on the most powerful transitions.

A solution for this problem was introduced by Shy and Yen (1986). They suggested using a low-pressure discharge for Lamb dip detection, while keeping the laser discharge tube at higher pressure. They found that this technique could be applied to the majority of ordinary

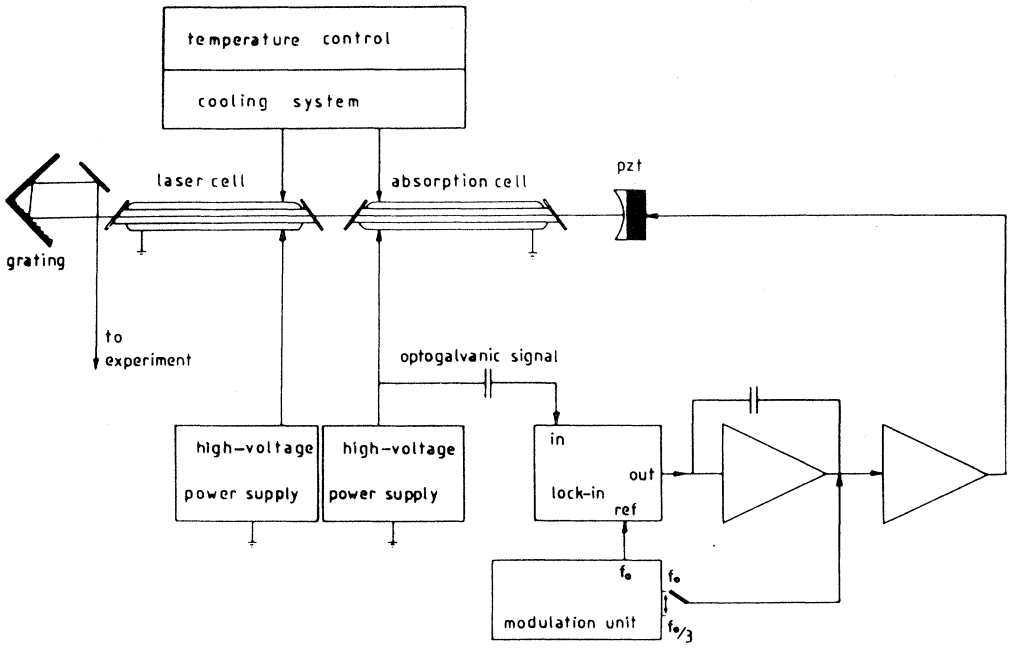

FIG. 31. High-accuracy CO laser stabilization circuit (from Schneider *et al.*, 1987).

lasing transitions with a frequency stability better than 1×10^{-9}.

A similar method was recently used by Schneider *et al.* (1987; see also Fig. 31) to stabilize a CO laser. They locked the CO laser to the absorption Lamb dip detected by the OG technique in an external low-pressure CO discharge and were able to obtain a relative stabilization in the 100 kHz range. A third derivative technique was applied in order to avoid frequency shifts due to asymmetry in the line shape. This locking method has particular importance for metrology. In fact, while optogalvanic CO_2 laser stabilization is simply an alternative to fluorescence detection—which ultimately gives better stability in the 30 kHz range—the CO laser stabilization by optogalvanic methods is innovative, since the CO molecule does not offer a similar fluorescence property. The CO transition frequencies can now be measured with an accuracy comparable to that of the CO_2 transitions, and a new series of calibrated wavelengths covers the infrared region.

The OG signal has also been used to frequency lock a dye laser on an atomic transition, following the usual stabilization schemes used in spectroscopy. The first frequency stabilization of a multimode cw dye laser on an OG signal from a hollow-cathode lamp was carried out by Green *et al.* (1977).

Yamaguchi and Suzuki (1982) proposed the extension of OG laser stabilization to diode lasers. They found that it was particularly effective for an AlGaAs diode laser in the near-infrared region. However, molecular spectra have a weak intensity in this region, and very few atomic absorption transitions occur. Menocal *et al.* (1989) have reported the frequency locking of a 1.5 μm distributed feedback diode laser to a neon indicator lamp.

D. Ion detection and plasma diagnostics

1. Positive-ion detection

Optogalvanic detection of ionic transitions was reported in Ba^+ and Eu^+ by Schenck and Smyth (1978); in U^+ by Keller *et al.* (1979) and by Drèze *et al.* (1982); and in I^+ by Rettner *et al.* (1981). Lorenzen and Niemax (1982) detected a Sr^+ transition by sub-Doppler Lamb dip spectroscopy and measured the isotopic shift. Molecular positive ions (N_2^+, CO^+) were observed by Walkup *et al.* (1983a, 1983b, 1983c). The ionic transitions are obviously more perturbed than atomic ones by the discharge environment, and the spectroscopic information is not as accurate. Detection of ionic transition can be, however, very useful for the study of ion mobility in the discharge (Walkup *et al.*, 1983a, 1983b, 1983c).

2. Photodetachment spectroscopy

The optogalvanic technique can be useful in diagnosing a discharge in which negative ions are present. In this case an OG signal comes from photodetachment of the electron from the negative ion, induced by the laser radiation when the photon energy is greater than the photodetachment energy. The reaction does not change the number of free charged particles, but the discharge impedance is greatly reduced due to the very different mobilities of free electrons and negative ions. This signal can be distinguished easily from the molecular absorption signal by its spatial and temporal properties. The first proposal came from Taillet (1969), who suggested using the method to determine the density of O^- ions in an oxygen discharge by irradiation with a fixed-frequency pulsed laser. The experimental method was set forth in detail by Bacal *et al.* (1979a, 1979b) in describing the measurement of H^- in a plasma using a ruby laser. The method was also applied by Pealat *et al.* (1985) to an analysis of magnetic multicusp discharges. By using UV lasers, one can observe many other negative ions. Greenberg *et al.* (1984), with a XeCl exciter laser, observed photodetachment phenomena in a NF_3 discharge.

Through the use of a tunable laser, photodetachment spectroscopy can also be employed to determine the electron affinity of atoms or radicals. Webster *et al.* (1983) observed a sudden increase in the discharge current at the energy threshold of this reaction in iodine when the laser was tuned from 420 to 380 nm. They determined a threshold energy for photodetachment of 3.0591 ± 0.0001 eV (Fig. 32). This result, obtained with a simple and inexpensive discharge tube, was more accurate than the complex determination made with a crossed-beam method.

The same technique was also used by Klein *et al.* (1983) to determine the electron affinity of the CN radical. In this case, a frequency-doubled dye laser was used, because the photodetachment threshold fell in the 320–330 nm region. The rotational structure of the radi-

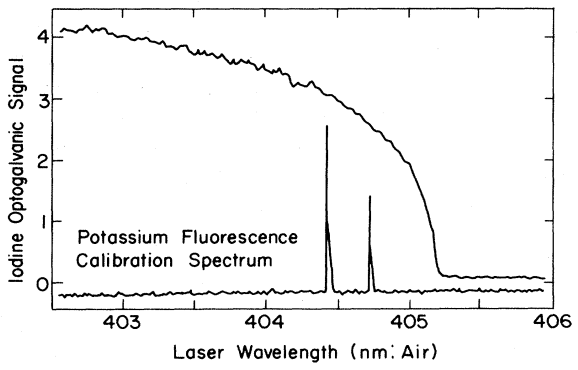

FIG. 32. Iodine photodetachment spectrum near the 405 nm threshold. The lower trace shows the potassium laser-induced fluorescence, which was used for calibration (after Webster *et al.*, 1983).

cal levels, not resolved in this experiment, made the determination of the affinity value (3.821±0.004 eV) both more complex and less accurate.

The photodetachment optogalvanic technique was applied to the study of negative-ion kinetics in an rf discharge. Gottscho and Gaebe (1986) used the technique in a low-pressure rf glow discharge at a frequency between 50 and 750 kHz in BCl_3 and Cl_2, while Kramer (1986) studied a 13.56 MHz discharge in chlorine. Similarly, Touzeau *et al.* (1989) monitored the density of O^- in a pure O_2 discharge. In all these cases, a pulsed dye laser (eventually frequency doubled), pumped by an excimer laser, was used. The experimenters determined the photodetachment energy for Cl^- (3.6118±0.0005 eV) and could monitor the anion densities and identify the negative ions from the temporal and spatial wavelength dependences of the optogalvanic signals.

3. Other applications

A multiphoton optogalvanic technique was suggested by Ausschnitt *et al.* (1978) to probe the ground- and excited-state densities and the translational temperatures of H and D atoms in a plasma. Two UV pulsed laser beams were overlapped inside the discharge. The laser frequencies f_1 and f_2 were chosen so that f_1+f_2 would be resonant with the $1S-2S$ two-photon transition, while neither $2f_1$ nor $2f_2$ were resonant with an intermediate level. In this way, a significant ionization from the ground state of hydrogen could be achieved by three-photon absorption only when both laser beams were present. Photoionization from the collisionally populated excited state was achieved by a single f_1 photon absorption. The optogalvanic signals observed in the presence of f_1 only and in the presence of both f_1 and f_2 laser beams gave a measurement of the relative population of the ground and excited states. The Doppler width of the $1S-2S$ transition was also monitored, and hence the translational temperature calculated, by tuning f_2. This technique gives a much better spatial and temporal resolution than other standard plasma diagnostic techniques, but without the difficulty of working at the Lyman α wavelength necessary in a fluorescence technique.

Another suggested application for optogalvanic spectroscopy is the study of Penning ionization (Shuker *et al.*, 1980; Ben-Amar *et al.*, 1981, 1984; Shuker *et al.*, 1983a). The excitation energy of the $7d\ ^2D_{5/2},^2D_{3/2}$ level of Ca^+ over the neutral-atom ground state is almost resonant (within kT) with the excitation energy of the $^3P_2$ metastable state of Ne. The time-resolved optogalvanic signal generated by the absorption of laser radiation from this metastable level can provide information about the kinetics of the Penning process. A similar Penning ionization process was observed by Nogar and Keaton (1985) in the production of O_2^+ ions in an O_2/Ne discharge, and by Reddy *et al.* (1989) in a Hg-Ar discharge.

E. Multiphoton excitation and detection in flames

The OG technique was first applied to flames by Green, Keller, Schenck, *et al.* (1976) shortly after its introduction. A flame can be considered as a region of very weak plasma (density less than 0.1%). When the OG effect occurs, an enhancement in ionization is observed. Since only enhanced ionization occurs, the OG effect in flames is often referred to as a "laser-enhanced ionization" (LEI), especially in works describing analytical applications. The experimental apparatus for OG studies of a flame does not differ substantially from that used with electrical discharges. To detect the enhancement in ionization produced by the OG effect, electrodes are inserted in the flame and kept at a negative voltage (about 10^3 volts) with respect to the burner. The experimental apparatus is not entirely satisfactory, since it introduces a perturbation in the flame dynamics. By contrast, optical techniques do not perturb the characteristic of the flame, but the signal may be perturbed by interference from scattered laser radiation.

The OG effect in flames has been used mainly for (a) determining the elemental concentration of atomic and molecular species in different zones of the flames and for (b) spatial mapping of ion and radical concentrations. Applications to ion mobility determinations and to studies of charge-transfer mechanisms have been made as well.

An explanation of the OG effect in flames was first provided by Green, Keller, Schenck, *et al.* (1976) and Alkemade (1977). A number of papers followed to deal with theoretical and experimental aspects of the OG effect in flames: Travis *et al.*, 1979; Smyth *et al.*, 1980; van Dijk and Alkemade, 1980; Axner *et al.*, 1983. Green *et al.* (1980) studied the electrical interferences to the signal due to the background ionization in the flame; Schenck *et al.* (1981) studied the temporal and spatial characteristic of the signal for cw lasers, while Berthoud *et al.* (1983) studied the effect of laser beam position and applied probe potential on the shape of the signal using a pulsed laser. Reviews of the first applications have been presented by Schenck and Hastie (1981), Travis and DeVoe (1981), Zorov *et al.* (1982), and Turk *et al.* (1983).

The experimental observation by Green, Travis, and Keller (1976) that OG laser absorption was more sensitive than laser-induced fluorescence suggested the use of the OG technique for analytical applications. An ionization enhancement factor of five to eight orders of magnitude has been observed. This is attributed to the lower ionization of the excited atom (Travis *et al.*, 1979). Turk, Travis *et al.* (1979) published some results on the detection limit of some metals seeded in a premixed air-acetylene flame. For some species the detection limits were 10 to 100 times better than for other flame-based techniques. The electrodes were a pair of parallel plates rather than rods. This arrangement reduced interference from background ionization in the flame. Turk and his co-workers used a flash-lamp-pumped dye laser with frequency-doubled capability. Detection limits $<10^{-9}$

were reported by Travis *et al.* 1982). The fundamental detection limit has been discussed by Matveev *et al.* (1978) and Travis *et al.* (1982). In order to improve the sensitivity, a two-step excitation approach has been used on several elements to populate levels closer to the ionization limit. The first application was made on sodium by Gonchakov *et al.* (1979); Turk, Mallard, *et al.* (1979) used two tunable dye lasers synchronously pumped by a nitrogen-pumped dye laser to detect a number of elements. Zorov *et al.* (1980) applied the technique to the determination of lithium and cesium concentration, while Salcedo Torres *et al.* (1981) determined indium concentration in an acetylene-air flame. Other applications of stepwise excitation include those of Turk, DeVoe, and Travis (1982) and Axner *et al.* (1983), which measured the detection limit on a number of metals using excimer-pumped dye lasers.

The first use of OG techniques to detect molecular species indigenous to a flame was made by Schenck *et al.* (1978). Bands of LaO in a premixed hydrogen/air flame with excitation in the 360–750 nm wavelength range were detected. Optogalvanic spectra have also been obtained for yttrium and scandium oxides, as well as for SrOH, CaO, CaOH, and BaOH. In all these cases the ionization limits were below the dissociation energy of the molecules. No signals were obtained from OH, CH, or other flame species where the dissociation energy was less than the ionization limit.

Multiphoton ionization of NO in flames has been reported by Mallard, Miller, and Smyth (1982) and by Rockney *et al.* (1982). Smyth and Mallard (1982) detected multiphoton ionization of PO in a premixed acetylene-air flame.

The OG technique has also been used to detect the presence of atoms and radicals directly involved in the combustion mechanism. Goldsmith (1982) detected H in an atmospheric-pressure hydrogen-air flame using resonant two-photon ionization detection. The two-photon scheme excited the transition $1S-2S$. A Nd:YAG laser provided a beam at 266 nm wavelength by fourth harmonic generation. The 223 nm wavelength radiation required to complete the excitation was obtained by diverting part of the frequency-doubled output of the Nd:YAG to pump a dye laser. The dye laser output was frequency doubled and then mixed with the Nd:YAG laser radiation. The two beams at 266 nm and 224 nm were focused in the flame and crossed at a 25 mrad angle. This geometrical scheme provides a detailed spatial resolution that allows the mapping of the H radical concentration throughout different regions of the flame.

Atomic oxygen has been detected (Goldsmith, 1983a) in a premixed atmospheric-pressure hydrogen/oxygen/argon flame using a similar experimental setup. A sensitivity of a few parts per million has been reached in the post-flame gases region (Goldsmith, 1983b). Resonant excitation and detection of these species using other optical techniques is not an easy task. Radiation in the vacuum-ultraviolet region of the spectrum is required due to the gap of about 10 eV between the ground state and the first excited state (Goldsmith, 1983c). Raman techniques cannot be applied due to the lack of structure in the ground state.

VI. CONCLUSIONS

Today the OG detection is a well-developed spectroscopic technology. It complements other optical techniques, like the traditional absorption and fluorescence spectroscopy or the optoacoustic spectroscopy.

The theoretical background and the fundamental mechanisms of the OG effect are well established and understood. Since a discharge is a complex medium, a complete description of the OG effect may require the knowledge of a large number of physical parameters. However, as shown in Sec. II, it is possible to build simple mathematical models that correctly reproduce the phenomenology of the experimental conditions. As shown in Sec. V, practical applications do not even require a complete theoretical modeling!

The different spectroscopic methods developed for the traditional spectroscopy can also be applied to the OG spectroscopy, including the saturation methods for sub-Doppler resolution. The OG technique cannot compete in ultimate resolution with the traditional methods, but in many cases a small loss in resolution and accuracy is the price to be paid for a more simple and economical experimental apparatus. We have shown that sometimes the application of the OG technique is the best detection method. A typical example is when absorption spectroscopy is not efficient because the sample is optically thin, and there is no fluorescence signal available—as is often the case in molecular infrared spectroscopy.

For all these reasons, we think that OG spectroscopy will be considered more frequently in laboratory application as a standard spectroscopical technique, especially for technological applications like laser stabilization and laser wavelength calibration.

ACKNOWLEDGMENTS

Our work in optogalvanic spectroscopy has benefited from our interactions with numerous friends and colleagues. We would like especially to thank Franco Strumia; Massimo Inguscio, who urged us to write this article and critically stimulated us through the process; and Graciela Bertuccelli, for her assistance in collecting the literature during the initial stage of this work.

APPENDIX: THE LITERATURE

1. Reviews of optogalvanic spectroscopy

King and Schenck, 1978
Goldsmith and Lawler, 1981
Ferguson, 1982

Camus, 1983 (atomic applications)
Webster and Rettner, 1983 (molecular applications)
Ochkin *et al.*, 1986

2. Discharge designs

a. Heat pipe

Camus, 1974

b. Hollow cathode:

Lawler *et al.*, 1981
Webster *et al.*, 1983
Inguscio, 1983
Miyazaki *et al.*, 1983a
Barbieri *et al.*, 1984

c. Radio-frequency discharges

Stanciulescu *et al.*, 1980a, 1980b, 1980c
Lyons *et al.*, 1981
Suzuki, 1981
Labastie, Biraben, and Giacobino, 1982

d. Microwave discharges

Suzuki *et al.*, 1983 (Rydberg states)

3. Linear spectroscopy

a. Single-step excitation

Katayama *et al.*, 1979	He
Grandin and Husson, 1981	Xe
Lemoigne *et al.*, 1983	Xe, Kr
Lemoigne *et al.*, 1984	Xe
Labastie, Biraben, and Giacobino, 1982	Xe
Labastie, Giacobino, and Biraben, 1982	Xe
Giacobino *et al.*, 1983	Xe

b. Two-step excitation

Camus *et al.*, 1979	Ba
Camus *et al.*, 1982	Ba
Camus *et al.*, 1983a	Ba
Camus *et al.*, 1983b	Ba
Delsart *et al.*, 1981	Kr

c. Three-step excitation

Broglia *et al.*, 1983	U

4. Optical-optical double resonance

a. Proposal

Vidal, 1980

b. Experiments

Inguscio, 1983	Ne
Wakata *et al.*, 1981	Na
Behrens *et al.*, 1983	Ga I, In I
Miyazaki *et al.*, 1983a	N_2
Miyazaki *et al.*, 1983b	Ne
Miyazaki *et al.*, 1983c	N_2
Miyazaki *et al.*, 1983d	N_2, H_2

5. Radio-frequency–optical double resonance

Beverini and Inguscio, 1980

6. Microwave-infrared double resonance

Hameau *et al.*, 1984	NH_3

7. Intermodulated optogalvanic spectroscopy (IMOGS)

a. Atoms

Lawler *et al.*, 1979a, 1979b	He I
Gerstenberger *et al.*, 1979	Cu I
Siegel *et al.*, 1981	Mo I
Lyons *et al.*, 1981	Ne I
Jackson *et al.*, 1981	He I, Ne I
Lorenzen and Niemax, 1982	Sr I, Sr II
Belfrage *et al.*, 1983a	Ne I
Behrens and Guthorlein, 1983	Mn I, Co I, La I, Yb I, Eu I, Eu II
Belfrage *et al.*, 1983b	Ne I, Mo I
Inguscio, 1983	Ca I, Ne I, U I
Barbieri *et al.*, 1984	U I
Bourne *et al.*, 1986	Zr I
Murnick *et al.*, 1986	Ar I
Chevalier *et al.*, 1987	Zr I
Moscatelli *et al.*, 1988	Ar I
Chevalier *et al.*, 1988	Zr I
Inguscio *et al.*, 1988	O I
Ernst *et al.*, 1989	O I

b. Molecules

Suzuki and Kakimoto, 1982	N_2

c. Zeeman IMOGS

Barbieri *et al.*, 1982b	Ca I, Ne I
Beverini, Bionducci, *et al.*, 1982	Ca I, Ne I
Beverini, Galli, *et al.*, 1982	Ca I, Ne I, Cu I
Barbieri *et al.*, 1982a	Ca I, Ne I
Hannaford *et al.*, 1983a	Zr I
Barbieri *et al.*, 1983	Ca I
Beverini *et al.*, 1985	Ca I, Ne I
Ernst, Grabinska, and Inguscio, 1989	Ne I

8. Polarization intermodulation excitation spectroscopy (POLINEX)

Hänsch *et al.*, 1981	He
Dabkiewicz *et al.*, 1981	He
Lyons *et al.*, 1981	Ne
Julien and Pinard, 1982	Ne
Pinard and Julien, 1983	Ne
Belfrage *et al.*, 1983a	Ne
Belfrage *et al.*, 1983b	Ne
Chevalier *et al.*, 1987	Zr

9. Two-photon optogalvanic spectroscopy (TOGS)

Goldsmith *et al.*, 1979	^{20}Ne I
Goldsmith and Smith, 1980	^{4}He I
Shuker *et al.*, 1983b	
Shuker *et al.*, 1984	

10. Stimulated level-crossing optogalvanic spectroscopy

a. Proposal

Beverini and Inguscio, 1980

b. Theory

Strumia, 1983
Beverini *et al.*, 1985

c. Level crossing at finite magnetic fields

Hannaford and Series, 1982a	^{89}Y I
Hannaford *et al.*, 1983a	^{89}Y I
Hannaford *et al.*, 1983b	^{89}Y I

d. Multimode saturation resonances

Hannaford and Series, 1982b	Zr I

e. Nonlinear Hanle effect (NLHE)

Hannaford and Series, 1981a	Zr I
Hannaford and Series, 1981b	Zr I
Julien and Pinard, 1982	Ne I

REFERENCES

Abramski, K. M., J. Van Spijker, and W. J. Witteman, 1985, Appl. Phys. B **36**, 149.

Ageev, V. A., V. D. Egorov, and M. I. Nedel'ko, 1982, Zh. Tekh. Fiz. **52**, 517.

Al-Chalabi, S. A. M., R. S. Stewart, R. Illingworth, and I. S. Ruddock, 1983, J. Phys. D **16**, 115.

Alkemade, C. Th. J., 1977, in *Proceedings of 20th Coll. Spectrosc. Intl. and 7th International Conference on Atomic Spectroscopy* (Sbornik VSCHT, Prague), p. 93.

Aoki, T., C. Yamada, and M. Kakayama, 1971, Jpn. J. Appl. Phys. **10**, 332.

Apel, C. T., R. A. Keller, E. F. Zalewski, and R. Engelman, Jr., 1982, Appl. Opt. **21**, 1465.

Apostol, D., C. Blanaru, Ch. Ionescu, I. I. Popescu, and V. Vasiliu, 1982, Rev. Roum. Phys. **27**, 581.

Arimondo, E., M. G. Di Vito, K. Ernst, and M. Inguscio, 1983, J. Phys. (Paris) **C7-44**, 267.

Arimondo, E., M. G. Di Vito, K. Ernst, and M. Inguscio, 1984, Opt. Lett. **9**, 530.

Arnett, K., R. Anderson, and R. Alexander, 1981, Am. J. Phys. **49**, 767.

Arnikar, H. J., 1982, Curr. Sci. **51**, 1103.

Ausschnitt, C. P., G. C. Bjorklund, and R. R. Freeman, 1978, Appl. Phys. Lett. **33**, 851.

Ausschnitt, C. P., G. C. Bjorklund, and R. R. Freeman, 1979, U.S. Patent 4, 166, 219, Bell Telephone Labs., Inc., abstract only.

Axner, O., T. Berglind, J. L. Heully, I. Lindgren, and H. Rubinsztein-Dunlop, 1983, J. Phys. (Paris) **C7-44**, 311.

Aymar, M., P. Camus, and A. El Himdy, 1982, J. Phys. B **15**, L759.

Aymar, M., E. Luc-Koenig, M. Chantepie, J. L. Cojan, J. Landais, and B. Laniepce, 1986, J. Phys. B **19**, 3881.

Babin, F., P. Camus, J. M. Gagné, P. Pillet, and J. Boulmer, 1987, Opt. Lett. **12**, 468.

Bacal, M., G. W. Hamilton, A. M. Bruneteau, H. J. Doucet, and J. Taillet, 1979a, J. Phys. (Paris) **C7-40**, 471.

Bacal, M., G. W. Hamilton, A. M. Bruneteau, H. J. Doucet, and J. Taillet, 1979b, Rev. Sci. Instrum. **50**, 719.

Bachor, H. A., P. J. Manson, and R. J. Sandeman, 1982, Opt. Commun. **43**, 337.

Barbieri, B., N. Beverini, G. Bionducci, M. Galli, M. Inguscio, and F. Strumia, 1982a, in *Rendiconti III Congresso Nazionale di Elettronica Quantistica e Plasmi,* edited by P. Caldirola, V. De Giorgio, and O. Svelto (Primi & C., Como), p. 337.

Barbieri, B., N. Beverini, G. Bionducci, M. Galli, M. Inguscio, and F. Strumia, 1982b, in *Rendiconti III Congresso Nazionale di Elettronica Quantistica e Plasmi,* edited by P. Caldirola, V. De Giorgio, and O. Svelto (Primi & C., Como), p. 340.

Barbieri, B., N. Beverini, G. Bionducci, M. Galli, M. Inguscio, and F. Strumia, 1983, in *Laser Spectroscopy VI,* Proceedings of the Sixth International Conference, Interlaken, Switzerland,

1983, edited by H. P. Weber and W. Lüthy (Springer-Verlag, Berlin/Heidelberg/New York/Tokyo), p. 133.
Barbieri, B., N. Beverini, M. Galli, M. Inguscio, and F. Strumia, 1984, Nuovo Cimento D **4**, 172.
Beenen, G. J., B. P. Lessard, and E. H. Piepmeier, 1979, Anal. Chem. **51**, 1721.
Beenen, G. J., and E. H. Piepmeier, 1981, Anal. Chem. **53**, 239.
Begemann, M. H., and R. J. Saykally, 1982, Opt. Commun. **40**, 277.
Behrens, H. O., and G. H. Guthorlein, 1983, J. Phys. (Paris) **C7-44**, 149.
Behrens, H. O., G. H. Guthorlein, and A. Kasper, 1983, J. Phys. (Paris) **C7-44**, 239.
Beigang, R., W. Makat, A. Timmermann, and P. J. West, 1983, Phys. Rev. Lett. **51**, 771.
Beigang, R., D. Schmidt, and P. J. West, 1983, J. Phys. (Paris) **C7-44**, 229.
Beigang, R., and A. Timmermann, 1983, J. Phys. (Paris) **C7-44**, 137.
Belfrage, Ch., P. Grafström, S. Kröll, and S. Svanberg, 1983a, Phys. Scr. **27**, 367.
Belfrage, Ch., P. Grafström, S. Kröll, and S. Svanberg, 1983b, J. Phys. (Paris) **C7-44**, 169.
Bell, W. E., and A. L. Bloom, 1961, J. Appl. Phys. **32**, 906.
Ben-Amar, A., G. Erez, S. Fastig, and R. Shuker, 1984, Appl. Opt. **23**, 4529.
Ben-Amar, A., R. Shuker, G. Erez, and E. Miron, 1981, Appl. Phys. Lett. **38**, 763.
Berman, P. R., 1976, Phys. Rev. A **13**, 2191.
Berman, P. R., 1978, Adv. At. Mol. Phys. **13**, 57.
Berthoud, T., J. Lipinsky, P. Camus, and J. L. Stehle, 1983, Anal. Chem. **55**, 959.
Beverini, N., G. Bionducci, M. Galli, M. Inguscio, and F. Strumia, 1982, Appl. Phys. B **29**, 161.
Beverini, N., K. Ernst, M. Inguscio, and F. Strumia, 1985, Appl. Phys. B **37**, 17.
Beverini, N., M. Galli, M. Inguscio, F. Strumia, and G. Bionducci, 1982, Opt. Commun. **43**, 261.
Beverini, N., and M. Inguscio, 1980, Lett. Nuovo Cimento **29**, 10.
Bickel, G. A., and K. K. Innes, 1985, Appl. Opt. **24**, 3620.
Bickerton, R. J., and A. von Engel, 1956, Proc. Phys. Soc. London, Sect. B **69**, 468.
Bjorklund, G. C., C. P. Ausschnitt, R. R. Freeman, and R. H. Storz, 1978, Appl. Phys. Lett. **33**, 54.
Bobulescu, R. C., C. Stanciulescu, N. Ceausescu, A. Surmeian, D. Popescu, and I. I. Popescu, 1979, Rev. Roum. Phys. **24**, 311.
Bobulescu, R. C., C. Stanciulescu, A. Surmeian, D. Popescu, I. I. Popescu, and C. B. Collins, 1980, Rev. Roum. Phys. **25**, 927.
Bourdet, G. L., and P. Houmault, 1986, Opt. Commun. **58**, 331.
Bourdet, G. L., A. Orzag, and Y. De Valence, 1973, C. R. Acad. Sci. **277**, 207.
Bourne, O. L., M. R. Humphries, S. A. Mitchell, and P. A. Hackett, 1986, Opt. Commun. **56**, 403.
Brandenberger, J. R., 1987, Phys. Rev. A **36**, 76.
Bréchignac, C., R. Vetter, and P. R. Berman, 1977, J. Phys. B **10**, 3443.
Bréchignac, C., R. Vetter, and P. R. Berman, 1978, Phys. Rev. A **17**, 1609.
Bridges, W. B., 1978, J. Opt. Soc. Am. **68**, 352.
Broglia, M., F. Catoni, A. Montone, and P. Zampetti, 1987, Phys. Rev. A **36**, 705.
Broglia, M., F. Catoni, and P. Zampetti, 1983a, J. Phys. (Paris) **C7-44**, 251.
Broglia, M., F. Catoni, and P. Zampetti, 1983b, J. Phys. (Paris) **C7-44**, 479.
Broglia, M., F. Catoni, and P. Zampetti, 1985, J. Opt. Soc. Am. B **2**, 570.
Brooks, M., and A. L. S. Smith, 1979, J. Phys. D **12**, 1249.
Brown, S. C., 1961, *Basic Data of Plasma Physics* (MIT, Cambridge, MA).
Brunker, S. A., and S. C. Haydon, 1983, J. Phys. (Paris) **C7-44**, 55.
Bulyshev, A. E., N. V. Denisova, and N. G. Preobrazhenskii, 1988, Opt. Spectrosc. (USSR) **64**, 590.
Bulyshev, A. E., and N. G. Preobrazhenskii, 1984, Dokl. Akad. Nauk SSSR **279**, 1357 [Sov. Phys. Dokl. **29**, 1034 (1984)].
Burkov, V. S., P. Ya. Misakov, P. A. Naumenkov, S. N. Raikov, and A. S. Khomyak, 1983, Dok. Akad. Nauk SSSR **27**, 27.
Caesar, T., and J. L. Heully, 1983a, Opt. Commun. **45**, 258.
Caesar, T., and J. L. Heully, 1983b, J. Phys. (Paris) **C7-44**, 261.
Camus, P., 1974, J. Phys. B **7**, 1154.
Camus, P., 1983, J. Phys. (Paris) **C7-44**, 87.
Camus, P., M. Dieulin, and A. El Himdy, 1982, Phys. Rev. A **26**, 379.
Camus, P., M. Dieulin, and A. El Himdy, 1983a, J. Phys. (Paris) **C7-44**, 271.
Camus, P., M. Dieulin, and A. El Himdy, 1983b, Phys. Scr. **27**, 125.
Camus, P., M. Dieulin, and C. Morillon, 1979, J. Phys. Lett. (Paris) **40**, L513.
Carlson, R. C., L. A. Cross, and T. M. Dunn, 1985, Chem. Phys. Lett. **113**, 515.
Carswell, A. J., and I. I. Wood, 1967, J. Appl. Phys. **38**, 3828.
Chellehmalzadeh, M. A., and C. B. Collins, 1979, Phys. Rev. A **19**, 2270.
Cherrington, B. E., 1979, IEEE Trans. Electron Devices **ED-26**, 148.
Chevalier, G., J. M. Gagné, and P. Pianarosa, 1987, Opt. Commun. **64**, 126.
Chevalier, G., J. M. Gagné, and P. Pianarosa, 1988, J. Opt. Soc. Am. B **5**, 1492.
Collins, C. B., 1983, J. Phys. (Paris) **C7-44**, 395.
Collins, C. B., S. M. Curry, B. W. Johnson, M. Y. Mirza, M. A. Chellehmalzadeh, J. A. Anderson, D. Popescu, and I. Popescu, 1976, Phys. Rev. A **14**, 1662.
Collins, C. B., B. W. Johnson, D. Popescu, G. Musa, M. L. Pascu and I. Popescu, 1973, Phys. Rev. A **8**, 2197.
Collins, C. B., F. W. Lee, H. Golnabi, F. Davanloo, P. A. Vicharelli, D. Popescu, and I. Popescu, 1981, J. Chem. Phys. **75**, 4852.
Dabkiewicz, Ph., T. W. Hänsch, D. R. Lyons, A. L. Schawlow, A. Siegel, Z.-Y. Wang, and G.-Y. Yan, 1981, in *Laser Spectroscopy V,* Proceedings of the Fifth International Conference, Jasper Park Lodge, Alberta, Canada, 1981, edited by A. R. W. McKellar, T. Oka, and B. P. Stoicheff (Springer-Verlag, Berlin/Heidelberg/New York), p. 178.
Delsart, C., J. C. Keller, and C. Thomas, 1981, J. Phys. B **14**, 3355.
De Marinis, E., A. Sasso, and E. Arimondo, 1988, J. Appl. Phys. **63**, 649.
Demuynck, C., and J. L. Destombes, 1981, IEEE J. Quantum Electron. **QE-17**, 575.
Den Hartog, E. A., D. A. Doughty, and J. E. Lawler, 1988, Phys. Rev. A **38**, 2471.
Dodd, J. M., 1983, J. Phys. B **16**, 2721.
Doughty, D. K., E. A. Den Hartog, and J. E. Lawler, 1985,

Appl. Phys. Lett. **46**, 352.
Doughty, D. K., and J. E. Lawler, 1983a, Phys. Rev. A **28**, 773.
Doughty, D. K., and J. E. Lawler, 1983b, Appl. Phys. Lett. **42**, 234.
Doughty, D. K., and J. E. Lawler, 1984, Appl. Phys. Lett. **45**, 611.
Dovichi, N. J., D. S. Moore, and R. A. Keller, 1982, Appl. Opt. **21**, 1468.
Drèze, C., Y. Demers, and J. M. Gagné, 1982, J. Opt. Soc. Am. **72**, 912.
Drouet, M. G., and J. P. Novak, 1971, Phys. Lett. A **34**, 199.
Druyvesteyn, M. J., and F. M. Penning, 1940, Rev. Mod. Phys. **12**, 87.
Duffey, T. P., D. Kammen, A. L. Schawlow, S. Svandberg, H. R. Xia, G. G. Xiao, and G. Y. Yan, 1985, Opt. Lett. **10**, 597.
Dumitras, D. C., D. C. Datu, N. Comaniciu, U. Draganescu, R. Alexandrescu, and I. Morjan, 1974, Rev. Roum. Phys. **26**, 485.
Engleman, R., Jr., and R. A. Keller, 1980, Opt. Lett. **5**, 465.
Engleman, R., Jr., R. A. Keller, and C. M. Miller, 1985, J. Opt. Soc. Am. B **2**, 897.
Erez, G., S. Lavi, and E. Miron, 1979, IEEE J. Quantum Electron. **QE-15**, 1328.
Ernst, K., M. Grabinska, and M. Inguscio, 1989, Opt. Commun. **73**, 43.
Ernst, K., and M. Inguscio, 1988, Riv. Nuovo Cimento **11**, N. 2.
Ernst, K., P. Minutolo, A. Sasso, G. M. Tino, and M. Inguscio, 1989, Opt. Lett. **14**, 554.
Feld, M. S., A. Sanchez, A. Javan, and B. J. Feldman, 1974, in *Méthods de Spectroscopie sans largeur Doppler de niveaux excités de systèmes moléculaires simples,* edited by J. C. Lehmann and J. C. Pebay-Peyroula (Editions du Centre National de la Recherche Scientifique 217, Paris), p. 87.
Feldmann, D., 1979, Opt. Commun. **29**, 67.
Ferguson, A. I., 1982, Philos. Trans. R. Soc. London, Ser. A **307**, 645.
Foote, P. D., and F. L. Mohler, 1925, Phys. Rev. **26**, 195.
Francesconi, M., L. Gianfrani, M. Inguscio, P. Minutolo, A. Sasso, and G. M. Tino, 1990, Appl. Phys. B **51**, 87.
Franklin, R. N., 1976, *Plasma Phenomena in Gas Discharges* (Clarendon, Oxford).
Freiberg, R. F., and L. A. Weaver, 1967, J. Appl. Phys. **38**, 250.
Fujimoto, T., and S. Ikeda, 1989, Opt. Commun. **72**, 286.
Fujimoto, T., Y. Uetani, Y. Sato, C. Goto, and K. Fukuda, 1983, Opt. Commun. **47**, 111.
Gagné, J. M., Y. Demers, P. Pianarosa, and C. Drèze, 1983, J. Phys. (Paris) **C7-44**, 355.
Ganguly, B. N., 1986, J. Appl. Phys. **60**, 571.
Ganguly, B. N., and A. Garscadden, 1985, J. Appl. Phys. **57**, 4856.
Garscadden, A., and S. L. Adams, 1966, Proc. IEEE **54**, 427.
Garscadden, A., P. Bletzinger, and E. M. Friar, 1964, J. Appl. Phys. **35**, 3432.
Gerstenberger, D. C., E. L. Latush; and G. J. Collins, 1979, Opt. Commun. **31**, 28.
Giacobino, E., F. Biraben, and P. Labastie, 1983, J. Phys. (Paris) **C7-44**, 505.
Goldsmith, J. E. M., 1982, Opt. Lett. **7**, 437.
Goldsmith, J. E. M., 1983a, J. Chem. Phys. **78**, 1610.
Goldsmith, J. E. M., 1983b, J. Phys. (Paris) **C7-44**, 277.
Goldsmith, J. E. M., 1983c, in *Laser-Based Ultrasensitive Spectroscopy and Detection V,* edited by R. A. Keller, Proc. Soc. Photo-Opt. Instrum. Eng. **426**, 145.
Goldsmith, J. E. M., A. I. Ferguson, J. E. Lawler, and A. L. Schawlow, 1979, Opt. Lett. **4**, 230.
Goldsmith, J. E. M., and J. E. Lawler, 1981, Contemp. Phys. **22**, 235.
Goldsmith, J. E. M., and A. V. Smith, 1980, Opt. Commun. **32**, 403.
Gonchakov, A. S., N. B. Zorov, Yu. Ya. Kuzyakov, and O. I. Matveev, 1979, Anal. Lett. **12**, 1037.
Gottscho, R. A., and C. E. Gaebe, 1986, IEEE Trans. Plasma Sci. **PS-14**, 92.
Gough, D. S., and P. Hannaford, 1985, Opt. Commun. **55**, 91.
Grandin, J. F., and X. Husson, 1981, J. Phys. B **14**, 433.
Green, R. B., G. J. Havrilla, and T. O. Trask, 1980, Appl. Spectrosc. **34**, 561.
Green, R. B., R. A. Keller, G. C. Luther, P. K. Schenck, and J. C. Travis, 1976, Appl. Phys. Lett. **29**, 727.
Green, R. B., R. A. Keller, G. C. Luther, P. K. Schenk, and J. C. Travis, 1977, IEEE J. Quantum Electron. **QE-13**, 63.
Green, R. B., R. A. Keller, P. K. Schenck, J. C. Travis, and G. G. Luther, 1976, J. Am. Chem. Soc. **98**, 8517.
Green, R. B., J. C. Travis, and R. A. Keller, 1976, Anal. Chem. **48**, 1954.
Greenberg, K. E., G. A. Hebner, and J. T. Verdeyen, 1984, Appl. Phys. Lett. **44**, 299.
Hameau, C., E. Arimondo, J. Wascat, and P. Glorieux, 1985, Opt. Commun. **53**, 375.
Hameau, C., J. Wascat, D. Dangoisse, and P. Glorieux, 1984, Opt. Commun. **49**, 423.
Haner, D. A., C. R. Webster, P. H. Flamant, and I. S. McDermid, 1983, Chem. Phys. Lett. **96**, 302.
Hannaford, P., D. S. Gough, and G. W. Series, 1983a, J. Phys. (Paris) **C7-44**, 107.
Hannaford, P., D. S. Gough, and G. W. Series, 1983b, in *Laser Spectroscopy VI,* Proceedings of the Sixth International Conference, Interlaken, Switzerland, 1983, edited by H. P. Weber and W. Lüthy (Springer-Verlag, Berlin/Heidelberg/New York/Tokyo), p. 95.
Hannaford, P., and G. W. Series, 1981a, J. Phys. B **14**, L661.
Hannaford, P., and G. W. Series, 1981b, in *Laser Spectroscopy V,* Proceedings of the Fifth International Conference, Jasper Park Lodge, Alberta, Canada, 1981, edited by A. R. W. McKellar, T. Oka, and B. P. Stoicheff (Springer-Verlag, Berlin/Heidelberg/NewYork), p. 94.
Hannaford, P., and G. W. Series, 1982a, Phys. Rev. Lett. **48**, 1326.
Hannaford, P., and G. W. Series, 1982b, Opt. Commun. **41**, 427.
Hänsch, T. W., D. R. Lyons, A. L. Schawlow, A. Siegel, Z. Y. Wang, and G. Y. Yan, 1981, Opt. Commun. **38**, 47.
Hänsch, T. W., and P. Toschek, 1970, Z. Phys. **236**, 213.
Hollberg, L., Long-Shen Ma, M. Hohenstatt, and J. L. Hall, 1983, in *Laser-Based Ultrasensitive Spectroscopy and Detection V,* edited by R. A. Keller, Proc. Soc. Photo-Opt. Instrum. Eng. **426**, 91.
Hurst, G. S., M. G. Payne, S. D. Kramer, and J. P. Young, 1979, Rev. Mod. Phys. **51**, 767.
Inguscio, M., 1983, J. Phys. (Paris) **C7-44**, 217.
Inguscio, M., P. Minutolo, A. Sasso, and G. M. Tino, 1988, Phys. Rev. A **37**, 4056.
Inguscio, M., A. Moretti, and F. Strumia, 1980, IEEE J. Quantum Electron. **QE-16**, 955.
Inguscio, M., A. Moretti, and F. Strumia, 1982, Appl. Phys. B **28**, 89.
Jackson, D. J., E. Arimondo, J. E. Lawler, and T. W. Hänsch, 1980, Opt. Commun. **33**, 51.
Jackson, D. J., H. Gerhardt, and T. W. Hänsch, 1981, Opt. Commun. **37**, 23.

Jirmann, J., and W. Durr, 1982, Electron. Lett. **18**, 69.
Johnston, T. F., Jr., 1978a, Coherent Radiat. Focus Sci. **2**, 1.
Johnston, T. F., Jr., 1978b, Laser Focus **14**, 58.
Julien, L., and M. Pinard, 1982, J. Phys. B **15**, 2881.
Kane, D. M., 1983, Opt. Commun. **47**, 317.
Kane, D. M., 1984, J. Appl. Phys. **56**, 1267.
Katayama, D. H., J. M. Cook, V. E. Bondybey, and T. A. Miller, 1979, Chem. Phys. Lett. **62**, 542.
Kavaya, M. J., R. T. Menzies, and U. P. Oppenheim, 1982, IEEE J. Quantum Electron. **QE-18**, 19.
Kawakita, K., K. Fukuda, Y. Adachi, and C. Hirose, 1985, J. Chem. Phys. **82**, 653.
Kawakita, K., T. Nakajima, Y. Adachi, S. Maeda, and C. Hirose, 1983, Opt. Commun. **48**, 121.
Keaton, G. L., N. S. Nogar, and S. W. Downey, 1987, Chem. Phys. Lett. **137**, 26.
Keller, R. A., R. Engleman, Jr., and B. A. Palmer, 1980, Appl. Opt. **19**, 836.
Keller, R. A., R. Engleman, Jr., and E. F. Zalewski, 1979, J. Opt. Soc. Am. **69**, 738.
Keller, R. A., B. E. Warner, E. F. Zalewski, P. Dyer, R. Engleman, Jr., and B. A. Palmer, 1983, J. Phys. (Paris) **C7-44**, 23.
Keller, R. A., and E. F. Zalewski, 1980, Appl. Opt. **19**, 3301.
Keller, R. A., and E. F. Zalewski, 1982, Appl. Opt. **21**, 3992.
Kenty, C., 1950, Phys. Rev. **80**, 95.
King, D. S., and P. K. Schenck, 1978, Laser Focus **14**, 50.
King, D. S., P. K. Schenck, K. C. Smith, and J. C. Travis, 1977, Appl. Opt. **16**, 2617.
Klein, R., R. P. McGinnis, and S. R. Leone, 1983, Chem. Phys. Lett. **100**, 475.
Koch, M. E., and C. B. Collins, 1979, Phys. Rev. A **19**, 1098.
Kohler, P., 1985, Appl. Opt. **24**, 1322.
Kolchenko, A. P., A. A. Puknov, S. G. Rautian, and A. M. Shalagin, 1973, Sov. Phys. JETP **36**, 619.
Kopeika, N. S., 1978, IEEE Trans. Plasma Sci. **PS-6**, 139.
Kopeika, N. S., 1982, Appl. Opt. **21**, 3989.
Kopeika, N. S., G. Eytan, and A. P. Kushelevsky, 1979, J. Appl. Phys. **50**, 11.
Kopeika, N. S., R. Gellman, and A. P. Kushelevsky, 1977, Appl. Opt. **16**, 2470.
Kopeika, N. S., T. Karcher, and C. S. Ih, 1979, Appl. Opt. **18**, 3515.
Kopeika, N. S., and A. P. Kushelevsky, 1978, Appl. Opt. **17**, 3933.
Kopeika, N. S., and J. Rosenbaum, 1976, IEEE Trans. Plasma Sci. **PS-4**, 51.
Kopeika, N. S., J. Rosenbaum, and R. Kastner, 1976, Appl. Opt. **15**, 1610.
Kramer, J., 1986, J. Appl. Phys. **60**, 3072.
Kravis, S. P., and S. C. Haydon, 1981, J. Phys. D **14**, 151.
Kroll, S., and A. Persson, 1985, Opt. Commun. **54**, 277.
Kushner, M. J., 1983, Appl. Opt. **22**, 1970.
Labastie, P., F. Biraben, and E. Giacobino, 1982, J. Phys. B **15**, 2595.
Labastie, P., E. Giacobino, and F. Biraben, 1982, J. Phys. B **15**, 2605.
Langlois, E., and J. M. Gagné, 1987, J. Opt. Soc. Am. B **4**, 1222.
Lawler, J. E., 1980, Phys. Rev. A **22**, 1025.
Lawler, J. E., and D. K. Doughty, 1983, J. Phys. (Paris) **C7-44**, 209.
Lawler, J. E., A. I. Ferguson, J. E. M. Goldsmith, D. J. Jackson, and A. L. Schawlow, 1979a, Phys. Rev. Lett. **42**, 1046.
Lawler, J. E., A. I. Ferguson, J. E. M. Goldsmith, D. J. Jackson, and A. L. Schawlow, 1979b, in *Laser Spectroscopy IV,* edited by H. Walther and K. W. Rothe (Springer-Verlag, Berlin/Heidelberg/New York), p. 188.
Lawler, J. E., A. Siegel, B. Couillaud, and T. W. Hänsch, 1981, J. Appl. Phys. **52**, 4375.
Lemoigne, J. P., J. P. Grandin, X. Husson, and H. Kucal, 1983, J. Phys. (Paris) **C7-44**, 209.
Lemoigne, J. P., J. P. Grandin, X. Husson, and H. Kucal, 1984, J. Phys. (Paris) **45**, 249.
Letokhov, V. S., and V. P. Chebotayev, 1977, in *Nonlinear Laser Spectroscopy* (Springer, Berlin).
Little, P. F., and A. von Engel, 1954, Proc. R. Soc. London, Ser. A **224**, 209.
Lorenzen, C. J., and K. Niemax, 1982, Opt. Commun. **43**, 26.
Lyons, D. R., A. L. Schawlow, and G. Y. Yan, 1981, Opt. Commun. **38**, 35.
Maeda, M., Y. Nomiyama, and Y. Miyazoe, 1981, Opt. Commun. **39**, 64.
Mallard, W. G., J. H. Miller, and K. C. Smyth, 1982, J. Chem. Phys. **76**, 3483.
Matveev, O. I., N. B. Zorov, and Yu. Ya. Kuzyakov, 1978, Vestn. Mosk. Univ. Khim. **19**, 537 [Moscow Univ Chem. Bull. **33**, 23 (1978)].
May, R. D., 1985a, J. Appl. Phys. **58**, 1169.
May, R. D., 1985b, Appl. Phys. Lett. **46**, 938.
May, R. D., and P. H. May, 1986, Rev. Sci. Instrum. **57**, 2242.
McDermid, I. S., and C. R. Webster, 1983, J. Phys. (Paris) **C7-44**, 461.
Meissner, K. W., and W. F. Miller, 1953, Phys. Rev. **92**, 896.
Menocal, S. G., N. Andreakis, J. S. Patel, J. Werner, C. E. Zah, T. P. Lee, and P. F. Liao, 1989, IEEE Photo. Technol. Lett. **1**, 285.
Miron, E., I. Smilanski, J. Liran, S. Lavi, and G. Erez, 1979, IEEE J. Quantum Electron. **QE-15**, 194.
Mirza, M. Y., and W. W. Duley, 1978, Proc. R. Soc. London, Ser. A **364**, 255.
Mirza, M. Y., and W. W. Duley, 1979, Opt. Commun. **28**, 179.
Miyazaki, K. H. Scheingraber, and C. R. Vidal, 1983a, Phys. Rev. Lett. **50**, 1046.
Miyazaki, K., H. Scheingraber, and C. R. Vidal, 1983b, Phys. Rev. A **28**, 2229.
Miyazaki, K., H. Scheingraber, and C. R. Vidal, 1983c, J. Phys. (Paris) **C7-44**, 411.
Miyazaki, K., H. Scheingraber, and C. R. Vidal, 1983d, in *Laser Spectroscopy VI,* Proceedings of the Sixth International Conference, Interlaken, Switzerland, 1983, edited by H. P. Weber and W. Lüthy (Springer-Verlag, Berlin/Heidelberg/New York/Tokyo), p. 93.
Moffatt, S., and A. L. S. Smith, 1981, Opt. Commun. **37**, 119.
Moffatt, S., and A. L. S. Smith, 1984, J. Phys. D **17**, 59.
Moscatelli, F. A., D. E. Murnick, and R. B. Robinson, 1988, J. Phys. B **21**, L495.
Muenchausen, R. E., R. D. May, and G. W. Hills, 1984, Opt. Commun. **48**, 317.
Murnick, D. E., W. R. Softy, and D. N. Stoneback, 1986, Phys. Lett. B **174**, 238.
Nakajima, T., N. Uchitomi, Y. Adachi, S. Maeda, and C. Hirose, 1983, J. Phys. (Paris) **C7-44**, 497.
Naveedullah, K., and A. S. Naqvi, 1985, Opt. Commun. **56**, 117.
Nestor, J. R., 1982, Appl. Opt. **21**, 4154.
Nestor, J. R., 1983, J. Phys. (Paris) **C7-44**, 387.
Nippoldt, M. A., and R. B. Green, 1983, Anal. Chem. **55**, 1171.
Nogar, N. S., and G. L. Keaton, 1985, Chem. Phys. Lett. **120**, 327.
Ochkin, V. N., N. G. Preobrazhenskii, N. N. Sobolev, and N.

Ya. Shaparev, 1986, Usp. Fiz. Nauk **148**, 473 [Sov. Phys. Usp. **29**, 260 (1986)].
Palmer, B. A., R. A. Keller, and R. Engleman, Jr., 1980, Report No. LA-8251-MS (Los Alamos National Laboratory, Los Alamos, NM).
Palmer, B. A., R. A. Keller, F. V. Kowalski, and J. L. Hall, 1981, J. Opt. Soc. Am. **71**, 948.
Pealat, M., J.-P. E. Taran, M. Bacal, and F. Hillion, 1985, J. Chem. Phys. **32**, 4943.
Pendrill, L. R., M. Pettersson, and U. Österberg, 1983a, Phys. Scr. **27**, 306.
Pendrill, L. R., M. Pettersson, and U. Österberg, 1983b, J. Phys. (Paris) **C7-44**, 489.
Penning, F. M., 1928, Physica **8**, 137.
Penning, F. M., 1957, "Electrical discharges in gases," Philips Technical Library (Servire BV, Katwijk aan Zee, Eindhoven).
Pepper, D. M., 1978, IEEE J. Quantum Electron. **QE-14**, 971.
Pfaff, J., M. H. Begemann, and R. J. Saykally, 1981, Bull. Am. Phys. Soc. **27**, 11.
Pfaff, J., M. H. Begemann, and R. J. Saykally, 1984, Mol. Phys. **52**, 541.
Pfau, S., A. Rutscher, and K. Wojaczek, 1969, Beitr. Plasma Phys. **9**, 333.
Pianarosa, P., Y. Demers, and J. M. Gagné, 1984, J. Opt. Soc. Am. B **1**, 704.
Piepmeier, E. H., and G. J. Beenen, 1982, Appl. Spectrosc. **36**, 235.
Pinard, M., and L. Julien, 1983, J. Phys. (Paris) **C7-44**, 129.
Piyakis, K. N., and J. M. Gagné, 1989, J. Opt. Soc. Am. B **6**, 7.
Popescu, D., R. C. Bobulescu, C. Stanciulescu, A. Surmeian, N. Ceausescu, I. I. Popescu, and C. B. Collins, 1980, Rev. Roum. Phys. **25**, 771.
Reddy, B. R., P. Venkateswarlu, and M. C. George, 1989, Opt. Commun. **73**, 117.
Reddy, M. N., and G. N. Rao, 1988, Phys. C **150**, 457.
Rettner, C. T., C. R. Webster, and R. N. Zare, 1981, J. Phys. Chem. **85**, 1105.
Richardson, W. H., L. Maleki, and E. Garmire, 1987, Phys. Rev. A **36**, 5713.
Rinneberg, H., and J. Neukammer, 1983, J. Phys. (Paris) **C7-44**, 177.
Rockney, B. H., T. A. Cool, and E. R. Grant, 1982, Chem. Phys. Lett. **87**, 141.
Roesch, L. P., 1983, Opt. Commun. **44**, 259.
Rosenfeld, A., S. Mory, and R. Konig, 1979, Opt. Commun. **30**, 394.
Rothe, E. W., G. S. Ondrey, and P. Anderson, 1986, Opt. Commun. **58**, 113.
Sakurai, T., N. Goto, and H. Morisawa, 1986, Opt. Commun. **61**, 266.
Salcedo Torres, L. E., N. B. Zorov, and Yu. Ya. Kuzyakov, 1981, Zh. Anal. Khim. **36**, 1433 [J. Anal. Chem. USSR **36**, 1016 (1982)].
Sansonetti, C. J., and K. H. Weber, 1984, J. Opt. Soc. Am. B **1**, 361.
Sasso, A., M. Ciocca, and E. Arimondo, 1988, J. Opt. Soc. Am. B **5**, 1484.
Sasso, A., M. G. Di Vito, and E. Arimondo, 1988, Opt. Commun. **66**, 270.
Sasso, A., M. Inguscio, G. M. Tino, and L. R. Zink, 1989, in *Non-Equilibrium Processes in Partially Ionized Gases,* edited by M. Capitelli and J. H. Bardsley, NATO ASI Series (Plenum, New York), in press.
Sasso, A., P. Minutolo, M. I. Schisano, G. M. Tino, and M. Inguscio, 1988, J. Opt. Soc. Am. B **5**, 2417.
Sasso, A., G. M. Tino, M. Inguscio, N. Beverini, and M. Francesconi, 1988, Nuovo Cimento D **10**, 941.
Saykally, R. J., M. H. Begemann, and J. Pfaff, 1981, in *Laser Spectroscopy,* Proceedings of the Fifth International Conference, Jasper Park Lodge, Alberta, Canada, 1981, edited by A. R. W. McKellar, T. Oka, and B. P. Stoicheff (Springer-Verlag, Berlin/Heidelberg/New York), p. 305.
Schenck, P. K., and J. W. Hastie, 1981, Opt. Eng. **20**, 522.
Schenck, P. K., W. G. Mallard, J. C. Travis, and K. C. Smyth, 1978, J. Chem. Phys. **69**, 5147.
Schenck, P. K., and K. C. Smyth, 1978, J. Opt. Soc. Am. **68**, 626.
Schenck, P. K., J. C. Travis, G. C. Turk, and T. C. O'Haver, 1981, J. Phys. Chem. **85**, 2547.
Schiffner, G., and F. Seifert, 1965, Proc. IEEE **53**, 1657.
Schneider, M., A. Hinz, A. Groh, K. Evenson, and W. Urban, 1987, Appl. Phys. B **44**, 241.
Schnell, S., and W. Lüthy, 1985, J. Phys. E **18**, 28.
Scholtz, A. L., and G. Shiffner, 1980, Appl. Phys. **21**, 407.
Schottky, W., 1924, Phys. Z **25**, 635.
Sekiguchi, H., A. Masuyama, T. Kasuya, and T. Suzuki, 1985, J. Appl. Phys. **58**, 154.
Series, G. W., 1981, Comments At. Mol. Phys. **10**, 199.
Shuker, R., 1983, J. Phys. (Paris) **C7-44**, 455.
Shuker, R., A. Ben-Amar, and G. Erez, 1980, J. Opt. Soc. Am. **70**, 1392.
Shuker, R., A. Ben-Amar, and G. Erez, 1981, Opt. Commun. **39**, 51.
Shuker, R., A. Ben-Amar, and G. Erez, 1982, Opt. Commun. **42**, 29.
Shuker, R., A. Ben-Amar, and G. Erez, 1983a, J. Appl. Phys. **54**, 5685.
Shuker, R., A. Ben-Amar, and G. Erez, 1983b, J. Phys. (Paris) **C7-44**, 35.
Shuker, R., A. Ben-Amar, and G. Erez, 1984, Opt. Commun. **49**, 263.
Shy, J. T., and T. C. Yen, 1986, Opt. Lett. **12**, 325.
Siegel, A., J. E. Lawler, B. Couillaud, and T. W. Hänsch, 1981, Phys. Rev. A **23**, 2457.
Singh, R., and G. N. Rao, 1989, Phys. Scr. **40**, 170.
Skolnick, M. L., 1970, IEEE J. Quantum Electron. **QE-6**, 139.
Smith, A. L. S., and S. Moffatt, 1979, Opt. Commun. **30**, 213.
Smith, P. W., and T. W. Hänsch, 1971, Phys. Rev. Lett. **13**, 740.
Smits, R. M. M., and M. Prins, 1979, Physica C **96**, 262.
Smyth, K. C., B. L. Bentz, C. G. Bruhn, and W. W. Harrison, 1979, J. Am. Chem. Soc. **101**, 797.
Smyth, K. C., R. A. Keller, and F. F. Crim, 1978, Chem Phys. Lett. **55**, 473.
Smyth, K. C., and W. G. Mallard, 1982, J. Chem. Phys. **77**, 1779.
Smyth, K. C., and P. K. Schenck, 1978, Chem. Phys. Lett. **55**, 466.
Smyth, K. C., P. K. Schenck, and W. G. Mallard, 1980, in *Laser Probes for Combustion Chemistry,* ACS Symposium Series 134, edited by D. R. Crosley (American Chemical Society, Washington, DC), Chap. 12.
Smyth, K. C., P. K. Schenck, W. G. Mallard, and J. C. Travis, 1978, Nat. Bur. Stand. (U.S.) Spec. Publ. 561, 865.
Sorem, M. S., and A. L. Schawlow, 1972, Opt. Commun. **5**, 148.
Stanciulescu, C., R. C. Bobulescu, A. Surmeian, D. Popescu, I. I. Popescu, and C. B. Collins, 1980a, Appl. Phys. Lett. **37**, 888.
Stanciulescu, C., R. C. Bobulescu, A. Surmeian, D. Popescu, I.

I. Popescu, and C. B. Collins, 1980b, Rev. Roum. Phys. **25**, 783.
Stanciulescu, C., R. C. Bobulescu, A. Surmeian, D. Popescu, I. I. Popescu, and C. B. Collins, 1980c, Rev. Roum. Phys. **25**, 915.
Strumia, F., 1983, J. Phys. (Paris) **C7-44**, 117.
Strumia, F., M. Inguscio, and A. Moretti, 1981, in *Laser Spectroscopy V,* Proceedings of the Fifth International Conference, Jasper Park Lodge, Alberta, Canada, 1981, edited by A. R. W. McKellar, T. Oka, and B. P. Stoicheff (Springer-Verlag, Berlin/Heidelberg/New York), p. 255.
Su, M. C., S. R. Ortiz, and D. L. Monts, 1987, Opt. Commun. **61**, 257.
Suri, B. M., R. Kapoor, G. D. Saksena, and P. R. K. Rao, 1985, Opt. Commun. **52**, 315.
Suzuki, T., 1981, Opt. Commun. **38**, 364.
Suzuki, T., T. Fukasawa, H. Sekiguchi, and T. Kasuya, 1986, Appl. Phys. B **39**, 247.
Suzuki, T., and M. Kakimoto, 1982, J. Mol. Spectrosc. **93**, 423.
Suzuki, T., and T. Kasuya, 1987, Phys. Rev. A **36**, 2129.
Suzuki, T., H. Sekiguchi, and T. Kasuya, 1983, J. Phys. (Paris) **C7-44**, 419.
Tachibana, K., 1986, Phys. Rev. A **34**, 1007.
Taillet, J., 1969, C. R. Acad. Sci. **269**, 52.
Tam, A. C., 1982, IEEE Trans. Plasma Sci. **PS-10**, 252.
Teets, R. E., F. V. Kowalski, W. T. Hill, III, N. W. Carlson, and T. W. Hänsch, 1977, Proc. Soc. Photo-Opt. Instrum. Eng. **113**, 80.
Tenenbaum, J., E. Miron, S. Lavi, J. Liran, M. Strauss, J. Oreg, and G. Erez, 1983, J. Phys. B **16**, 4543.
Thomason, W. H., and D. C. Elbers, 1975, Rev. Sci. Instrum. **46**, 409.
Tochigi, K., S. Maeda, and C. Hirose, 1986, Phys. Rev. Lett. **57**, 711.
Tonks, L., and I. Langmuir, 1929, Phys. Rev. **34**, 876.
Touzeau, M., G. Gousset, J. Jolly, D. Pagnon, M. Vialle, C. M. Ferreira, J. Loureiro, M. Pinheiro, and P. A. Sa, 1989, in *Non-Equilibrium Processes in Partially Ionized Gases,* edited by M. Capitelli and J. H. Bardsley, NATO ASI Series (Plenum, New York), in press.
Travis, J. C., and J. R. DeVoe, 1981, in *Lasers in Chemical Analysis,* edited by C. M. Hieftje, J. C. Travis, and F. E. Lytle (The Humana Press, Clifton, NJ), p. 92.
Travis, J. C., P. K. Schenck, G. C. Turk, and W. G. Mallard, 1979, Anal. Chem. **51**, 1516.
Travis, J. C., G. C. Turk, and R. B. Green, 1982, Anal. Chem. **54**, 1006A.
Turk, G. C., 1981, Anal. Chem. **53**, 1187.
Turk, G. C., J. R. DeVoe, and J. C. Travis, 1982, Anal. Chem. **54**, 643.
Turk, G. C., W. G. Mallard, P. K. Schenck, and K. C. Smith, 1979, Anal. Chem. **51**, 2408.
Turk, G. C., J. C. Travis, and J. R. DeVoe, 1983, J. Phys. (Paris) **C7-44**, 301.
Turk, G. C., J. C. Travis, J. R. DeVoe, and T. C. O'Haver, 1979, Anal. Chem. **51**, 1890.
Uchitomi, N., T. Nakajima, S. Maeda, and C. Hirose, 1983, Opt. Commun. **44**, 154.
Uetani, Y., and T. Fujimoto, 1984, Opt. Commun. **49**, 258.
Valentini, H. B., 1985, Opt. Commun. **53**, 313.
van Den Hoek, W. J., and J. A. Visser, 1980, J. Appl. Phys. **51**, 174.
van de Weijer, P., and R. M. M. Cremers, 1985a, Opt. Commun. **53**, 109.
van de Weijer, P., and R. M. M. Cremers, 1985b, Opt. Commun. **54**, 273.
van Dijk, C. A., and C. Th. J. Alkemade, 1980, Combust. Flame **38**, 37.
Van Roozendael, M., M. Godefroid, M. Herman, and G. W. Hills, 1985, in *Ninth Colloquium on HIgh Resolution Molecular Spectroscopy,* edited by G. Nivellini, A. Trombetti, and F. Tullini (Cooperativa Libraria Universitaria Editrice, Bologna), p. 16.
Van Roozendael, M., G. W. Hills, and M. Herman, 1986, Opt. Commun. **58**, 319.
Vasudev, R., and R. N. Zare, 1982, J. Chem. Phys. **76**, 5267.
Vidal, C. R., 1980, Opt. Lett. **5**, 158.
von Engel, A., 1965, *Ionized Gases,* 2nd ed. (Clarendon, Oxford).
Wada, A., Y. Adachi, and C. Hirose, 1986, J. Phys. Chem. **90**, 6645.
Wada, A., Y. Adachi, and C. Hirose, 1987, J. Chem. Phys. **86**, 5904.
Wada, A., Y. Adachi, and C. Hirose, 1988, Opt. Commun. **66**, 203.
Wakata, H., S. Saikan, and M. Kimura, 1981, Opt. Commun. **38**, 271.
Walkup, R., R. W. Dreyfus, and Ph. Avouris, 1983a, Phys. Rev. Lett. **50**, 1846.
Walkup, R., R. W. Dreyfus, and Ph. Avouris, 1983b, J. Phys. (Paris) **C7-44**, 441.
Walkup, R., R. W. Dreyfus, and Ph. Avouris, 1983c, in *Laser Spectroscopy VI,* Proceedings of the Sixth International Conference, Interlaken, Switzerland, 1983, edited by H. P. Weber and W. Lüthy (Springer-Verlag, Berlin/Heidelberg/New York/Tokyo), p. 72.
Walsh, C. J., 1985, J. Phys. D **18**, 789.
Webster, C. R., 1982, Appl. Opt. **21**, 2298.
Webster, C. R., I. S. McDermid, and C. T. Rettner, 1983, J. Chem. Phys. **78**, 646.
Webster, C. R., and R. T. Menzies, 1983a, J. Chem. Phys. **78**, 2121.
Webster, C. R., and R. T. Menzies, 1983b, J. Phys. (Paris) **C7-44**, 429.
Webster, C. R., and C. T. Rettner, 1983, Laser Focus **19**, 41.
White, J. C., R. R. Freeman, and P. F. Liao, 1980, Opt. Lett. **5**, 120.
Yamaguchi, S., and M. Suzuki, 1982, Appl. Phys. Lett. **41**, 597.
Yan, G.-Y., K.-I. Fujii, and A. L. Schawlow, 1990, Opt. Lett. **15**, 142.
Yasuda, Y., N. Sokabe, and A. Murai, 1985, Opt. Commun. **55**, 319.
Zalewski, E. F., R. A. Keller, and R. Engleman, Jr., 1979, J. Chem. Phys. **70**, 1015.
Zorov, N. B., Yu. Ya. Kuzyakov, and O. I. Matveev, 1982, Zh. Anal. Khim. **37**, 520 [J. Anal. Chem. USSR **37**, 400 (1982)].
Zorov, N. B., Yu. Ya. Kuzyakov, O. I. Matveev, and V. I. Chaplygin, 1980, Zh. Anal. Khim. **9**, 1701 [J. Anal. Chem. USSR **35**, 1108 (1981)].